

VISUAL ACUITY PREDICTION BASED ON
TRANSIENT SWEEP VISUAL EVOKED POTENTIALS AND
THE EFFECT OF IMAGE DEGRADATION

by

Joan Parkinson

Submitted in partial fulfilment of the requirements
for the degree of Master of Science

at

Dalhousie University
Halifax, Nova Scotia
March 2016

© Copyright by Joan Parkinson, 2016

TABLE OF CONTENTS

LIST OF TABLES.....	viii
LIST OF FIGURES.....	ix
ABSTRACT.....	xi
LIST OF ABBREVIATIONS AND SYMBOLS USED.....	xii
ACKNOWLEDGEMENTS.....	xv
CHAPTER 1:INTRODUCTION.....	1
1.1 Background.....	1
1.2 Purpose of the Study.....	3
1.3 Hypothesis and Research Questions.....	3
CHAPTER 2: LITERATURE REVIEW	4
2.1 Transmission of Visual Information.....	4
2.1.1 Central Neurosensory Retina- Basic Anatomy.....	5
2.1.2 Central Neurosensory Retina- Signal Processing.....	7
2.1.3 Optic Nerve to Visual Cortex.....	9
2.2 Visual Acuity.....	13
2.2.1 Minimum Recognizable Visual Acuity.....	13
2.2.2 Minimum Resolvable Visual Acuity.....	15
2.2.3 Effect of Refractive Errors and Accommodation.....	17
2.3 Experimental Image Degradation.....	21
2.3.1 Optical Defocus.....	21

2.3.2	Bangerter Foils.....	22
2.4	Standard Visual Evoked Potential.....	23
2.4.1	Flash Visual Evoked Potential.....	24
2.4.2	Pattern Visual Evoked Potential.....	25
2.5	Sweep Visual Evoked Potential.....	28
2.5.1	Early Design and Methodology.....	31
2.5.2	Infant Visual Acuity and Visual Development.....	34
2.5.3	Abnormal Ocular or Cortical Conditions.....	34
2.5.4	Experimental Image Degradation.....	36
2.5.5	Considerations: Technology and Acuity Determination.....	37
2.6	M-sequence and Visual Evoked Potential.....	39
2.6.1	Visual System Nonlinearities and the M-Sequence.....	39
2.6.2	VERIS™ System.....	40
2.7	Wavelet Analysis.....	41
 CHAPTER 3: METHODS		45
3.1	Preliminary Actions.....	45
3.2	Overview of Study Design.....	45
3.3	Ethical Considerations.....	50
3.3.1	Research Ethics Board Approval.....	50
3.3.2	Risk/Benefit Analysis.....	50
3.3.3	Informed Consent.....	50
3.4	Sample.....	51

3.4.1	Recruitment Procedures.....	51
3.4.2	Inclusion and Exclusion Criteria.....	51
3.4.3	Study Population.....	52
3.4.4	Sample Size Calculation.....	54
3.5	Preliminary Procedures- General.....	54
3.5.1	Orthoptic Evaluation.....	54
3.5.2	Electrode Placement.....	55
3.5.3	Viewing Conditions.....	55
3.6	Image Degradation.....	56
3.6.1	Optical Defocus (Plus Lenses).....	56
3.6.2	Image Obscuration (Bangerter Foils).....	59
3.7	Technology Assessment: Use of Pattern Visual Evoked Potential.....	62
3.7.1	Removal of LCD Monitor Flash Artefact: Preliminary Trials with PVEP.....	62
3.7.2	Removal of Aliasing with LCD Monitor.....	63
3.8	Sweep Visual Evoked Potential (Population- Averaged Estimates)....	63
3.8.1	Acquisition.....	64
3.8.2	Measurement of Waves and Linear Regression.....	65
3.8.3	Automated Wavelet Analysis.....	66
3.8.4	Additional Analysis Models.....	68
3.9	Sweep Visual Evoked Potential (Individual Estimates).....	71
3.10	Statistical Consideration.....	72

CHAPTER 4: RESULTS.....	73
4.1 Data Presentation.....	73
4.2 Comparison between Expert and Wavelet Analysis Techniques (Individual Data).....	74
4.3 Effect of Image Degradation on the SVEP Response Curve (Group Data).....	77
4.3.1 Effect of Optical Defocus (Plus Lenses).....	77
4.3.2 Effect of Image Obscuration (Bangerter Foils).....	81
4.3.3 Comparison of Image Degradation Techniques on SVEP Acuity.....	84
4.4 Initial Models Related to SVEP Response Curve Parameters (Group Data).....	87
4.4.1 Model 1: SVEP Predicted Acuity by Linear Extrapolation.....	87
4.4.2 Model 2: SVEP Predicted Acuity Related to Response Amplitude Ratios.....	90
4.4.3 Models 1&2: Measurement Repeatability.....	94
4.5 Additional and Combined Models for SVEP Predicted Acuity (Group Data).....	98
4.6 Additional and Combined Models for SVEP Predicted Acuity (Individual Data).....	102
4.6.1 Additional Models for SVEP Predicted Acuity.....	102
4.6.2 Combined Models for SVEP Predicted Acuity and Agreement with ETDRS Acuity.....	105
4.6.3 Model Combinations for SVEP Predicted Acuity.....	110
4.7 Review of Normative SVEP Response Curves and Subgroups (Individual Data)	112

CHAPTER 5: DISCUSSION.....	116
5.1 Transient Sweep Visual Evoked Potential.....	116
5.1.1 Population Design Considerations.....	116
5.1.2 Technical Considerations and Modifications.....	117
5.1.3 SVEP Trials and Response Curve Characteristics.....	119
5.1.4 Challenges to Expert Markings and Use of Wavelet Analysis.	121
5.2 SVEP Parameters Related to Image Degradation: Initial Analysis Models.....	122
5.2.1 Image Degradation Data: Expert versus Wavelet Analysis.....	123
5.2.2 SVEP Acuity Predictions: Linear Regression Model 1.....	125
5.2.3 SVEP Acuity Predictions: Analysis by Ratio Model 2.....	129
5.2.4 Data Repeatability.....	130
5.3 Transient SVEP Parameters: Additional and Combined Analysis Models.....	132
5.4 Transient SVEP: Normative Subgroups.....	137
5.5 Limitations and Future Work.....	138
5.6 Conclusion.....	140
APPENDIX A. Removal of Flash Artefact- PVEP Acquisition Details.	143
APPENDIX B. Holladay Visual Acuity Conversion Chart.....	144
APPENDIX C. SVEP Responses and Marking Challenges as Note by the Expert.....	145
APPENDIX D. MATLAB® Codes.....	146
APPENDIX E. MATLAB® Code for Receiver Operating Curve.....	148

APPENDIX F.	Analysis of Individual Data Related to the Presence of Repeated Measures.....	149
REFERENCES.....		150

LIST OF TABLES

Table 1	Participant Characteristics and Test Summary.....	53
Table 2	Statistics for SVEP Models (Group Data).....	101
Table 3	Combination Analyzes of Various SVEP Parameter Models.....	111

LIST OF FIGURES

Figure 1.	Approximate Anatomical Demarcations of the Macula (Right Eye).....	6
Figure 2.	Basic Anatomy of the Left Occipital Lobe Showing the Foveal Representation and Visual Field Correlates.....	12
Figure 3.	The Optics of Basic Refractive States and Fogging Technique.....	19
Figure 4.	Historical Samples Showing Technique of Extrapolation to Zero Related to Contrast Sensitivity and Eventual Translation to SVEP.....	29
Figure 5.	Historical Samples of SVEP Tracings using Central Masking and Optical Defocus	33
Figure 6.	Wavelet Analysis Process Showing a Signal Waveform that can be Matched using Wavelets that Vary in Frequency.....	44
Figure 7.	Effect of Monitor Type and Modifications on Pattern Visual Evoked Potentials.....	47
Figure 8.	Flow Chart of SVEP Study Design.....	49
Figure 9.	The Effect of Plus Lenses on ETDRS Visual Acuity.....	58
Figure 10.	The Effect of Bangerter Foils on ETDRS Visual Acuity.....	61
Figure 11.	Illustration of a SVEP Response Curve Showing Analysis Models (1-6) Based on Response Curve Parameters.....	70
Figure 12.	Linear Regression between the Expert and Wavelet Analysis (WA) Using Group Data with Optical Defocus and Bangerter Foils (BF).....	76
Figure 13.	Effect of Increasing Power of Plus Lenses on ETDRS Visual Acuity and SVEP Linear Extrapolated Visual Acuity using Wavelet Analysis and Group Data	79
Figure 14.	Effect of Increasing Power of Bangerter foils (BF) on ETDRS Visual Acuity and SVEP Linear Extrapolated Visual Acuity using Wavelet Analysis (WA) and Group Data.....	82
Figure 15.	Summary Comparison between ETDRS Visual Acuity and SVEP Predicted Acuity.....	86
Figure 16.	Comparison between ETDRS Visual Acuity (VA) and SVEP Linear	

	Extrapolated VA using Expert and Wavelet Analysis (WA) with Group Data	89
Figure 17.	Comparison between ETDRS Visual Acuity (VA) and Two Ratios Based on SVEP Response Amplitudes at Designated Points on the SVEP Response Curve.....	93
Figure 18.	Bland-Altman Analysis Comparing Expert and Wavelet Analysis (WA) using Control Trial Data for SVEP Linear Extrapolated Visual Acuity Levels and Response Amplitude Ratios.....	96
Figure 19.	Various Models for SVEP Visual Acuity Prediction using Linear Regression between ETDRS Visual Acuity and SVEP Response Curve Parameters.....	99
Figure 20.	Models for SVEP Visual Acuity Prediction using SVEP Response Curve Parameters Compared to ETDRS Visual Acuity	103
Figure 21.	Combination of all Models (1-6) for SVEP Visual Acuity Prediction using SVEP Response Curve Parameters and ETDRS Visual Acuity Levels.....	106
Figure 22.	Receiver Operating Curve for SVEP Individual Data and Chart Illustrating the Method Related to ROC Calculation.....	108
Figure 23.	Variation in Normative SVEP Response Curves.....	113
Figure 24.	Combination of all Models (1-6) for SVEP Visual Acuity Prediction (SVEP Response Curve Parameters Compared to ETDRS Visual Acuity) for Two Subgroups	114
Figure 25.	Individual Data Comparing ETDRS Visual Acuity and SVEP Predicted Visual Acuity in Relationship to Octaves of Difference and Various Methods of Recording Visual Acuity.....	135

ABSTRACT

Purpose: To investigate the accuracy of a new transient sweep visual evoked potential (SVEP) technology to estimate optotype visual acuity (VA) under various viewing conditions and to compare the standard model for SVEP VA estimation (linear regression) with innovative analysis models.

Methods: VERIST™ 6.4 software (Electro-Diagnostic Imaging, Inc.) was used for transient SVEP recordings. Several technical adjustments were required to resolve a flash artefact inherent to LCD monitors. Thirteen participants (ages: 21-59; 7 males; mean VA -1.11 logMAR) underwent an orthoptic examination, pattern visual evoked potentials, and SVEP testing under normal conditions and with image degradation by lenses (+0.50 to +3.00) and/or Bangerter foils (BF) (8 foils: VA ~0.1 to light perception). SVEP response curves were obtained by two techniques: subjective wave marking (Expert) and objective Wavelet Analysis (WA) (MATLAB®, Natick MA). The Haar wavelet was used to decompose the raw waves into the summation of high-frequency wavelet coefficients and to create automated SVEP response curves. Analysis models were used to determine optotype VA from SVEP response curves in a population-based data set: 1) linear regression; 2) amplitude ratios; 3) peak position; 4) peak amplitude; 5) points >1.6 x noise level; 6) area under the curve. These models and their possible combinations were applied to individual data to test for clinical application of the technique. Predictive relationships were determined by linear regression and repeatability was assessed using Bland-Altman plots

Results: Although good coefficients of determination were seen between Expert and WA (R^2 lens data: 0.92; BF data: 0.95), WA showed superiority for noise assessment, reduced data variability and repeatability. WA was eventually used of all data analysis. Population- averaged (“group”) data revealed that SVEP results underestimated optotype VA when no or minimal image degradation was used and overestimated optotype VA with marked image degradation. Of all 6 analysis models, Model 2 (ratio between low and peak spatial frequency stimuli) and Model 5 (number of data points above 1.6 x the noise level) showed the most consistency for both image degradation conditions (lens and BF) and highest R^2 values (all above 0.91). Individual data showed more variability with lower R^2 values for all models (range: 0.33 to 0.49) but improved R^2 values with all Models 1-6 combined (0.62). However, Bland-Altman plots showed substantial variance with midrange acuities (15-25 c/d). Binary combinations optimized the R^2 value to 0.65 with model combinations of 1,2,4 and 1,2,4,5. Receiver operating curve for individual data revealed good sensitivity/specificity for high and low levels of ETDRS acuity with area under the curve values of 0.90 and 0.94 respectively with poor values for intermediate acuity levels (~0.57). Subsequent review of raw data revealed high and low normative amplitude groups with R^2 values of 0.80 and 0.63 respectively using model combination 1-6.

Conclusion: Automated WA shows precedence over the Expert technique and provides objectivity for SVEP data that inherently shows substantial variability. Coefficients of determination between SVEP predicted acuity and optotype acuity can be optimized by using new analysis models and model combinations. Normative SVEP response curves appear to fall into normative high and low peak amplitude groups with much better R^2 values between SVEP and optotype acuity with normative high amplitudes.

LIST OF ABBREVIATIONS AND SYMBOLS USED

a.k.a.	Also Known As
AUC	Area Under the Curve
c/d	Cycles Per Degree
CI	Confidence Interval
cm	Centimeter
D	Lens Diopter
e.g.	Example
ETDRS	Early Treatment Diabetic Retinopathy Study
ETDRS-SVEP	Early Treatment Diabetic Retinopathy Study Chart Visual Acuity Minus Sweep Visual Potential Test Predicted Visual Acuity
FVEP	Flash Visual Evoked Potential
ISCEV	International Society for Clinical Electrophysiology of Vision
LED	Light Emitting Diode
LGN	Lateral Geniculate Nucleus
LP	Light Perception
Log	Logarithmic
MAR	Minimum Angle of Resolution
m	Meter
mm	Millimeter
MAR	Minimum Angle of Resolution
Min	Minute
MR	Manifest Refraction

M-Sequence	Maximal Length Sequence
nV	Nanovolt
OLED	Organic Light Emitting Diode (Monitor)
OZ	Occipital Lobe Location (Midline)
PappVEP	Pattern Appearance Visual Evoked Potential
PVEP	Pattern Visual Evoked Potential
PVEP-CRT	Pattern Visual Evoked Potential using Cathode Ray Tube Monitor
PVEP-LCD	Pattern Visual Evoked Potential using Liquid Crystal Display Monitor
PVEP-LCDm	Pattern Visual Evoked Potential using Liquid Crystal Display Monitor with Modified M-Sequence
RGC	Retinal Ganglion Cell
ROC	Receiver Operating Curve
SD	Standard Deviation
sec	Seconds
SEM	Standard Error of the Mean
SNR	Signal to Noise Ratio
spf	Spatial Frequency
SVEP	Sweep Visual Evoked Potential
TM	Trade Mark
V1	Primary Visual Cortex
VA	Visual Acuity
VEP	Visual Evoked Potential
VERISTM	Visual Evoked Response Imaging System

WA	Wavelet Analysis
WC	Wavelet Coefficient
yrs	Years
μV	Microvolt
™	Trademark
®	Registered
~	Approximately
'	Arc minutes
“	Arc seconds

ACKNOWLEDGEMENTS

It is with great sincerity that I express my gratitude to everyone who has contributed to my success with this thesis. My supervisor, Francois Tremblay was patient and tolerant of my *unending questions* and quietly moved this project towards fruition. He was truly invested in success and would not consider that perhaps this technique “just doesn’t work”. My supervisory committee and examiners took time from their other numerous activities to thoroughly review my project and attend to details, for which I am very grateful. My course professors at Dalhousie University and Mount St, Vincent University were excellent teachers, engaged, and tolerant of my *unending questions*. My colleges at the IWK Health Centre Eye Clinic have been wonderful and altogether have created an atmosphere that encourages learning and high patient care standards that promote my endeavors. And last, but not least, I thank my friends and family who have been willing to “lend an ear” for discussions that likely had a bit too much jargon and went a bit too long. My kind husband, Chris Morrone, was encouraging, patient with my wanderings at unusual hours, and accepting that many home activities necessarily were “put on hold”. And lastly, thanks to my children, Ben, Kate and Nathan who are my role models for “pushing through rough spots” and maintaining curiosity. Here’s to *unending questions* and science that is fascinating and the essence of long chats ‘round the kitchen table late into the night.

CHAPTER 1: INTRODUCTION

1.1 Background

Comparisons between objective and subjective measurements of human visual function are of ongoing interest to vision researchers and clinicians. This project involves using various testing conditions to determine the capability of an objective visual function test (visual evoked potential) to match or predict the subjective identification of letters or optotypes – commonly referred to as visual acuity (VA).

A precise and objective method to predict VA would be advantageous to clinicians and researchers for many reasons. The measurement of VA is a key component in judging the integrity of the visual pathway (Levi, 2011); as such, VA contributes to diagnosis, treatment evaluation, and medico-legal documentation (Kim, Weber, & Szabo, 2012; Rubin, 2006). Visual acuity levels relate to disability categories (low vision, legal blindness) and can impact education, employability, mobility and the overall psychosocial well-being of individuals (Allen & Birse, 1991; Lang, 2000; Lee, Cunningham, Nakazono, & Hays, 2009; MacCuspie, 1996; McCreath, 2010; Reinhardt & D'Allura, 2000). However, reliance on subjective reporting of VA using standard charts introduces human error (Arditi & Cagenello, 1993; Chen S., Chandna, Norcia, Pettet, & Stone, 2006; Reeves, Wood, & Hill, 1991), may involve unintentional misrepresentation or feigning (Lim, Siatkowski, & Farris, 2005; Moore, Al-Zubidi, Yalamanchili, & Lee, 2012), and may exclude populations with communication barriers due to age, cognitive ability, or physical impairments (Hyvarinen, 1988; McLeod, Wisnicki, & Medow, 2000; Ray & Maahs, 1999; Zambone, Ciner, Appel, & Graboyes, 2000).

When routine subjective VA is unobtainable or doubted, clinicians may employ a variety of tools to estimate VA such as the potential acuity meter and laser interferometer (Cavallerano,

1991; Faulkner, 1983; Minkowski, Palese, & Guyton, 1983), stereoacuity (Donzis, Rappazzo, Burde, & Gordon, 1983; Goodwin & Romano, 1985), visual evoked potentials (Prager et al., 1999; Tyler, Apkarian, Levi, & Nakayama, 1979; Xu, Meyer, Yoser, Mathews, & Elfervig, 2001), and preferential looking (McDonald et al., 1985; Nelson, 1998) But as yet, despite a variety of tools and in the presence of various pathological conditions, the validity of these VA estimation techniques has been questioned (Arai, Katsumi, Paranhos, Lopes De Faria, & Hirose, 1997; Friedman, Munoz, Massof, Bandeen-Roche, & West, 2002; Parkinson & Tremblay, 2009; Vianya-Estopa, Douthwaite, Funnell, & Elliott, 2009; Woodhouse, Morjaria, & Adler, 2007).

Of the auxiliary tests used to estimate VA, the visual evoked potential (VEP) is an objective test requiring no reports of a vision level from the patient (Chiappa, 1989; Fahle & Bach, 2006). The VEP measures the cortical response to stimuli as received by scalp electrodes placed at the occipital lobe. The pattern visual evoked potential (PVEP) most often measures the cortical response to checkerboard stimuli using check sizes ranging from low to high spatial frequencies. The PVEP estimates correlate well with VA (Bobak, Bodis-Wollner, & Guillory, 1987; Harter & White, 1968); however, the VA estimates with PVEP remain broadly categorical in routine clinical practice (Prager et al., 1999; Xu et al., 2001). To improve upon PVEP acuity estimates, the sweep visual evoked potential (SVEP) has been developed (see review Almoqbel, Leat, & Irving, 2008). The SVEP quickly “sweeps” through multiple spatial frequencies and shows precise VA estimates in some populations, but may not be predictive of VA in various disease conditions (Arai et al., 1997; Gottlob et al., 1990). The capacity of the SVEP to predict visual acuity needs clarification prior to incorporating the SVEP as a local clinical tool.

1.2 Purpose of the study

The purpose of this study is to characterize a new transient SVEP technique. Models of vision loss (temporary induced image blur or obscuration) used with visually normal participants will assist in comparing the response of the SVEP to simulated vision loss. The information gained by this study will assist in the eventual deployment of the SVEP for our clinic population.

1.3 Hypothesis and Research Questions

Hypothesis

Variations of image clarity will show similar and predictable changes when comparing SVEP and optotype visual acuity measures.

Research Questions

- What is the effect of optical defocus (using plus lenses) on SVEP visual acuity predictions?
- What is the effect of image obscuration (using Bangerter foils) on SVEP visual acuity predictions?
- Can an automated wavelet analysis of SVEP data be as accurate as an expert analysis?

CHAPTER 2: LITERATURE REVIEW

2.1 Transmission of Visual Information

Visual acuity and PVEPs are highly dependent on the integrity of the central retina and the transfer of visual information from this area through the optic nerve to the visual cortex. Anomalous function of the central retina can cause vision loss (central scotoma), yielding deficits of visual acuity (Deutman, Hoyng, & van Lith-Verhoeven, 2006; Kanski & Milewski, 2002; Rotenstreich, Fishman, & Anderson, 2003; Szlyk, Fishman, Grover, Revelins, & Derlacki, 1998; Trobe, 2001) and suboptimal PVEPs (Brigell, 2001; Holder, 2006; Parkinson & Tremblay, 2009; Vottonen, Kaarniranta, Paakkonen, & Tarkka, 2013). Under normal circumstances, individuals show a decrement in visual acuity with increasing eccentricity from the central retina (foveola) (Bishop, 1981; Levi, 2011) and small central masks of 3-9 degrees will reduce the PVEP amplitude (Sokol, 1986). The PVEP is not only sensitive to small central masks but is also resistant to peripheral masks beyond the central 8-12 degrees thus demonstrating the limited retinal area that contributes to the PVEP- as opposed to a simultaneously recorded pattern electroretinogram that is much more sensitive to peripheral stimulation (Parkinson, Waterhouse, & Tremblay, 2009; Sakaue, Katsumi, Mehta, & Hirose, 1990).

Due to the relationship of visual acuity and PVEPs to the central retina and with consideration of our photopic experimental conditions, the following sections will focus on transmission of visual information from this retinal area as related to a black/white achromatic stimulus.

2.1.1 *Central Neurosensory Retina- Basic Anatomy*

The central retina can be anatomically divided into concentric rings within the macula termed (from most central to more peripheral): the foveola, fovea, parafovea and perifovea (Bishop, 1981; Forrester, Dick, McMenemy, & Roberts, 2008; Hildebrand & Fielder, 2011; Knob, 2014) (see Figure 1). The foveola, fovea, and parafovea are the anatomical areas most related to VA and PVEP.

The foveola is a circular area (.35 mm diameter) located at the center of fovea; this area has only cone photoreceptors (highest density of the retina-200,000/mm²), is free from overlying blood vessels and ganglion cells, subtends a visual angle of ~1.4 degrees, and yields optimal levels of visual acuity (Bishop, 1981; Hildebrand & Fielder, 2011; Rodieck, 1998). The concentration of cones reduces with increased eccentricity from the foveola (approximately 20,000/mm² at the foveal border and further reduces by 25% beyond this point) and visual acuity rapidly declines (Bishop, 1981; Hildebrand & Fielder, 2011).

The fovea (1.5 mm diameter) increases the visual angle subtended from the foveola center to ~ 5 degrees, continues to be rod photoreceptor free, but retinal ganglion cells and a retinal nerve fiber layer are present- both increasing in thickness with eccentricity (Hildebrand & Fielder, 2011; Massey, 2006). The ganglion cell layer gains maximal thickness in the narrow parafovea (.5 mm diameter); this area increases the visual angle subtended from the central foveola to ~ 8.4 degrees, and has increased rod photoreceptors (rod:cone ratio of 4:1) (Bishop, 1981; Hildebrand & Fielder, 2011; Massey, 2006).

The perifovea which extends to the edge of the macula, is highly vascularized, shows increasing ratios of rod:cones, and increases the visual angle subtended from the center of the foveola to ~ 18.4 degrees (Bishop, 1981; Hildebrand & Fielder, 2011).

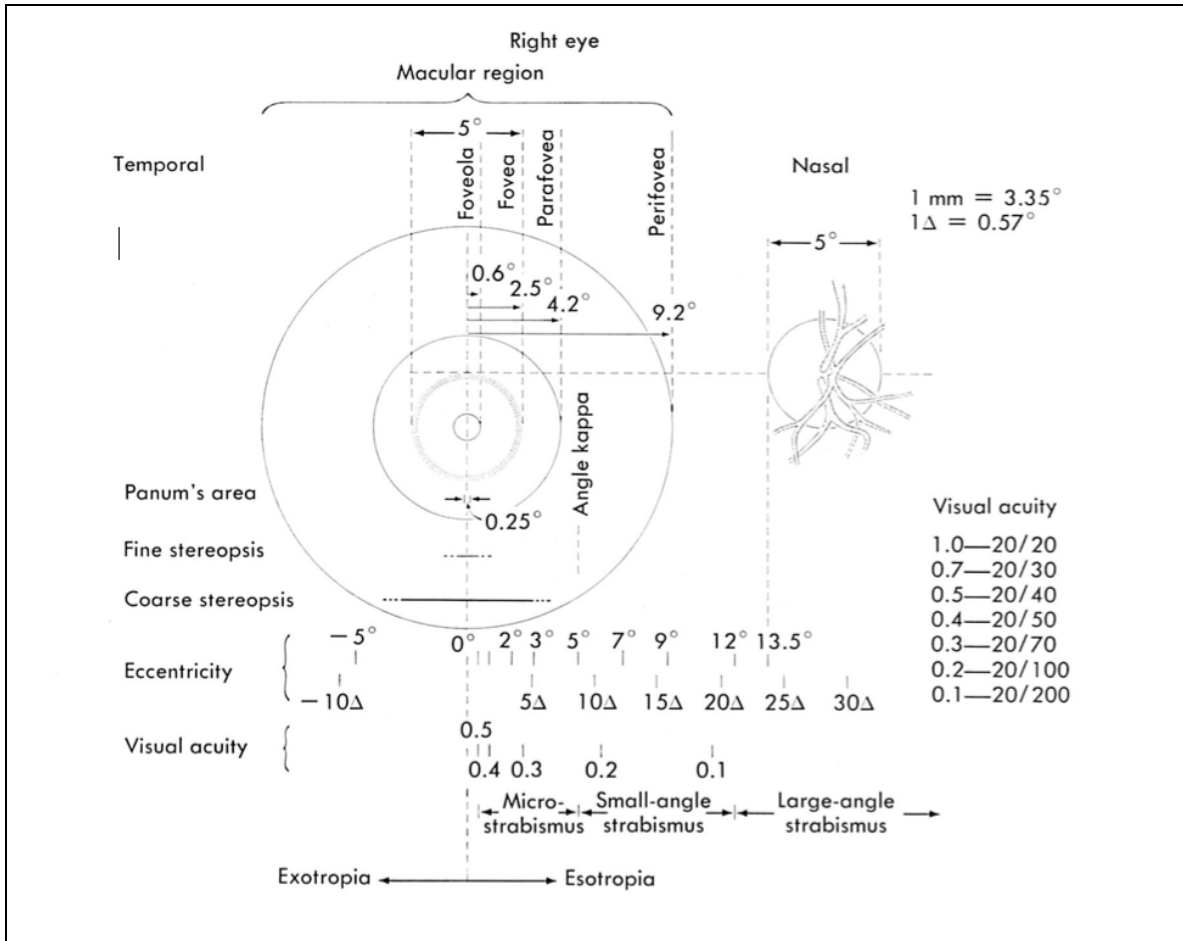


Figure 1: Approximate Anatomical Demarcations of the Macula (Right Eye). Snellen visual acuity estimates for degrees of eccentricity from the foveola and the potential degrees of associated strabismus are shown. Adapted from “Binocular Vision” by P.O. Bishop, 1981, *Adler’s Physiology of the Eye: Clinical Applications* R.A. Moses (Ed.), 7th ed. p. 579. Copyright 1981 by The C.V. Mosby Company.

2.1.2 Central Neurosensory Retina- Signal Processing

The anatomical configuration of the central retina alone does not fully account for the capacity of the visual system to discern fine details and high spatial frequencies (Forrester et al., 2008). Other than appropriate phototransduction of photons of light by the photoreceptors, the transfer of the resulting electrical information anteriorly through a complex retinal circuitry, multiple neuron types and receptive fields, and exclusive or convergent neural connections are required for normal visual function. Inhibitory processes assist in defining the visual image, such as lateral inhibition afforded by retinal horizontal cells, ON and OFF bipolar cells, and antagonistic center/surround retinal ganglion cell receptive fields (Rodieck, 1998).

Although the central retina is mainly populated by cone photoreceptors, rods are also present starting in the parafovea. Other than differing in retinal distribution, cone and rods differ in type of photopigments/opsins, retinal circuitry, and visual function: cones contribute more so to spatial and image resolution and color vision; rods are highly sensitive to light, movement and stimulus contrast (Forrester et al., 2008; Massey, 2006). Of particular interest, is the capability of the two types of photoreceptors to transmit either highly specific or summated visual information. This capacity is related to the nature of their synaptic terminals, the type and availability to secondary neurons (bipolar cells, horizontal cells) and following this, the type and availability to the tertiary neuron- retinal ganglion cells that will transmit the visual information to the brain via the optic nerve.

The bipolar cells can be broadly classified as rod or cone associated and then into two main types based on their response to the synaptic transmission received from the photoreceptors. There is a marked contrast between the types and availability of bipolar cell interactions for cones versus rods. At the first cone/bipolar cell synapse the visual information is channeled into two separate functional pathways known as the ON and OFF pathway (Masland,

2012; Massey, 2006). The ON bipolar cells respond to light with depolarization and the OFF bipolar cells respond to light with hyperpolarization. Both types of bipolar cells then synapse with retinal ganglion cells (RGC) with sign conserving synapses (Massey, 2006; Rodieck, 1998). Rods have one type of bipolar cell (reacts to light similar to the ON cone system) but has no direct contact with ganglion cells (access to the cone ON and OFF systems is provided to the rods via amacrine-cone system interactions) (Massey, 2006).

The high spatial resolution provided by the cone system is related to an exclusive $\sim 1:1$ ratio between central cones and midsize bipolar cells; the 1:1 ratio then extends to midsize ganglion cells (Massey, 2006). However, the cone system also provides convergence of information via diffuse cone bipolar cells that may contact with up to 20 cone pedicles (Forrester et al., 2008). The rods show higher convergence with up to 30-50 rods to a single rod bipolar cell (Rodieck, 1998). The convergence of rod synaptic information contributes to high sensitivity but reduced resolution.

It is estimated that humans have ~ 1.2 million RGCs that can be subdivided into 20 different cell types that are arranged in several rows in the parafovea and then sparsely distributed in the peripheral retina (Forrester et al., 2008). Action potentials are generated by RGCs and their axons form the retinal nerve fiber layer that eventually creates the optic nerve (Chalam et al., 2011; Massey, 2006). The ON and OFF bipolar cells synapse with ON-center and OFF-center RGC receptive fields respectively; this affords enhanced edge and contrast detection along with lateral inhibition as afforded by horizontal cells (Rodieck, 1998).

Recordings from the receptive fields of ganglion cells show tuning of various cell types to visual stimuli or changes in stimuli involving such factors as brightness, color, movement or shape

(Marc, 2011) and reveal generally smaller receptive field sizes in the central compared to the peripheral retina (Rodieck, 1998).

Midget and parasol (diffuse) RGCs are predominant in the retina and constitute approximately 70% and 10% of the ganglion cell population respectively (Rodieck, 1998). Midget ganglion cells occupy the central retina (Rodieck, 1998) and all central synapses are exclusive with midget bipolar cells (1:1 ratio) (Forrester et al., 2008). The midget ganglion cells synapse in the parvocellular layers of the lateral geniculate nucleus (LGN); the parvocellular system contributes to perception of color, high spatial resolution. Also present in the central retina are parasol ganglion cells that synapse mainly with diffuse bipolar cells, show more signal convergence with larger receptive fields, and gather information from groups of photoreceptors (Rodieck, 1998). Parasol RGCs synapse in the magnocellular layers of the LGN; the magnocellular system contributes to the perception of contrast and movement (Forrester et al., 2008).

2.1.3 Optic Nerve to Visual Cortex

The integrity of the RGCs, optic nerve, and the visual pathway to the occipital cortex is crucial for optimal visual evoked potentials and visual acuity. The origin of the optic nerve (optic disc) is located ~12-15 degrees nasal to the fovea (Chalam et al., 2011). Foveal and macular fibers are highly represented in the optic nerve with approximately 90% of retinal ganglion cell axons derived from the macular area- particularly nasal axons extending from the fovea to the optic disc (maculopapillary bundle) (Forrester et al., 2008).

The optic nerve pathway to the primary visual cortex extends from the posterior globe to the optic chiasm where nasal retinal fibers from each eye decussate to join the temporal fiber of the contralateral eye and follow a lateral route to synapse at either the right or left LGN

(Forrester et al., 2008). Retinotopic organization is maintained in the LGN with a large macular representation; the predominant layers are: 1,4, and 6 (contralateral nasal fibers); 2,3 and 5 (ipsilateral temporal fibers) with small koniocellular layers present below each major layer (Forrester et al., 2008; Rodieck, 1998).

Traditionally, it has been understood that the flow of information was unidirectional (anterior to posterior) and that mainly midget ganglion cells projected to the upper/dorsal layers of the LGN (cone related-parvocellular layers 3-6) and mainly parasol ganglion cells project to the lower layers (rod related- magnocellular layers 1&2) (Rodieck, 1998). However recently, it is suspected that up to 10 axon classes may have conduits for projections to the LGN, that extraretinal sources contribute, and that substantial cortical feedback exists (Casagrande & Ichida, 2011).

After the LGN, the optic nerve fibers course through the optic radiations and terminate at the primary visual cortex (V1) in the posterior occipital lobe. The visual cortex shows a marked increase in cells compared to the LGN (> 100 times) (Levi, 2011). Similar to the LGN, V1 is retinotopically organized with alternating layers of cells and receptive fields, and has bilateral representation that yields a striped (striated) appearance related to the input from each eye (ocular dominance columns) (Rodieck, 1998). Other than processing the visual information from the LGN (brightness level, temporal and spatial frequencies), the cellular activity of V1 yields information regarding: binocularity, stimulus orientation and direction; LGN interactions and feedback; interactions and feedback between V1 and higher processing centers (Casagrande & Marion, 2011).

The extensive LGN macular representation is mirrored in V1 with a large posterior foveal representation (Casagrande & Marion, 2011; Horton & Hoyt, 1991) (see Figure 2). The posterior

foveal representation and the placement of the active VEP electrode at the mid-occipital location (2 cm above the inion) yields optimal PVEP recording and is agreeable with estimates that the PVEP reflects the central ~ 10 degrees of retinal activity (Parkinson et al., 2009; Sakaue et al., 1990; Sokol, 1986).

Although the PVEP reflects foveal activity and a relationship between visual acuity and PVEP results does exist (Regan, 1973), the cognitive interpretation of V1 activity requires the transfer to and feedback from extrastriate locations (Boyd & Matsubara, 2011; Casagrande & Marion, 2011); recordable PVEP does not insure a higher level cognitive interpretation of the V1 activity.

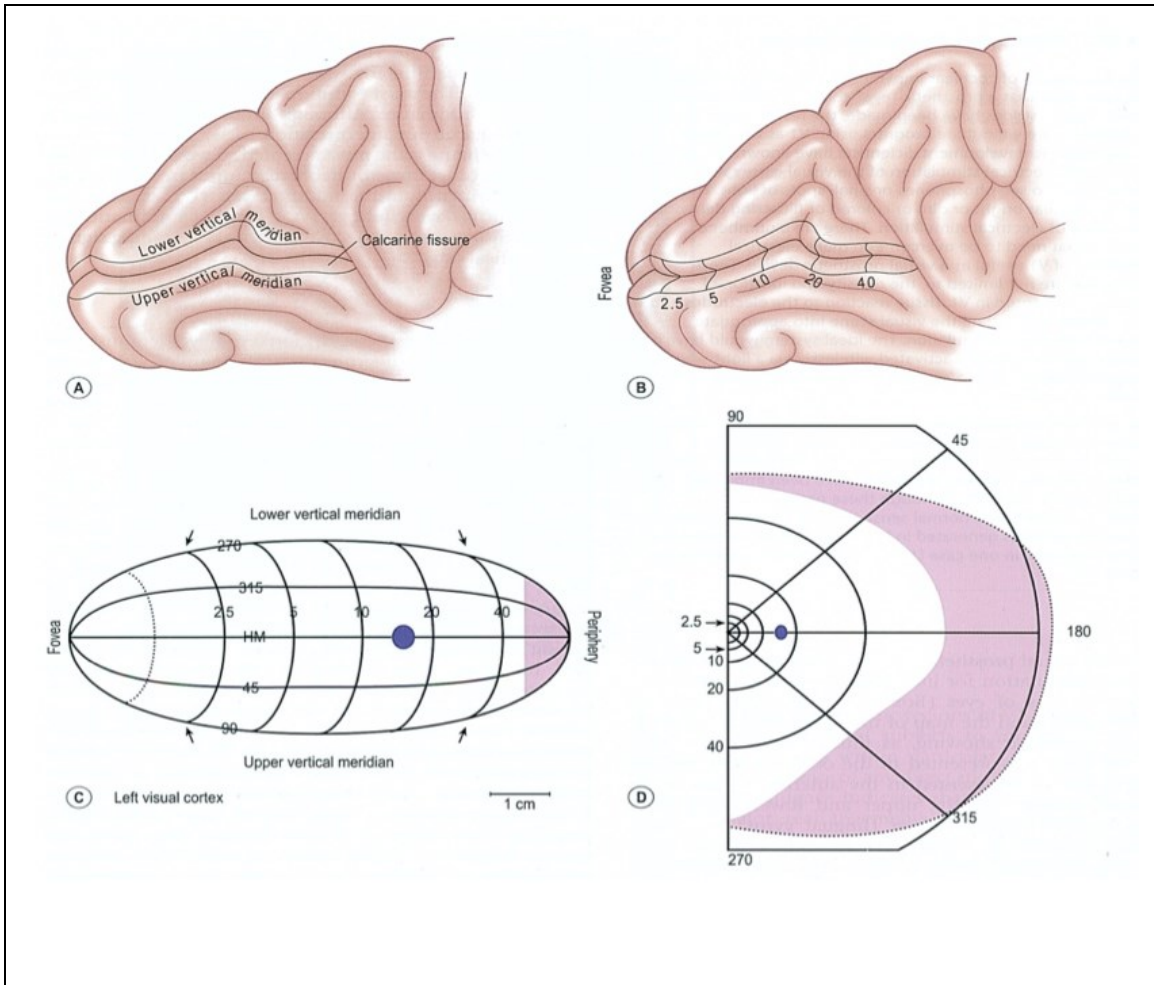


Figure 2: Basic Anatomy of the Left Occipital Lobe Showing the Foveal Representation and Visual Field Correlates. A. The calcarine fissure (location of the primary visual cortex-VI). B. Foveal representation and visual field demarcations from the fovea to approximately 45 degrees peripherally. C. Schema of the calcarine fissure in B. flat mounted showing visual field distribution and blind spot in blue. Purple area indicates the monocular crescent. HM = horizontal meridian. D. The right visual field representation of C. showing the monocular crescent in purple. Adapted from “Processing in the Primary Visual Cortex,” by V. Casagrande and R. Marion R, 2011, in *Adler’s Physiology of the Eye*, (11th ed., p.587). Copyright 2011 by Saunders Elsevier. Reproduced there with permission from the publisher Horton & Hoyt (1991).

2.2 Visual Acuity

Routine VA measurement (see also section 1.1) involves the determination of a subjective psychophysical threshold that is related to many factors including: subject attention level and intellectual capacity; testing methodology including test object contrast and luminance; integrity of the ocular media, retinal and visual pathways. There are several types of visual acuity that either coincide well with retinal cone mosaic or otherwise show thresholds that exceed anatomical expectations and relate more so to complex visual processing. For example, related to foveal cone size ($\sim .5$ min arc) the Nyquist sampling limit would predict that resolution of two separate points or lines would require $2x$ the spatial period (1 min of arc; 0.017°). This prediction is agreeable with the two types of acuity that are investigated in this report- minimum recognizable acuity (the correct identification of an optotype on a vision chart) and minimum resolvable acuity (ability to discern the separation between two features of an object such as lines; “grating acuity”) (Levi, 2011). However, due to complex visual processing, under certain conditions the Nyquist limit is exceeded. This occurs with two types of acuity: minimum visible acuity – the ability to detect one feature on a blank background (human threshold $\sim .5$ sec arc or 0.00014°); minimum discriminable acuity – the ability to detect the alignment of two features (human threshold ~ 3 sec arc or 0.0008°) (Levi, 2011). Minimum discriminable acuity is also known as “Vernier” or “hyperacuity”.

2.2.1 *Minimum Recognizable Visual Acuity*

The most commonly measured type of VA is minimum recognizable (“recognition”) acuity. This measurement indicates the capability of a person to correctly identify optotypes that gradually reduce in visual angle subtended on the retina and also reduce in the distance between the features of the optotypes –the minimum angle of resolution (MAR).

There are a variety of formats to report recognition VA; a fraction notation is common with the numerator being the viewing distance and the denominator reflecting the MAR. The norm for visual acuity MAR has been set at one minute of arc, for example: 20/20 = viewing distance of 20 feet/ normal MAR at 20 feet (1 min of arc); 20/40= viewing distance of 20 feet/ abnormal MAR (2 minutes of arc). According to local protocol, this example could be recorded in metric (6/6, 6/12) or as a decimal (1.0, .50).

The Snellen visual acuity chart has been the standard recognition VA measurement tool for many years. However due to inconsistencies that became apparent with this chart (non-geometric progression of letter size and spacing from line to line, differing numbers of letters on each line, use of letters that vary in readability), new logarithmic VA charts were developed that resolved the inconsistencies and allowed the reporting of VA in logMAR units (Ferris, Kassoff, Bresnick, & Bailey, 1982). A common logMAR chart is the Early Treatment Diabetic Retinopathy Study (ETDRS) chart (Early Treatment Diabetic Retinopathy Group, 1985). There are five letters on each line of the ETDRS chart (each letter = .02 logMAR units, each line = .10 logMAR units). Related to the acuity example in the previous paragraph, using the ETDRS chart: 6/6 = 0.0 and 6/12 = +.30 logMAR. The ETDRS test results may be summarized in terms of octaves, an octave difference represents a reduction by half or a doubling of the stimulus spatial frequency (equivalent to 3 lines on the ETDRS chart).

As recognition VA results are used to judge the stability or decline in visual function, consistency in testing methodology is needed as well as an understanding of the test/retest variations within the normal population. The original ETDRS testing procedures required participants (adults) to start at the largest letters on the vision chart and progress until they could no longer guess correctly; however, due to time constraints, an equally reliable method (ETDRS-

Fast) was devised that required only one letter of each line to be read to the point of inaccuracies (test/retest values: ETDRS: ± 0.08 logMAR; ETDRS-Fast: ± 0.06 logMAR) (Camparini, Cassinari, Ferrigno, & Macaluso, 2001). Other studies with visually normal adult participants using the ETDRS charts have found test/retest values of ± 0.11 logMAR (Rosser, Cousens, Murdoch, Fitzke, & Laidlaw, 2003) and ± 0.09 (Arditi & Cagenello, 1993). Due to test/retest variations, a typical benchmark to determine a clinically significant change in recognition VA is 0.20 logMAR (Rosser et al., 2003).

2.2.2 *Minimum Resolvable Visual Acuity*

Although recognition acuity is generally considered the clinical “gold standard”, this is not obtainable in all circumstances (e.g. infants, persons with cortical impairment), or the subjective report of recognition acuity may be questioned. In these circumstances, the minimum resolvable acuity can be measured by various means, including VEP/SVEP testing. Minimum resolvable acuity involves gratings of alternating light and dark patterns- often in stripes (square or sine wave) or checkerboards; acuity thresholds are determined by increasing spatial frequencies in cycles per degree (c/d) until responses become immeasurable or inaccurate. Related to the retinal cone mosaic, at least two cones are required to process a wave cycle (period from start of a white stripe to the end of the next black stripe). Gradual increases in spatial frequency beyond this Nyquist limit results in a perceived image that is losing contrast and eventually dissolves to gray; the eventual modulation to zero with humans occurs at spatial frequencies of ~ 80 c/d with 3 mm pupil size (Levi, 2011). In clinical settings, square wave stimuli (fundamentally a sine wave but there is a constant luminance across each stripe that changes abruptly midway through the cycle) may be preferred due to the associated high contrast and increased likelihood to obtain a response. Sine waves (a “pure” waveform with sinusoidal

changes in luminance across each stripe) are also used as they are more resistant to blur and maintain a sine wave morphology despite modulation (Levi, 2011). Loss of amplitude or a phase shift can occur with modulation of gratings causing blur and illusions such as spurious resolution (e.g. blurring of one stripe creates adjacent dark edges) (Duckman, 2006). With computer generated stimuli, other than the limits of ocular resolution, the image resolution also depends on the computer monitor pixel number and spacing; a mismatch can lead to aliasing (various image aliases, moirés, and interference patterns).

Although constants exist to convert grating acuity thresholds to recognition acuity values (spatial frequency in $c/d = 180/$ metric denominator for recognition acuity) (Duckman, 2006), debates exist regarding the equivalence of the two types of acuity. Cortical processing requirements differ – VEP/SVEP response to a grating pattern indicates activity in the visual cortex but does not require higher cortical interactions required to identify an optotype. Also, difficulties in comparison arise as grating patterns are used for ages or health conditions when recognition acuity testing is not possible and control acuity tests that might be used may not equate to standardized recognition acuities such as ETDRS (optokinetic nystagmus, fixation preference, Allen pictures etc.).

Currently, clinicians may use grating acuity to document a visual behavior, but recognition acuities that are eventually tested may differ significantly; this has been corroborated by several reports indicating that grating acuities tend to overestimate recognition acuity when it is possible to obtain or eventually compare both types of acuity (Hyvarinen, 1991; Kushner, Lucchese, & Morton, 1995; Woodhouse et al., 2007). Age may be a factor with overestimation occurring in young visually normal children and underestimation occurring when recognition acuity nears maturation (Hargadon, Wood, Twelker, Harvey, & Dobson, 2010; Stiers,

Vanderkelen, & Vandenbussche, 2003). Although several grating acuity methods may each document visual maturation well in infants (Teller, VEP, SVEP) and show good test/retest results for the individual methods, the between comparisons of the methods may show poor agreement and prediction of an acuity level for an individual infant may not be valid (Prager et al., 1999).

Using linear regression techniques, early estimates of infant visual acuity with PVEP predicted that visual acuity levels changed from 6/90 (age 2 months) to 6/6 (age 6 months) (Sokol, 1978); Teller card estimates were fairly agreeable at 6 months of age (binocular best level- 6 /15) (Vistech Consultants, 1986). However, eventually with child recognition logMAR acuity charts that are equivalent to adult vision charts, indications are that recognition acuity does not reach 6/6 levels until about 5-6 years of age (Leone, Mitchell, Kifley, & Rose, 2014; Mulla, 2007). Grating acuity results by SVEP testing also provide a recognition acuity estimate via linear regression (Norcia & Tyler, 1985b; Tyler et al., 1979); however, an overestimation of visual acuity may occur in infants (3 – 52 weeks) compared to Teller cards (Riddell et al., 1997) and challenges exist as estimated recognition acuity levels may show inaccuracies particularly in populations with a variety of ocular disease (Arai et al., 1997; Gottlob et al., 1990).

2.2.3 *Effect of Refractive Errors and Accommodation*

Visual processing of fine image details and high spatial frequencies requires optimal refraction of the incoming light rays from the object of regard to a focal point on central retinal cone photoreceptors¹. Several ocular structures including cornea, aqueous, lens, and vitreous, have refractive indices that contribute to the refraction of the incoming light rays; the optimal refractive ability of an eye to focus parallel light rays from an object at optical infinity (≥ 6

¹ The term focal point is often used to describe ocular refraction but it should be considered that the structures of the eye cause diffraction, light scatter, and aberrations; a precise focal point is not achieved and a point spread function exists (Forrester et al., 2008; Ginis, Perez, Bueno, & Artal, 2012).



meters) is termed emmetropia (Keirl, 2007). The emmetropic eye is considered, therefore, to have no refractive error. However, light rays are divergent at distances closer to the viewer than optical infinity, the convergence of such light rays to a focal point by emmetropes is afforded by ocular accommodation- a reflexive/voluntary process that increases the convexity of the crystalline lens (Glasser, 2011; Rabbetts & Mallen, 2007). Accommodation is inherent but related to the flexibility of the crystalline lens which declines with age- a noticeable deficit typically occurs at age 40-50 years in humans (Forrester et al., 2008; Rabbetts & Mallen, 2007)










Refractive error (ametropia) is common (Schor & Miller, 2011). Two main categories exist based on the location of the focal point relative to the retina: myopia- focal point is located anteriorly; hyperopia- focal point lies theoretically posterior to the retina (Corboy, 2003). Also, if unequal curvatures of the ocular refracting surfaces are present, two focal lines are created which are positioned at various locations juxtaposed to the retina (astigmatism) (Corboy, 2003). If the hyperopia is minimal and accommodative ability is present, hyperopes frequently self-correct their refractive error by accommodating to focus the incoming light rays from infinity (hyperopia is latent- no glasses are needed); in fact, when good visual acuity can be maintained, correction of hyperopia by prescription lenses may be rejected until accommodation declines with age (Milder & Rubin, 1991) (see Figure 3). Accommodation to focus light rays from infinity is not useful for myopes and may only be partially useful for astigmats. For all types of ametropia, if lenses are worn to focus light rays from infinity, accommodation will occur for near viewing relative to age.

Clinicians can measure ocular refractive errors objectively by using a retinoscope and lenses, subjectively by verbal responses to the placement of lenses, or by combining these techniques (Corboy, 2003; Franklin, 2007); the result of this process is commonly referred to as

a “refraction”. Accommodation may be temporarily suspended in young people by using eye drops (cycloplegic refraction) whereas adults are most frequently done without drops (“dry” manifest refraction). Manifest refraction (MR) is often preferred for adults as cycloplegia can induce spherical and chromatic aberrations and yield measurement of the full amount of latent hyperopia- possibly leading to a lens prescription that may not be tolerated (Franklin, 2007; Hiraoka et al., 2013; Milder & Rubin, 1991). Dry MR techniques often include initial relaxation of accommodation by introducing convex lenses to move the light rays anterior to the retina (creates pseudomyopia, a.k.a. “fogging”) (Corboy, 2003) (see Figure 3).

Figure 3: The Optics of Basic Refractive States and Fogging Technique. Illustration showing three basic refractive states of the eye and examples of the focal point for each type based on light rays entering the eye from infinity. An example of latent hyperopia is illustrated showing increased crystalline lens convexity indicating accommodation to focus light rays on the retina. Glasses correction is shown (see below). The fogging technique utilizes a plus lens (over basic glasses correction, if indicated) to focus light rays anterior to the retina (pseudomyopia) with resulting image degradation for all refractive states as shown.

-  — Symbolizes convex lens (plus lens; e.g. +1.00)
-  — Symbolizes concave lens (minus lens; e.g. - 1.00)

Basic Refractive States	Focal point Light Rays from Infinity	Self Correction (Latent Hyperopia Accommodation)	Glasses Correction	Fogging with Plus Lenses (Pseudomyopia)
Emmetropia		Not Applicable	Not Applicable	
Myopia		Not Applicable		
Hyperopia				

2.3 Experimental Image Degradation

Temporary image degradation is common in ophthalmic clinical practice and vision research. In clinical practice since the early 1900's, pharmacological image degradation of the dominant eye (defocus by use of atropine to prevent accommodation) has been used to treat amblyopia- a common developmental anomaly related to ocular dominance that results in reduced visual perception of the non-dominant eye (von Noorden & Campos, 2002). A variety of singular or combined techniques to degrade the image of the dominant eye (penalization) evolved using medication, lens modifications, or various filters (Loudon, 2007; von Noorden & Campos, 2002). Related to this historical context and this thesis are two methods of image degradation: optical defocus and Bangerter foils.

2.3.1 *Optical Defocus*

A common method of temporary optical defocus utilizes convex lenses that will refract the image light rays to a focal point anterior to the retina; sign convention for convex lenses is + (“plus lens”). Such anterior displacement of a point of focus that was previously on the retina will blur (“fog”) the retinal image inducing pseudomyopia. However, if the point of focus was theoretically posterior to the retina (hyperopia), anterior displacement of the focal point by the plus lens will correct or partially correct for the hyperopia (Corboy, 2003; Fannin & Grosvenor, 1996) (see Figure 3). The use of concave lenses (“minus lens” indicated by a minus sign) moves the focal point behind the retina and stimulates accommodations so this is less often used for optical defocus. The power of a lens to refract light rays is measured in lens diopters using the following formula:

$$\text{Lens Diopter} = 1 / \text{focal length in meters}$$

Fogging of the image for one or both eyes is used in clinical practice for assessment of refractive error (Corboy, 2003; Rabbetts & Mallen, 2007), testing visual acuity with nystagmus (Evans, Biglan, & Troost, 1981; von Noorden & Campos, 2002), and non-organic vision loss (Milder & Rubin, 1991; Moore et al., 2012). Optical defocus has been used in VEP research for many years (Anand et al., 2011; Berman & Seki, 1982; Bobak et al., 1987; Harter & White, 1968; Regan, 1973; Tyler et al., 1979).

2.3.2 Bangerter Foils

Due to the objections of some children to wearing an eye patch for the treatment of amblyopia, the practice of placing adhesive material on eyeglasses (over the lens of the dominant eye) was promoted in 1953 by Swiss ophthalmologist, Alfred Bangerter (Loudon, 2007). The technique was published in 1960 (as cited in Agervi, 2011) and the foils became commercially available as Bangerter Occlusion Foils (Ryser Optik, St. Gallen, Switzerland). To the present day, the Bangerter foil (BF) has been predominantly used for amblyopia treatment (Agervi et al., 2009; Iacobucci, Archer, Furr, Martonyi, & Del Monte, 2001) but they have also been used for a variety of clinical circumstances where monocular occlusion is beneficial (Galli, 2012; Malhotra, Then, Richards, & Cheek, 2010; Rutstein, 2012; Sagili, Malhotra, & Elston, 2005). The foils have also been utilized in vision research to study the effect of monocular image degradation on axial length (Read, Collins, & Sander, 2010), stereopsis (Odell, Hatt, Leske, Adams, & Holmes, 2009), and development of motor fusion (Abrams, Duncan, & McMurtrey, 2011). They have been used to simulate reduced vision in low vision research (Watson et al., 2012) and VEP research (Bach, Maurer, & Wolf, 2008; Chen Z. et al., 2014; Kurtenbach, Langrova, Messias, Zrenner, & Jagle, 2013; Mackay, Bradnam, Hamilton, Elliot, & Dutton, 2008; Watson et al., 2012).

A presumed advantage of the BFs for research and clinical applications is the availability of a variety of foil densities with manufacturer estimates of the resultant VA when viewing through the foils. However, some researchers have reported inconsistencies for the VA produced by the foils, either inequality with the manufacturer VA estimates or inconsistencies between foils labeled as the same density (Odell, Leske, Hatt, Adams, & Holmes, 2008; Repka & Gramatikov, 2006; Rutstein et al., 2011). With further examination using a subset of the foils (0.8, 0.6, 0.4, 0.3), investigators did detect a lack of ordinal change in microbubble density from 0.8 to 0.3 and the point spread and modulation transfer function was only obviously different with the 0.8 compared to the other filters that were quite similar (Perez, Archer, & Artal, 2010). This group also compared image degradation by foils to optical defocus and revealed that the foils produce a monotonic decrease in contrast and optical defocus is more prone to spurious resolution with phase shifts occurring that cause light and dark images that assist in object identification. Despite some inconsistencies, the BFs are in frequent use, with clinicians typically testing acuities with individual foils prior to administering them to patients.

2.4 Standard Visual Evoked Potential

Visual evoked potentials are routinely used for patients and for vision research to evaluate the transmission of visual information from the eye to the visual cortex via the optic nerve and visual pathway. The response of the visual cortex to a light or a pattern stimulus can be objectively recorded by time-locking the trigger for the visual stimulus and recording the resulting cortical response using surface scalp electrodes. Various electrode placements exist, but commonly one main active electrode is placed at the posterior skull midline, 2 cm above the inion (most obvious occipital bone protuberance) to align with the calcarine fissure (location-OZ); ground and reference electrodes are commonly placed at the earlobe and forehead

respectively (Odom et al., 2006; American Encephalographic Society, 1994). The recordings are differentially amplified (active versus reference electrodes) and analyzed for waveform morphology, amplitude, and implicit time with individual results compared to normative databases.

Visual evoked potentials are dependent on the cortical status of the subject and the integrity of the incoming visual information transmitted to the optic nerve from the retina. It is recommended that routine VEPs be done with natural, non-dilated pupils (Brigell, 2001; Odom et al., 2006). Recordings can be affected by unknown normal variants of occipital lobe orientation within the skull (Baseler, Sutter, Klein, & Carney, 1994; Fahle & Bach, 2006) or variations in skull conductivity (Wendel, Vaisanen, Seemann, Hyttinen, & Malmivuo, 2010). As well, the ocular media, refractive state, retinal health, and concentration of the subject need to be considered during interpretation of the results. The clarity of the recordings is also subject to the presence of muscle artefact (facial grimacing, head movements, etc.) that may create noise interference; the acceptable signal-to-noise ratios (SNR) are calculated from normative data bases. To promote comparable recordings from one center to another, the International Society for Clinical Electrophysiology of Vision (ISCEV) sets standards for VEP acquisition (Odom et al., 2006).

2.4.1 Flash Visual Evoked Potential

Establishment of the electroencephalogram as a clinical tool in neurology and the discovery of a human visual evoked potential in response to a flash of light has been attributed to the work of Hans Berger in the early 1900s (Brazier, 1986). Further work identified the disruption of the recording with the appearance of a pattern and the optimization of the response by using an opal glass bowl with a ring of lamps to produce diffuse and uniform flashes (Adrian

& Matthews, 1934); this apparatus was an early prototype of the Ganzfeld used currently for computer generated flash visual evoked potential (FVEP).

The FVEP yields the response of the visual cortex to light but not to pattern details. The test has specific uses, for example, if ocular media opacities are present (e.g. cataract, corneal scar) that prevent a view of ocular fundus, the FVEP bright flash is transmitted through ocular opacities and the transfer of this information to the visual cortex can be recorded; if activity is present, this is beneficial in determining if the opacity should be surgically removed. The test is not affected by uncorrected refractive errors or instability of fixation (Fahle & Bach, 2006) and therefore can be useful, as well, in cases of nystagmus (e.g. albinism) or with persons unable to attend to a fixed target.

The FVEP is affected by age with a gradual decrease in amplitude and shortening of implicit time from infancy to adulthood (Neveu, Jeffery, Burton, Sloper, & Holder, 2003; Schanel-Klitsch, Siegfried, & Kavanagh, 1987). Other than individual inconsistencies related to age, the FVEP varies between individuals for wave amplitude and implicit time, provides no visual acuity estimate, and can be noisy related to patient photosensitivity (Brigell, 2001; Fahle & Bach, 2006; Harding, 2006; Odom et al., 2006). Although the FVEP is appropriate to answer particular clinical questions, the PVEP was developed to address some of the inherent faults of the FVEP.

2.4.2 Pattern Visual Evoked Potential

The PVEP was developed in the 1960s with Cobb and colleagues, among others, measuring electroencephalograms using pattern stimuli such as black and white bars (Cobb, Morton, & Ettliger, 1967). Computer generated checkerboard patterns yield optimal responses but stimuli can also be vertical or horizontal stripes (sine or square wave); despite the stimulus

type, typical testing protocols utilize various spatial frequencies to tune patient responses (Brigell, 2001; Fahle & Bach, 2006; Odom et al., 2006). There is a gender effect with PVEP with females showing shorter implicit times and larger amplitudes and, as with the FVEP, there is an PVEP age effect with amplitudes that are larger in children and implicit times that reduce during early visual maturation then increase with aging at greater than ~ 60 yrs (Emmerson-Hanover, Shearer, Creel, & Dustman, 1994). As opposed to the FVEP, the PVEP shows a relationship to visual acuity, has a fairly consistent implicit time for individuals, and shows more consistent normative values between individuals (Brigell, 2001; Harding, 2006; Regan, 1973). However, PVEP amplitude is also more sensitive to fatigue, concentration, and variable fixation compared to the FVEP. The representation of the visual field also differs between the two tests as the FVEP represents a response from the complete visual field where as the PVEP represents approximately the central 10 degrees of visual field (see Section 2.1.1).

An important design factor for the PVEP is that the display should not be contaminated with a flash component. The common black and white checkerboard pattern alternates between black and white squares (pattern reversal) such that the mean luminance during acquisition remains constant (Brigell, 2001). Cathode ray tube monitors have been used for VEP testing in the 1900's to date. However, CRT technology is being phased out and replaced with liquid crystal display (LCD) monitors. Comparisons between the CRT and LCD monitors has revealed discrepancies in VEPs; the LCD monitor can produce delays in implicit times and a flash component related to a transient reduction in luminance during pattern reversal- particularly black squares changing to white (Fox, Barber, Keating, & Perkins, 2014; Karanjia, Brunet, & ten Hove, 2009; Matsumoto et al., 2013; Matsumoto et al., 2014; Nagy et al., 2011). Consideration of this artefact for PVEP acquisition going forward and either stimuli modification such as

reducing stimulus contrast (Matsumoto et al., 2013; Matsumoto et al., 2014), calculating a correction factor, or creating new normative data banks may need to be implemented.

Two main types of PVEP acquisition techniques are in routine use: transient and steady state. The early VEPs that were done related to electroencephalograms were a steady state type of recording with flashes at a rate of 8-12 per second (8-12 Hz) (Adrian & Matthews, 1934; Harding, 2006). The indication of steady state relates to the relatively high rates of stimulus presentation that creates a constant cortical response lacking a resting phase. The VEP can be analyzed from the resulting electroencephalogram by using Fourier analysis; the recording frequency will match the stimulus frequency (with harmonics) but will have a phase lag due to transmission time (Regan, 1989). The mathematical construct of the wave frequency to components of amplitude and phase (time) provides a result that would be similarly interpreted amongst examiners, and the SNR is easily obtained (Regan, 1989).

Transient PVEP recordings have stimulus presentation rates of approximately 3 Hz and requires a longer overall testing time, particularly when various spatial frequencies are evaluated. The transient PVEP allows easier identification of wave morphology and direct measurement of wave amplitude and implicit time; this tends to be the preferred over the steady state PVEP for most clinicians. However, the interpretation of the transient PVEP recordings may not be as straight forward as with the steady state PVEP and exact amplitude and implicit time values may vary between examiners (Brigell, 2001). Also, the SNR for the transient PVEP requires post recording calculations unlike the steady state SNR that is visible as recordings are taking place.

Other types of PVEP exist including: pattern onset- offset also known as pattern appearance (PappVEP). The PappVEP displays black and white checkerboard patterns that are flashed alternately with a blank gray screen equal in overall contrast; the sweep PVEP (provides

a rapid presentation of spatial frequencies) (see Section 2.5); the multifocal PVEP (provides PVEP responses from a wide range of the visual field (Hood, 2006). Of these three tests, the PappVEP is more often done as a routine clinical VEP test depending on local preferences (Odom et al., 2006) and has been adapted to provide a SVEP (Bach et al., 2008; Kurtenbach et al., 2013). The PappVEP can be useful in cases of unstable fixation (nystagmus) or shifting fixation as may occur in cases of feigning vision loss (Fahle & Bach, 2006; McBain, Robson, Hogg, & Holder, 2007); due to the difference in stimulus presentation, the PappVEP has a slightly different waveform.

2.5 Sweep Visual Evoked Potential

The SVEP is a pattern type of visual evoked potential test that displays multiple spatial frequencies over a short period of time and provides an amplitude response curve that can be used to extrapolate visual acuity estimates.

In early stages of SVEP development, recording of steady state PVEPS were done on individuals while various lens powers were systematically presented; the sensitivity of the PVEP amplitude to blur vs. clear retinal images were graphed and using evoked potentials for ocular refraction was proposed (Regan, 1973). Although this technique did not eventually replace retinoscopy, as this is fairly rapid in most clinical situations, the obvious utility of the steady state PVEP for quickly assessing poor vs. good vision was intriguing. Partially based on earlier work indicating that the relationship between logarithmic contrast values and VEP amplitudes was linear (Campbell & Maffei, 1970), a method of predicting visual acuity based on a linear function that extrapolated from the peak of the PVEP spatial frequency response curve to a zero response location on the X axis was used to predict the visible spatial frequency threshold

(Sokol, 1978). This extrapolation technique was eventually used for SVEP data to predict visual acuity (Tyler et al., 1979) (See Figure 4).

Figure 4: Historical Samples Showing Technique of Extrapolation to Zero Related to Contrast Sensitivity and Eventual Translation to SVEP. Adapted from: “Electrophysiological evidence for the existence of orientation and size detection in the human visual system” by F.W.Campbell and L. Maffei , 1970, in *Journal of Physiology* 207, p 638; “Measurement of infant visual acuity from pattern reversal evoked potentials” by S.Sokol, 1978, in *Vision Research* 18, pp. 34,35 with data replotted from “Independence of evoked potentials and apparent size” by D. Regan and W. Richards, 1971, in *Vision Research* 11, p 681; “ Rapid assessment of visual function: an electronic sweep technique for the pattern visual evoked potential” by C.W.Tyler et al., 1979, in *Investigative Ophthalmology and Visual Science* 18 (7), p. 707.

Year	Author	Technique	Data Sample
1970	Campbell	Extrapolate to Zero PVEP Amplitude vs. Contrast	
1971	Regan	PVEP Amplitude vs Check Size (100% Contrast)	 A. B.
1978	Sokol	A. Regan 1971 Data Replotted in Sokol 1978 B. Sokol Original Data 1978	
1978	Sokol	PVEP Amplitude vs. Check Size Infant Visual Development	 RD 3 mos. RD 5 mos.
1979	Tyler	SVEP Predictions vs. Psychophysical VA Various conditions	 RETINAL LOCATION CONTRAST LUMINANCE DEFOCUS

The steady state SVEP technology developed by Tyler and co-investigators at the Smith-Kettlewell Eye Research Institute in the 1970-1980's is the most often reported method in SVEP literature (Norcia & Tyler, 1985a, 1985b; Tyler et al., 1979). Their system known as DIVA (Digital Infant Visual Assessment, a.k.a. Digital Instrumentation for Visual Assessment) and updated modifications (NuDIVA, PowerDiva) became available to various researchers from approximately 1990 (Gottlob et al., 1990). Other steady state SVEP technology available at the time included the Enfant 4010 (Neuroscientific Corp., Farmindale, NY. (as cited in Katsumi et al. 1996) currently available as Enfant® (Diopsys Inc., Pine Brook, NJ.). Systems for SVEP were also devised for local use by other researchers (Hajek & Zrenner as cited in Kurtenbach et al., 2013) and (France & Ver Hoeve, 1994; Kurtenbach et al., 2013; Struck, Ver Hoeve, & France, 1996; Ver Hoeve, France, & Bousch, 1996). Recently and related to this thesis, prototypes of transient SVEP tests are being investigated (software by VERIS™, Electro-Diagnostic Imaging, Inc., San Francisco, CA.)

Over several decades, SVEP techniques were refined and progressed from normal populations to infants and persons otherwise unable to respond to acuity testing and eventually to predict visual acuity in disease states.

2.5.1 Early Design and Methodology

Tyler et al. (1979) plotted the results of steady state SVEP under various conditions. Their findings indicate that with visually normal subjects (adults), the best acuity estimate occurs with a linear change in spatial frequencies and in conditions of high luminance, high contrast (90%) and square wave stimuli. They promoted linear changes in spatial frequencies as this allowed a gradual approach to the visual acuity threshold level. Tyler et al. also presented stimuli

in the direction of low to high spatial frequencies due to a slight shift related to hysteresis (the effect of previous evoked potentials on current potentials) when moving in the opposite direction as noted by Regan (1977).

The early report by Tyler et al. (1979) also revealed the SVEP was responsive to increased levels of central masking and optical blur or reductions in either contrast or luminance, but all showed high linear correlation coefficients ($r = 0.87-0.99$); however, the results of optical blur was singled out as a much more gradual slope than the other conditions (see Figure 5). The SVEP was sensitive to optical blurring of greater than .25 D and success using the SVEP for refraction in children as young as 6 months of age was mentioned. The test was also useful in an example of apparent feigning of vision loss. However, due to nonhomogeneous SVEP responses across the spatial frequency spectrum in various individuals or with ocular pathology, they cautioned that the SVEP technique may not be applicable in all circumstances. Due to this caution, Tyler et al. promoted interocular comparisons when possible and the use of log changes in spatial frequencies to give equal weight throughout the response curve to view nonhomogeneous results- to the detriment of the linear change in spatial frequencies that allowed more weight for VA predictions by approaching threshold more gradually.

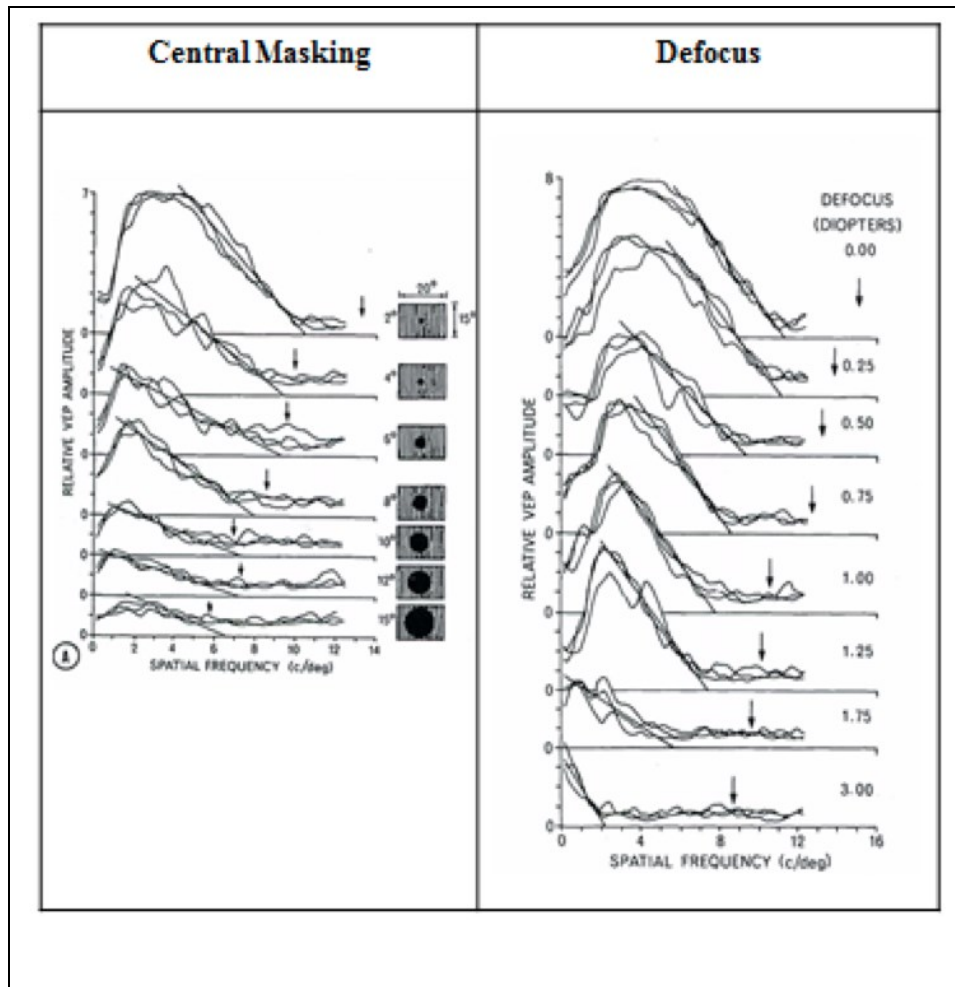


Figure 5: Historical Samples of SVEP Tracings Using Central Masking and Optical Defocus. Arrows indicate psychophysical measurement of visual acuity and linear regression extrapolation to the x-axis indicates the SVEP predicted acuity. Central masking example shows the sensitivity of the SVEP to the central visual field with decline of the SVEP responses with increased central mask size. However, at many locations the SVEP extrapolation is close to the psychophysical visual acuity. The defocus sample shows substantial difference between the SVEP predicted acuity and the psychophysical visual acuity. Adapted from “Rapid assessment of visual function: an electronic sweep technique for the pattern visual evoked potential” by C.W. Tyler et al., 1979, *Investigative Ophthalmology and Visual Science*, 18 (7), pp.706, 708.

2.5.2 *Infant Visual Acuity and Visual Development*

Moving forward with Tyler's SVEP technology, as described above with slight variations, infant visual acuity and early visual development was explored. Norcia & Tyler (1985b) reported on SVEPs performed on 197 infants from 1-53 weeks of age with results indicating visual development of SVEP acuities from 4.5 c/d to 20 c/d at age 1 month to age 8-13 months respectively; infants could reach adult SVEP acuity levels at approximately age 8 months. This was quite agreeable with Sokol (1978) who predicted 6/6 acuity levels with steady state PVEP at age 6 month (see Section 2.2.1) (see Figure 4). Norcia & Tyler (1985b) added a SNR calculation (accepted 3:1 ratio) that was visible on the recording as well as an active monitor of the response phase. Both of these assisted in obtaining reliable recordings and consistency in marking the linear regression line; the phase was typically constant at the peak amplitude of the response with a phase lag occurring when visual threshold was approached. The chosen SVEP recordings included either a single recording or vector averages. Challenges occurred when multiple peaks were visible in the recording- at which time the phase monitor contributed to the final analysis.

Further reports on the test/retest reliability with the Norcia-Tyler SVEP was calculated for 25 infants with results showing that the best predicted visual acuities for individuals (either single sweeps or averages) were reliable within ± 0.38 octaves at 95% confidence; however, the range of acuities for individuals was up to 2 octaves (1 octave change = doubling of the spatial frequency) (Norcia & Tyler, 1985a).

2.5.3 *Abnormal ocular or cortical conditions*

Following the encouraging reports of SVEPs in normal infants, the research effort moved in the direction of predicting VA in ocular or cortical pathologies and comparing the VA predictions to behavioral resolution acuity or recognition acuity.

Infant SVEP testing was done on normal and abnormal preterm infants (suspects for cortical blindness); results showed that normal preterm infants had SVEP results that did not significantly differ from a normal cohort of age-matched infants, but obviously abnormal SVEP were detected in the suspects for cortical blindness (Norcia, Tyler, Picuch, Clyman, & Grobstein, 1987).

Gottlob et al. (1990) used the Norcia and Tyler SVEP technology (DIVA) to test a variety of visual disorders in children (3 weeks- 11 years old), often using the best single sweep for analysis and log changes in spatial frequencies in cases of low vision. Results indicated optotype testing, when possible, correlated well with SVEP predictions; however, a trend for SVEP to underestimate acuity in well seeing patients and overestimate acuity in poorly seeing patients occurred; reliability was also questioned in amblyopia, optic nerve and neurological disorders. The concern about SVEP with optic nerve conditions was echoed by Arai et al.(1997) who used the Infant 4010 to assess a variety of ocular disorders in 100 patients (age: 7-90 yrs.).

Research using SVEP has involved patients with various syndromes, developmental delays, or cortical impairments. With Down syndrome, the SVEP predictions (compared to a variety of tests: Teller cards, picture tests, logMAR letters) were found to underestimate VA starting at approximately age 2 yrs.; however, all testing formats revealed an overall reduced acuity in Down syndrome compared to a normal cohort (John, Bromham, Woodhouse, & Candy, 2004). With spastic cerebral palsy patients (age 6 months to 4 yrs. old), abnormal SVEPs correlated well with the degree of motor deficit (da Costa, Salomao, Berezovsky, de Haro, &

Ventura, 2004). Another group of children with cerebral palsy and periventricular damage without retinopathy (age 9 months to 12 yrs.) showed a good relationship between SVEP and grating acuity cards but relatively better acuity values with the grating cards (Tinelli et al., 2008).

Other than comparing predicted VA levels, comparisons have been made between SVEP response curves in various populations. An insight into cortical vision impairment using SVEP was offered by investigators who found that affected children (age 7 months to 4 yrs.) showed improved responses to SVEP under low luminance- perhaps related to abnormal light modulation capabilities in these children (Good & Hou, 2006). As well, the SVEP response curves of very low birth weight preterm infants with no cerebral or retinal pathology showed reduced sensitivity for spatial, contrast and Vernier acuity compared to an age-matched group of term infants (Hou et al., 2011). In autism spectrum disorder, despite equal SVEP predicted acuities, the SVEP response curves differed in affected children compared to neurotypical children (age 5 to 7 years), specifically for low spatial frequency stimuli localizing to the right occipital lobe; these results aligned with other right hemisphere anomalies found in this disorder (Pei, Baldassi, & Norcia, 2014).

2.5.4 Experimental Image Degradation

As previously mentioned, Tyler et al. (1979) noted that the SVEP response curve differed in optical defocus compared to a variety of other stimulus conditions (see Section 2.5.1). As optical blur may occur during routine clinical electrophysiology related to uncorrected refractive errors or over accommodation during testing, the effect of optical blur required further investigation. In a SVEP study involving visually normal adults and the Infant 4010 system, the SVEP predictions tended to underestimate acuity with mild optical defocus (+.50 & +1.00 D.; ~ 6/12 ETDRS) and tended to overestimate acuity with more defocus (> +1.50 D.; < 6/19 ETDRS);

two individuals revealed approximately 1.5 to 2.0 octaves difference between the SVEP predicted vision and ETDRS in conditions of reduced vision ($\sim 6/24$ to $6/45$ ETDRS) (Katsumi et al., 1996).

Bangerter foils have also been used in two SVEP studies (pattern onset stimuli) to provide comparison between SVEP predicted acuity and recognition acuity under conditions of visual obscuration. The first study included adults (visually normal with BFs and subset with ocular pathology) and a steady state protocol that included an automated heuristic (practical solution) algorithm to create the regression line for acuity prediction (Bach et al., 2008). The automated system promoted by Bach and co-investigators avoided an inconsistency (“notch” in mid to high spatial frequencies) that was present in many SVEP response curves; their system was able to predict the recognition acuity within ± 0.3 logMAR. Using a slightly different automated SVEP design with only visually normal adults, other investigators found that 80 % of their SVEP predictions were within ± 0.2 logMAR of the recognition acuity; they found no obvious benefit to using the algorithm promoted by Bach et al. in 2008 (Kurtenbach et al., 2013).

2.5.5 Considerations: Technology and Acuity Determination

When reviewing literature involving SVEP research since the 1970s it is important to consider the changes in stimulus display and acquisition technology since that time. During the early years of investigations, the limited resolution afforded by television monitors or early computer monitors could have caused raster effects or aliasing with attempts to create high spatial frequency stimuli (Bobak et al., 1987; Katsumi et al., 1996); ameliorating this by increasing the viewing distance would reduce stimulus luminance and attention of the subject. Display resolution has improved (e.g. 1920 X 1080 pixels) and future consideration now relates

to the change from LCD to CRT monitors and the related flash effect and increase in implicit time seen with PVEP (see Section 2.4.2).

As with any new technique, changes have occurred in the criterion and methods for steady state SVEP prediction of acuity since the initial proposals. Most of the analysis has involved the commonly used DIVA system. Initial methods included a linear progression of spatial frequencies to provide a more gradual approach and the method of adjustment with the average of three settings to determine the final threshold; noise level was documented on recordings but no phase recording was visible and examples show a SNR of less than 1 (Tyler et al., 1979). Investigations by Norcia and Tyler with newborns to age 1 year, added a simultaneous phase recording that was visible in the output and provided a guide as to when threshold was being approached (phase lag occurred); criteria included a peak response being three times the average response amplitude and a constant phase (Norcia & Tyler, 1985b). Another study by the same authors regarding SVEP measurement error revealed that for individual infants, the recordings were precise and taking the best estimate was as good as the vector average; however, predictions related to response curve with multiple peaks were problematic (Norcia & Tyler, 1985a).

Using the DIVA system with children, Gottlob et al. (1990) corroborated with Norcia and Tyler regarding the validity of the best single sweep rather than the vector average; however, with an infant study using NuDIVA, results indicated that an average of several sweeps was more reliable (Lauritzen, Jorgensen, & Michaelsen, 2004). Further SVEP testing using the Enfant system with adults found the repeatability good for both single sweeps and sweep averages (Ridder, Tong, & Floresca, 2012) and there was good agreement between the Enfant and PowerDiva systems (Ridder, Waite, & Melton, 2014).

In attempts to standardize SVEP methods for prediction of visual acuity and with no available ISCEV standards for these tests, various changes in criteria continue to be investigated as well as tools to automate the determination of acuity. Testing of various criteria have been studied using PowerDiva with results that indicated a reduced SNR of ≥ 1 provided a more accurate prediction of logMAR visual acuity than the routine criteria of ≥ 3 as is chosen by the PowerDiva software (Yadav, Almoqbel, Head, Irving, & Leat, 2009). A heuristic algorithm for predicting visual acuity has been proposed (Bach et al., 2008) (see Section 2.4.4). Automated calculations became available with the NuDIVA system, but some researchers advised manual scrutiny of the results (Lauritzen et al., 2004). However more recently, two automated systems, *Enfant* and *PowerDiva* have been found to predict agreeable visual acuities (limit of agreement-0.23 logMAR) with visually normal adults (Ridder et al., 2014). However, it is still unknown how automated predictions will handle abnormal SVEP response curves (markedly reduced amplitudes or multiple peaks); such challenges are more commonly seen in cases of reduced VA or with cortical/ocular anomalies either alone or in combination. Wavelet analysis may be helpful in the analysis of such complex waveforms.

2.6 M-sequence and Visual Evoked Potential

2.6.1 Visual System Nonlinearities and the M-Sequence

Although experimental testing of the human visual system may show linear outputs, both the system as a whole and various components show substantial nonlinearity (Campbell & Maffei, 1970; Howard & Rogers, 1995; Pinter & Nabet (Eds), 1992; Sokol, 1978; Tyler et al., 1979; Victor, 1992). The presence of nonlinearity can be detected in cellular responses to stimuli (e.g. ceiling effects, specialization, inhibitory or facilitatory interactions) and psychophysical thresholds can be influenced by adaptation or learning (Howard & Rogers, 1995; Schiffman,

1976; Underwood, 1966). Nonlinearities related to hysteresis can occur and can be particularly problematic in visual electrophysiology (Howard & Rogers, 1995; Regan, 1977; Sutter, 1992). Although stochastic (randomized) sampling is a highly recommended research practice (M. Bland, 2000; Polit, 2008; Underwood, 1966), to address electrophysiological hysteresis and other factors, a deterministic computerized approach using pseudorandomized binary code m-sequences (maximal length sequence) was developed by Erich Sutter and co-workers (Sutter, 1991; Sutter & Tran, 1992; Sutter & Vaegan, 1990). By using a fast m-transform, a rapid analysis of responses from multiple small retinal locations could be detected by cross correlation of visual white noise and the m-sequence generated stimuli; the technique afforded an ability to decompose and assess multiple orders of the response and acquire an orthogonal (independent) data set as well as access to kernels (hysteresis related responses) (Sutter, 1991, 1992; Sutter & Tran, 1992).

2.6.2 *VERIS™ System*

The m-sequence related technology (see Section 2.6.1) was further developed by Erich Sutter and Duong Tran at the Smith Kettlewell Eye Research Institute, and eventually became commercially available as the VERIS™ (Visual Evoked Response Imaging System) through EDI (Electro-Diagnostic Imaging, Inc., San Francisco). The VERIS™ m-sequence related technology allowed recordings of multifocal electroretinograms that afforded previously unavailable detailed information about retinal topography and related ocular disease; the VERIS™ multifocal visual evoked potential, although not in current widespread clinical use, is showing potential for clinical application (Herbik, Geringswald, Thieme, Pollmann, & Hoffmann, 2014; Jampel et al., 2011; Mendoza-Santiesteban et al., 2010; Perez-Rico et al., 2014; Wu, Ayton, Guymer, & Luu, 2014; B. Young, Eggenberger, & Kaufman, 2012). The VERIS™

software can also be used for routine visual electrophysiology testing including PVEP, FVEP, flash and pattern electroretinograms, and electro-oculograms. The VERIS™ system provides versatility in both recording and analysis settings; m-sequence modifications and a recent version of a transient SVEP were utilized in this thesis.

2.7 Wavelet Analysis

Wavelet analysis (WA) has been actively investigated as a method for signal analysis for approximately the last 30 years (Aboufadel & Schlicker, 1999; Hubbard, 1996; Walker, 2008), although wavelets in mathematics were mentioned as early as 1909 by Haar as cited in Aboufadel & Schlicker, 1999). The wavelet concept was first proposed by Grossman and Morlet (1984) but improved comprehension and the term wavelet became more widespread after the work of Stephane Mallat (Hubbard, 1996; Mallat, 1987, 1989). The Fourier analysis (Fourier, 1822) was the main focus of development in the 1800's to recent times and is still widely used in electrical engineering, communication, and biotechnology (Hubbard, 1996; James, 2002; Wolfe, Kluender, & Levi, 2009), as well as for steady state PVEP and SVEP (see Sections 2.4.2 and 2.5). The development of WA has been encouraged by advances and the widespread availability of computer technology and, related to vision, computational visual investigations (Mallot, 2000; Marr, 1982).

Wavelet analysis appears to offer some advantages over Fourier analysis under certain circumstances. The Fourier transform allows the decomposition of electrical signals into a frequency spectrum related to sine and cosine functions, this type of analysis is most useful for linear data and stationary signals (frequencies repeat over time e.g. sound waves, x-rays, visible light), whereas for the analysis of nonstationary signals (frequencies vary over time e.g. biological waveforms including evoked potentials that require exact latency calculations) or

nonlinear data, clinicians may prefer more information related to timing (Hubbard, 1996; Polikar, 2006). For example, when comparing steady state and transient VEPs, the Fourier analyzed steady state VEPs provide an optimal view of frequency responses but only an indirect evaluation of time (phase assessment) compared to typically obvious latency calculations available with the transient VEP (see Sections 2.4.2 and 2.5).

Eventual modification to the Fourier transform to afford improved analysis of time and frequency yielded the short-term Fourier transform. This method allowed analysis of segments or windows of nonstationary signals- essentially finding stationary segments within the nonstationary signal (Polikar, 2006). However, inherent to general signal analysis, is improved resolution of high frequency components in the time domain and low frequency components in the frequency domain, consequently small short-term segments could show optimal high frequency but inadequate low frequency information for complex nonstationary signals (Hubbard, 1996; Polikar, 2006). Wavelet analysis has attempted to address this deficiency by providing broad simultaneous analysis of both time and frequency components of electrical signals (Hubbard, 1996; Misiti, Misiti, Oppenheim, & Poggi, 2010).

A wavelet is a series of oscillations that start and end at zero amplitude (“finite energy”), show a variety of fluctuations between the endpoints, and have an integral of zero (the positive and negative components are equal- “admissibility condition”) (Hubbard, 1996; Sadowsky, 1996; Walker, 2008; R. K. Young, 1993). Families of wavelets exist with the many prototypes (“mother” wavelets) named after the developers or based on appearance (Haar, Morlet, Daubechies, symlet, Mexican hat). The basics of wavelet analysis include the decomposition of a waveform by matching or fitting wavelet types to the waveform in question; this is usually done with computer software such as Wavelet Toolbox™ (The Mathworks, Inc., Natick MA). The

wavelet can be compressed or dilated (“scale” variations) to match the frequencies of the signal waveform and, in regards to timing, a discrete area of the signal can be chosen for analysis (discrete wavelet transform) or a continuous time analysis can be done (continuous wavelet transform) (Hubbard, 1996; Misiti et al., 2010). The transforms generate coefficients related to the correlation between the wavelet and signal waveform and these coefficients can be used to analyze, remove noise, or reconstruct the waveform. A scalogram can be created (color coded related to coefficients) that provides a visual model of the transform and multiresolution techniques afford an ability to sequentially examine the frequency characteristics of the wavelet analysis (Hubbard, 1996; Misiti et al., 2010) (see Figure 6).

Although WA provides simultaneous time-frequency characteristics that may show an advantage in some circumstances compared to Fourier analysis, inherent limits to the technique do exist² (small wavelets relate more so to time, large wavelets relate more so to frequency), and the technique is still in early stages of development. Diverse applications are being investigated (Hubbard, 1996; Siddiqi et al., 2014; Walker, 2008) including vision science where WA automated analysis of electrophysiological waveforms may ultimately prove very useful (Barraco, Persano Adorno, Brai, & Tranchina, 2014; Thie, Sriram, Klistorner, & Graham, 2012).

² The Heisenberg Uncertainty Principle related to particle position and momentum being a probability rather than an exact measurement also applies to signal analysis. Precision in time will always have some variability in frequency and vice versa (Hubbard, 1996; Polikar, 2006).

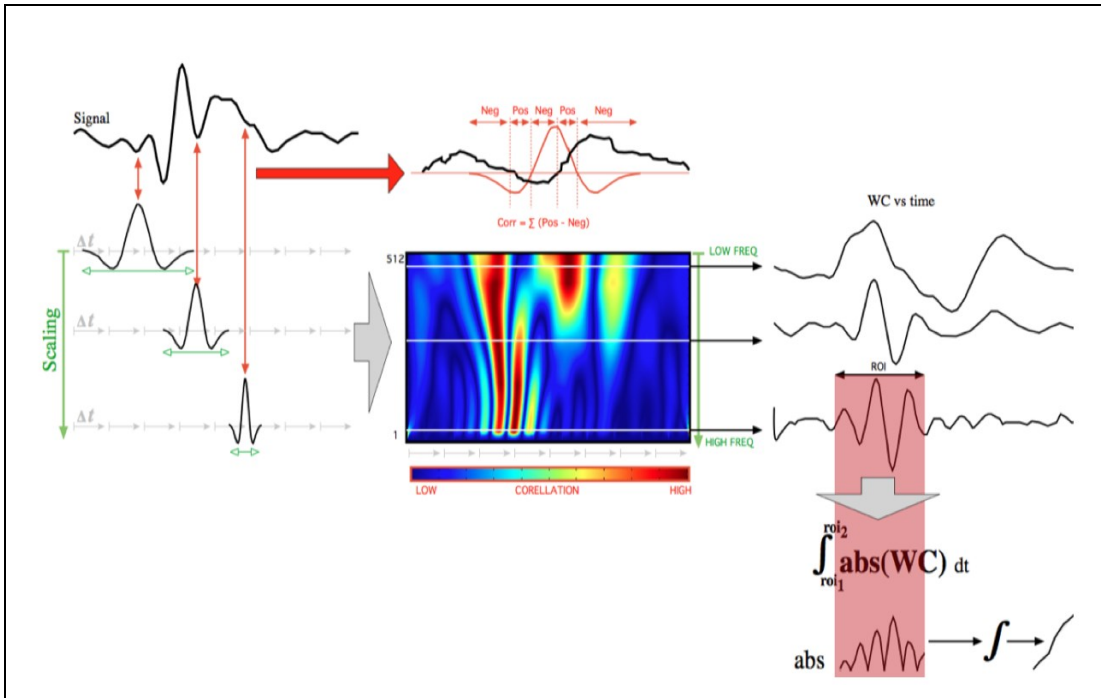


Figure 6: Wavelet Analysis Process Showing a Signal Waveform that can be Matched using Wavelets that Vary in Frequency. The correlation coefficients that are generated can be summarized in color coded scalograms that can be used to quantify signal characteristics.

CHAPTER 3: METHODS

3.1 Preliminary Actions

The main focus of this project was to explore the SVEP test and implement the SVEP for our clinical population. Although our laboratory uses transient visual evoked potentials, we initially considered obtaining and testing the steady state SVEP technology that has prevailed in the literature since the SVEP was established (DIVA). Certain barriers emerged that required forethought and preliminary actions:

- 1) The steady state SVEP system (DIVA) was found not to be commercially available and attempts to contact the developers were not successful.
- 2) Correspondence to other researchers revealed that they either obtained the DIVA software via direct contact with the developers or, if that was problematic, they devised their own system.
- 3) Correspondence with EDI (Electro-Diagnostic Imaging, Inc.), the designers of the VERIS™ system used in our clinic, resulted in permission for us to study their new transient SVEP software that was under development.
- 4) Use of the EDI transient SVEP required technical modifications:
 - A. The SVEP test required a high resolution LCD monitor. We detected a flash artefact with the new LCD monitor that needed to be removed prior to proceeding with the SVEP; we resolved the artefact with a novel m-sequence modification.
 - B. The high resolution LCD monitor showed aliasing with high spatial frequency stimuli; software modifications were needed prior to SVEP trials.

3.2 Overview of Study Design

In order to evaluate the potential of the new transient SVEP technique to predict ETDRS visual acuity, we designed a prospective, quantitative and quasi-experimental study using visually normal adult participants who underwent trials using two types of simulated vision loss by image degradation (defocus by plus lenses and image obscuration by Bangerter foils).

After insuring eligibility, informed consent was obtained prior to gathering baseline orthoptic data. Pattern visual evoked potentials were recorded to detect and resolve a technical issue related to computer monitor type used for stimulus display; modifications were applied prior to running SVEP trials (see Figure 7 and Appendix A). Participants were randomly assigned to undergo either image degradation by plus lenses or by Bangerter foils (see Section 3.6). However as individual responses to each type of image degradation was of interest, several individuals agreed to undergo testing with both.

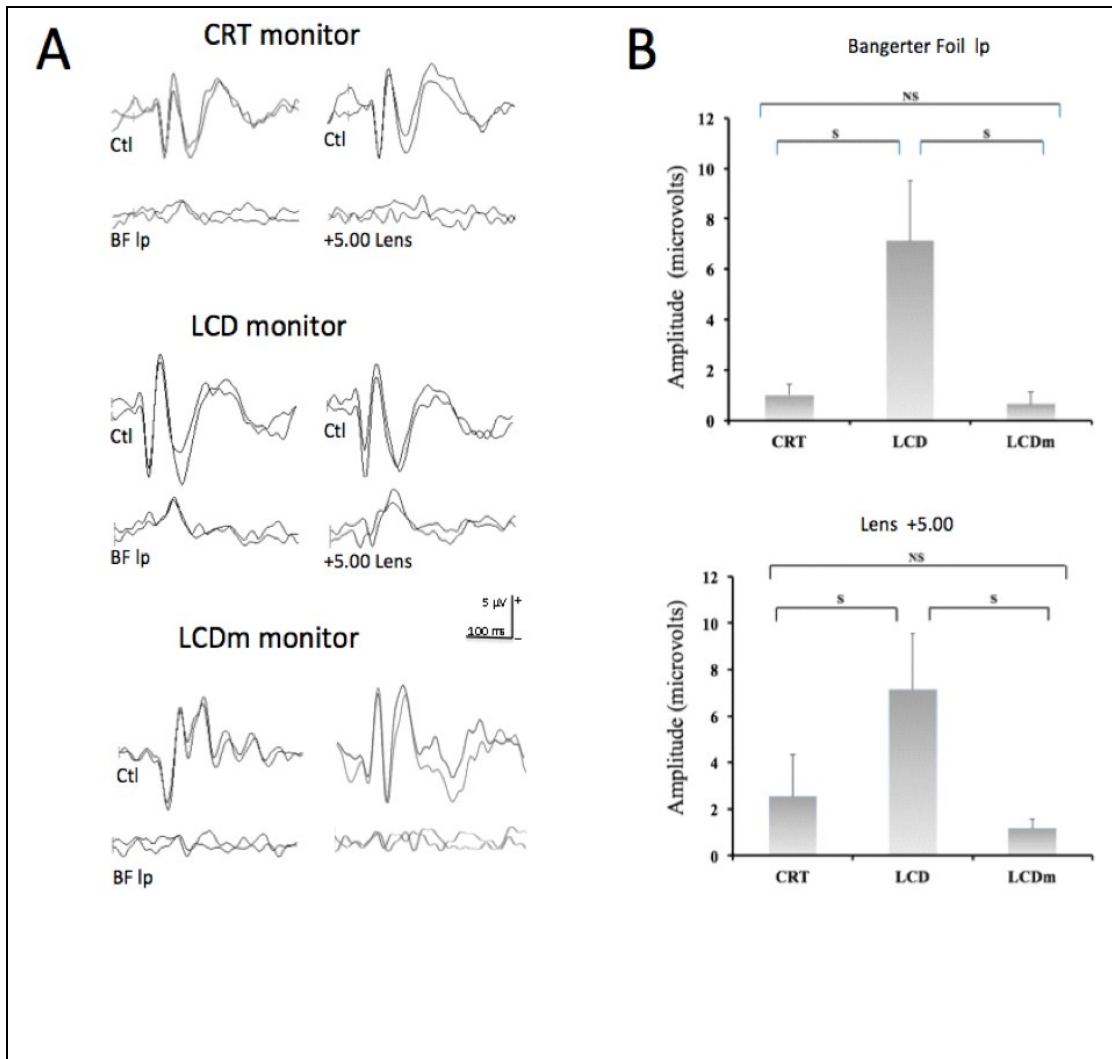


Figure 7: Effect of Monitor Type and Modifications on Pattern Visual Evoked Potentials. A: Samples of control recordings and resulting waveforms using Bangerter foil (light perception) and +5.00 lens. LCD monitor shows persistent defined waveforms despite image obscuration (a flash effect) compared to the CRT and LCDm monitor conditions. LCD= liquid crystal display monitor; CRT= cathode ray tube monitor; LCDm= liquid crystal display monitor with modified m-sequence; Ctrl= control trial; BF Ip = light perception Bangerter filter. B: Bar histogram showing amplitude differences under the two conditions (one-way ANOVA, BF Ip- $F(2,12) = 32.13, p = .000$; +5.00- $F(2,12) = 15.99, p = .000$. Bonferroni post hoc for both LP and +5.00 lens: LCD vs. both CRT and LCDm are significantly different ($p = .000$) and CRT vs. LCDm are not significantly different (LP: $p = 1.000$; +5.00: $p = .689$). NS= not significant; S= significant.

The data from each participant was then analyzed manually by an expert (considered gold standard) and, in parallel, submitted to an in-house wavelet analysis paradigm developed exclusively for that purpose (see Figure 8). The results from those two analyses were compared to determine the viability of automated WA versus manual assessment by the Expert.

The concatenated data from all the participants (population-averaged data) resulted in a series of SVEP response curves corresponding to each of the image degradation conditions (6 lenses plus two controls, or 8 Bangerter foils plus two controls). These were analyzed using the standard model of previous studies (linear regression) as well as with five additional innovative analysis models proposed by our study. As eventual clinical results of the SVEP will need to be discerned on an individual basis, equations derived from population-averaged results with the 6 analysis models (linear regressions between the SVEP and ETDRS visual acuity) were applied to individual data. A detailed diagram of this protocol can be found in Figure 8.

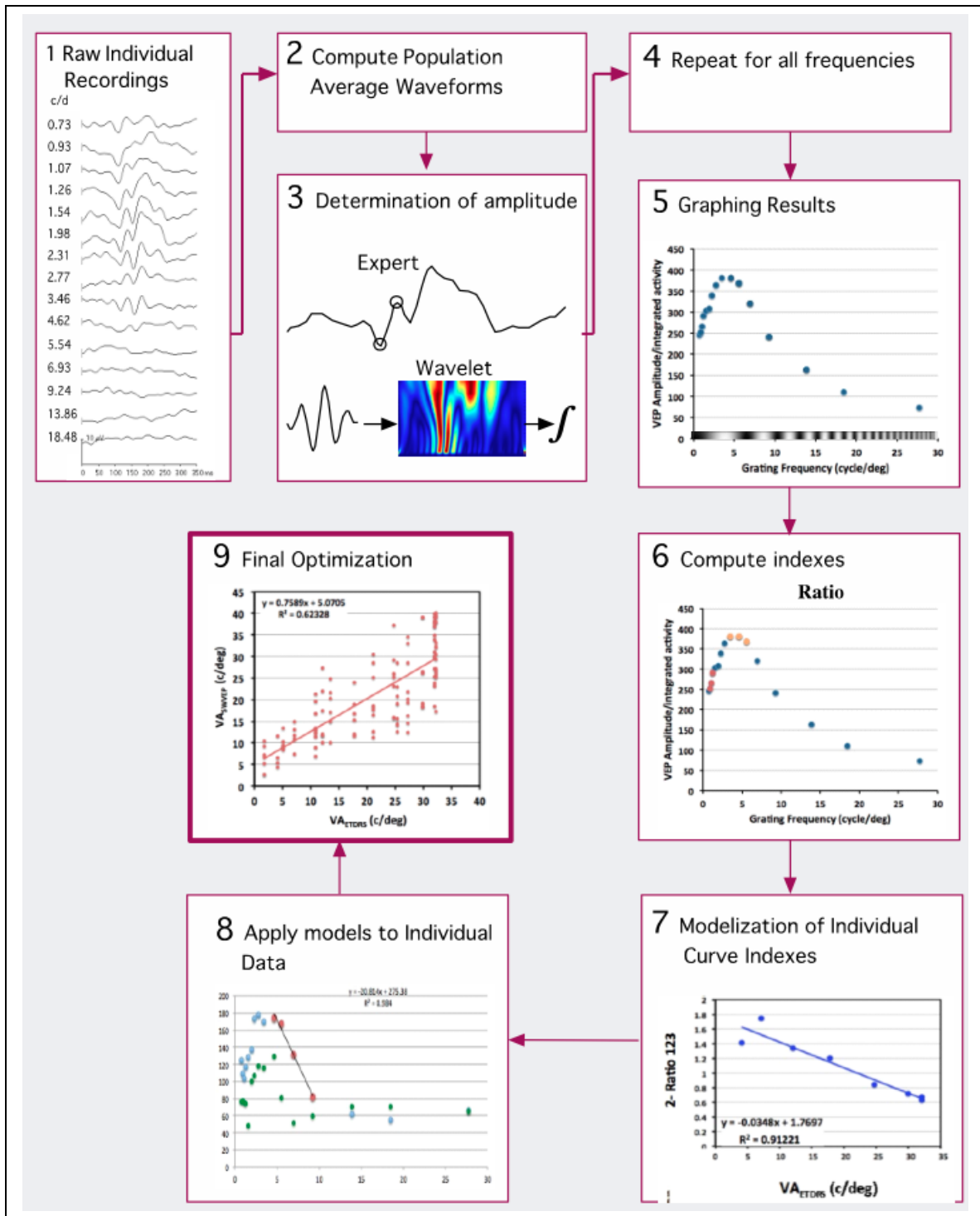


Figure 8: Flow Chart of SVEP Study Design.

3.3 Ethical Considerations

3.3.1 Research Ethics Board Approval

According to the guidelines regarding research at the IWK Health Centre, an application to the IWK Health Centre Research Ethics Board was submitted and subsequently approved.

3.3.2 Risk/Benefit Analysis

The VEP test is used routinely for patient evaluation at the IWK Health Centre Visual Electrodiagnostic Laboratory and is rarely, if ever, associated with harm to patients. However, the potential risks as well as clarification about benefits of participating in the study were discussed with the participants.

Potential risks included: 1) allergy to the skin preparatory compounds or to occlusive eye patches; 2) a slight skin irritation at the location of the electrode; 3) test fatigue. Regarding these risks, participants were advised that a staff ophthalmologist or the ophthalmology resident on-call would be contacted if there was a concern about an apparent allergic reactions or skin irritation. If participants appeared to be tired, or at their request, a break from testing was given; testing was reinitiated if the participant was agreeable. Participants were assured that if they had any concerns, testing could be discontinued at any time. To assure participant confidentiality, all study information was stored and protected as per the IWK Research Ethics Board guidelines.

Regarding benefits, the participants were informed that the study was purely investigational and would not provide benefits to individual participants.

During the study, no issues arose regarding risks or benefits.

3.3.3 Informed Consent

The risks, benefits and study procedures were discussed with the participants. They were given information and consent forms and, if agreeable, provided written informed consent. The participants were advised that they may be requested to return for optional repeat testing

sessions. If they agreed to return for further testing, at that time, the basic testing procedures were reviewed and continued consent was assured.

3.4 Sample

3.4.1 Recruitment Procedures

Advertisements were posted at the Eye Clinic of the IWK Health Centre and patients or family members accompanying patients could become aware of the study. Students and staff at the IWK Eye Clinic became aware of the study during routine staff/research meetings and their acquaintances through posters or casual conversation. As fellow vision researchers became aware of the study, they offered to participate and returned for repeat sessions if they were agreeable. Potential participants were contacted by Joan Parkinson via phone or email.

3.4.2 Inclusion and Exclusion Criteria

Inclusion Criteria:

- Between the age of 18-60 years
- Good visual acuity (6/7.5 or better)
- Alert and cooperative with good attention span

Exclusion Criteria:

- Ocular disease
- High refractive errors (spherical corrective lenses of greater than ± 8.00 diopters and/or astigmatic correction of greater than ± 4.00 diopters).
- Neurological disease, developmental delay, poor cooperation or reduced attention span including extreme fatigue or recent use of sedative drugs
- Positive family history of optic atrophy
- Presence of nystagmus

- Known allergy to skin preparation compounds used for VEP testing, electrode paste, occlusive eye patches.
- Inability to communicate in English
- Lack of consent

Individuals were not excluded based on religion, cultural background, or physical disability as long as they had the capacity to perform VEP/SVEP testing. The age range reflected our interest in mature visual systems as developmental changes can still occur in early teens in humans (Daw, 2006), PVEP measurements are most stable between ages 20-50 yrs. (Emmerson-Hanover et al., 1994) and adults over the age of 60 were excluded related to declines in visual function occurring with increasing age (Dagnelie, 2013; Tielsch, 2000). Individuals with high power corrective lenses were excluded as these lenses may cause a distortion of the image or can be associated with an underlying ocular anomaly (Appel & Brilliant, 1999; Hersh, Spinell, & Astorino, 1999).

3.4.3 Study Population

To fully investigate the new SVEP test, modifications in software, hardware, and acquisition protocols were required. We ran some early trials involving over 25 recording sessions with the principle investigators and volunteer visual research associates. It was apparent that initial testing of the system would require a small number of participants with repeated testing on a variety of stimulus conditions. A total of 13 participants (age range: 21-59 yrs.; 7 males) met the inclusion and exclusion criteria as outlined above (see Table 1). In this report we will highlight the most informative experimental findings that occurred post system modifications and refinement of analysis techniques.

Table 1: Participant Characteristics and Test Summary

ID	Age (yr)	Sex	Test Eye	VA Dom	Rx Dom	DM	PVEP	SVEP	Plus Lens	BF
01	55	M	R/B	-.10	-4.75+1.0	Plano	x	x	x	x
02	58	F	L/B	-.10	+3.75+.75	Plano	x	x	x	x
03	44	M	B	-.20	None	+0.50	x	x	x	x
04	26	F	L/B	-.14	None	+0.50	x	x	x	x
05	25	M	B	-.14	-1.50	Plano		x		
06	59	M	R/B	-.06	+1.25	Plano	x	x	x	x
07	23	M	L	-.10	None	+1.00	x		x	x
08	23	F	R	-.06	-0.75	Plano	x	x	x	x
09	56	F	R	+0.04	None	+0.50	x	x	x	x
10	21	M	R	-.08	None	+0.75	x	x	x	x
11	28	F	R	-.08	-7.00	Plano	x		x	x
12	25	F	R	-.14	None	Plano	x			x
13	21	M	L	-.10	-2.00	Plano		x	x	x

ID = Participant identification number; R = Right eye; L = Left eye; B = Both eyes open (not included in analyses); VA= ETDRS visual acuity; Rx = glasses prescription; Dom = Dominant eye; DM = Dry manifest refraction; M= male; F= Female; PVEP = Pattern visual evoked potential; SVEP = Sweep visual evoked potential; BF = image degradation testing with Bangerter foils; Plus Lens = image degradation testing with plus lenses.

3.4.4 *Sample Size Calculation*

No laboratory normative data base is yet available for transient SVEP sample size estimates; however, sample sizes with similar studies using a variety of SVEP methods have been relatively small: 6-10 (Yadav et al., 2009), 10 (Kurtenbach et al., 2013), 12 (F. M. Almoqbel, Yadav, Leat, Head, & Irving, 2011).

3.5 Preliminary Procedures- General

3.5.1 *Orthoptic Evaluation*

After insuring baseline eligibility and obtaining informed consent, orthoptic data was obtained (further ophthalmic history, distance VA measurements of both eyes and lensometry) to assure that the ophthalmic inclusion/exclusion criteria were met. High contrast VA was measured at 3 m using a retro- illuminated ETDRS illuminator cabinet™ and original series ETDRS charts (Precision Vision, LaSalle Ill.). An ETDRS –Fast method was used to determine VA (see Section 2.2.1).

When ophthalmic inclusion was confirmed, further testing was undertaken. The dominant eye was determined by: 1) asking the participant to point to a distant object; 2) alternating occlusion of one eye at a time to determine the dominant eye as being the “aiming eye”- the eye aligned with the distant object; 3) repeating this procedure to test for consistency. If no clear ocular dominance was present, the eye with the better acuity was chosen as the dominant eye. Following this, both eyes were fogged with +1.50 spherical lenses (working distance for retinoscopy, see Section 2.2.3), the participant viewed a large optotype at the end of the examining lane (3 m) and the dominant eye was checked for latent hyperopia or uncorrected refractive error by retinoscopy. In our group of 13 participants, the right eye was dominant in 9 (70%) and VA of the dominant eyes ranged from -0.14 to +0.04 logMAR. Refractive corrections

were worn by 7 (54%) with minimal interocular difference and over refraction of the dominant eyes in these cases was plano. A small amount of latent hyperopia was detected in 5 (31%) but correction of the refractive error was not accepted when viewing the ETDRS chart and one person was emmetropic by dry manifest refraction (see Table 1).

3.5.2 Electrode Placement

The skin was prepped for dermal electrodes by initially cleaning the skin with an isopropyl alcohol swab and then rubbing each location with slightly abrasive Nuprep® Skin Prep Gel (D.O.Weaver & Co., Aurora, CO.). The 10 mm diameter gold dermal electrodes (SAFELEAD™, Grass Technologies, Astro-Med Inc., West Warwick, RI) were filled with EC2® Electrode Cream (Grass Technologies) and placed at three locations: reference electrode at FPz (forehead); active electrode at MO (middle occipital- 2 cm above the inion); ground electrode on the earlobe. The ground and active electrode were secured by small clips and the reference electrode was secured by transpore tape (Transpore™ Medical Tape, 3M™ Company, St. Paul, MN). Impedance was checked using Model-F-EZM5 Grass® Electrode Impedance Meter (Grass Technologies) and kept at or below 5 kilo-ohms. Impedance was rechecked periodically during testing, and additionally, if signal noise interference appeared during data acquisition.

3.5.3 Viewing Conditions

Viewing conditions were adjusted to align with the participant's midline and eye level at a viewing distance of two meters. Ambient room lighting was reduced with only dim red light present during PVEP and SVEP testing (lux meter range: 4-9 lux). The non-dominant eye was covered with a black occlusive patch (MYI™ Orthoptic Eye Patch, The Fresnel Prism and Lens

Co., Eden Prairie, MN.). Participants were instructed to blink as needed during testing, and to remain generally relaxed but alert.

3.6 Image Degradation

3.6.1 Optical Defocus (Plus Lenses)

To determine the effect of optical defocus on SVEP results, these tests were recorded with participants viewing through various amounts of plus lenses to fog VA by inducing temporary pseudomyopia. This models various clinical scenarios: an examinee arrives for visual evoked potential testing with uncorrected refractive errors, inappropriate lenses, or self-induced refractive error due to over accommodation (see Sections 2.2.3, 2.3, 2.54).

After the initial orthoptic examination and measurement of VA, the non-dominant eye was occluded with a black occlusive patch and a full aperture plus lens was placed in front of the test eye to fog the visual acuity. During this testing, participants wore standard trial frames or if they wore glasses, a Halberg lens clip (Keeler Instruments Inc., Broomall, PA.) was used as a lens holder. The vision was initially fogged to the level of ETDRS ≤ 1.0 (6/60) and then the lens was reduced in +0.50 spherical lens steps (e.g. +3.00, +2.50, +2.00, +1.50, +1.00, +.50); visual acuity was recorded with each reduction and fogging was maintained throughout. Twelve participants (age range: 21-58 yrs.) contributed to baseline VA decrement values as a function of plus lenses (See Figure 9). A trial with a +5.00 spherical lens was used with a small subset of participants to induce an extreme blur for evaluation of a suspected flash artefact with the LCD monitor.

Participants then underwent SVEP testing with optical defocus with lenses ranging from +0.50 to +3.00 (presented in +.50 steps with random order) or a subset of lenses. Transpore tape

was used around the periphery of the lens to omit incoming peripheral stimulation around the lens edge.

Effect of Plus Lenses

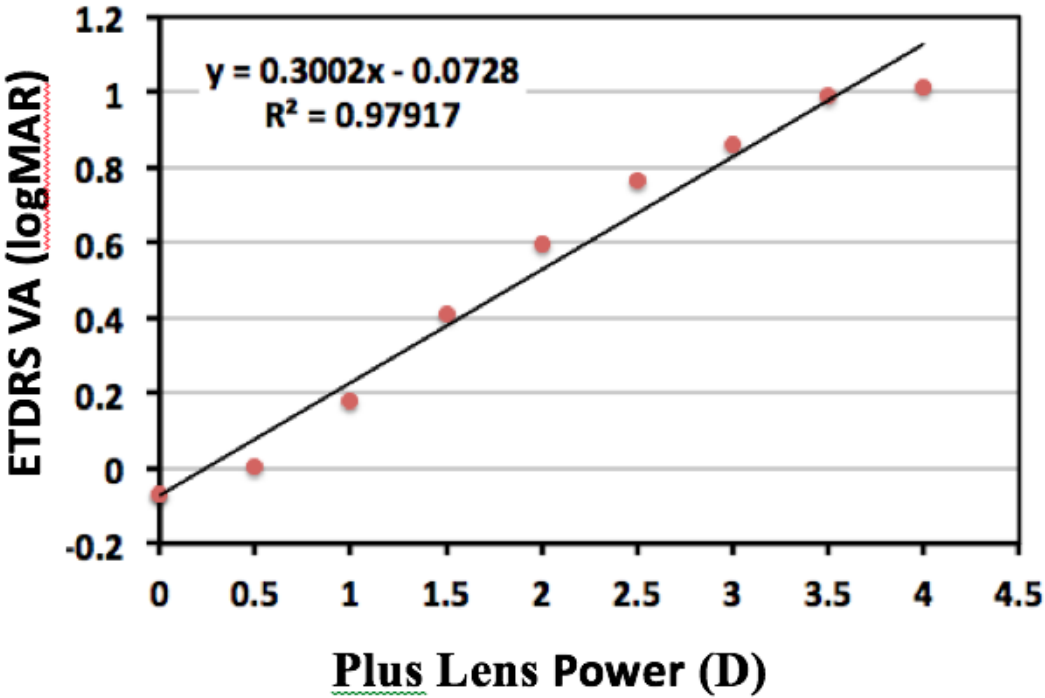
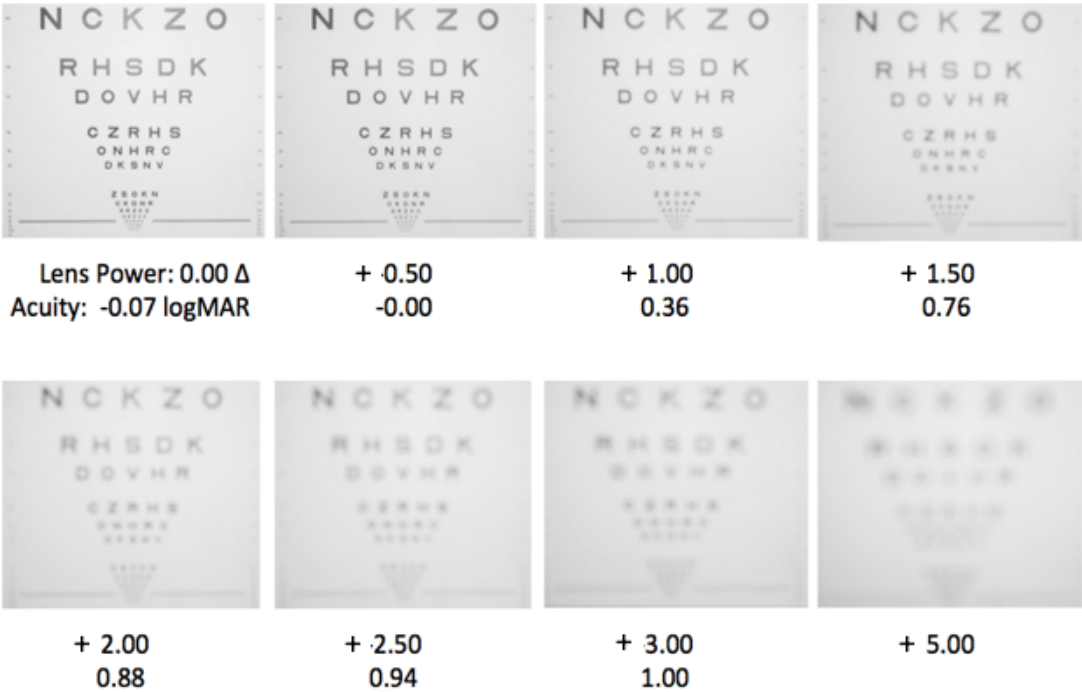


Figure 9: The Effect of Plus Lenses on ETDRS Visual Acuity. Top: Photographs of image degradation of the ETDRS chart with increasing powers of plus lenses. Bottom: Linear regression between ETDRS visual acuity and increasing plus lenses ($R^2: 0.98$).

3.6.2 *Image Obscuration (Bangerter Foils)*

To determine the effect of reduced VA related to visual obscuration on SVEP test results, these tests were recorded with participants viewing through various levels of Bangerter Occlusion foils (Distributor: The Fresnel Prism and Lens Co. Bloomington, MN.) to temporarily reduce vision acuity. This models a common clinical scenario: an examinee arrives for visual evoked potential testing with reduced visual acuity due opaque ocular media (e.g. cataract, corneal scar) or reduced contrast as may occur with optic neuropathies.

Related to previous reports of BF inconsistencies (see Section 2.3.2), the foils were tested under our conditions using a retro-illuminated ETDRS chart (conditions agreeable with the backlit computer monitors used for our VEP testing). It became apparent that the reduction in VA related to each BF power as noted on the manufacturer information was not agreeable under our testing conditions. We retested VA without backlighting on our chart and noted that the VA levels were then more agreeable with the manufacturer suggested values. We re-evaluated the foils and obtained an order of progressive VA decrements for seven foils for our test conditions (range from least to most visual degradation: .8, .6, .4, .3, .2, .1, <.1). The light perception BF was consistent irrelevant to chart retro-illumination. These foils were labeled and then used consistently for all participants to induce gradients of visual obscuration.

The foils were then used in a similar manner to the lenses in the optical defocus experiments. Prior to the test visit, BFs were adhered to plano trial lenses so they could be placed alternately over the dominant eye, either in a trial frame or a Halberg clip. During testing, the vision of the dominant eye was initially fogged to the level of ETDRS ≤ 1.0 (6/60) with the strongest foil available (<.1) while the non-dominant was occluded with a black occlusive patch. The foil was then reduced in order from <.1 to .8 foil with the resultant ETDRS acuity recorded. Nine participants (age range: 25-58 yrs.) contributed to baseline VA decrement values as a

function of BF (see Figure 10). A trial a light perception level BF was used with a small subset of participants to induce extreme obscuration for evaluation of a suspected flash artefact with the LCD monitor.

Participants then underwent SVEP testing with the BFs over the dominant eye with foils ranging from $<.1$ to $.8$ (presented random order) or a subset of foil strengths. Transpore tape was used around the periphery of the lens to omit peripheral visual stimulation around the lens edge.

Effect of Bangerter Filters

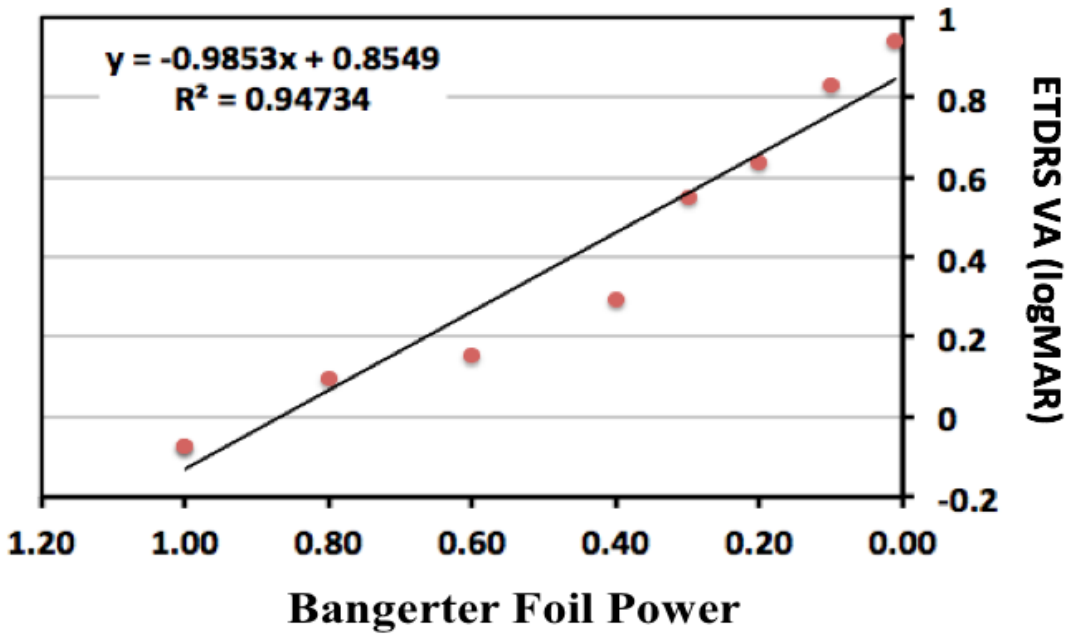
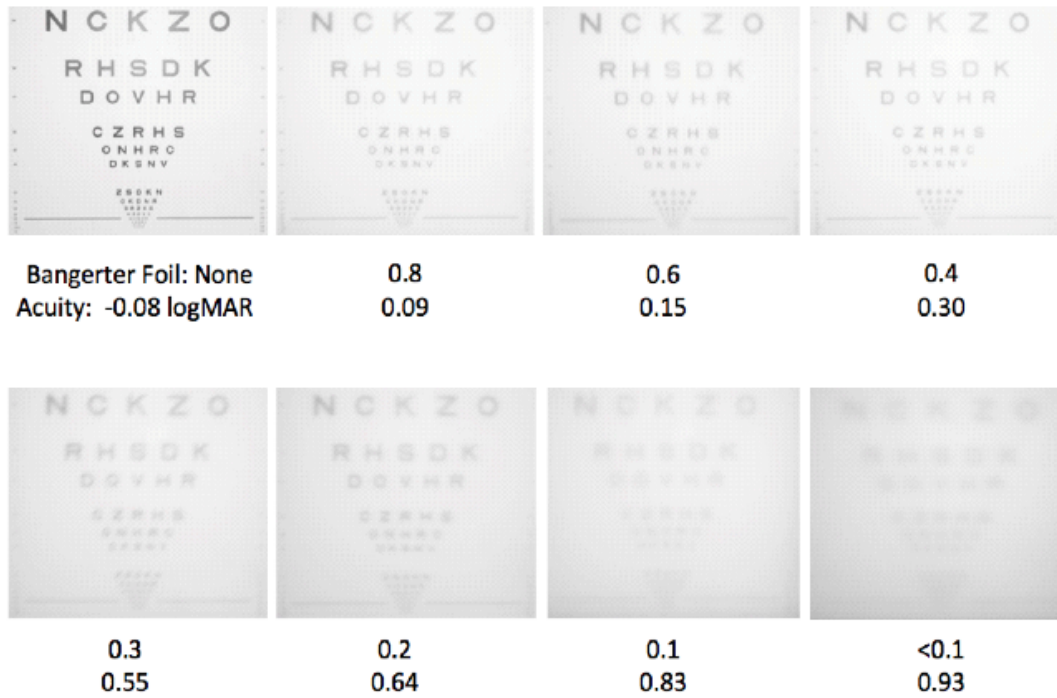


Figure 10: The Effect of Bangerter Foils on ETDRS Visual Acuity. Top: Photographs of image degradation of the ETDRS chart with increasing powers of Bangerter foils. Bottom: Linear regression between ETDRS visual acuity and increasing Bangerter foils (R^2 : 0.95).

3.7 Technology Assessment: Use of Pattern Visual Evoked Potential

Two major technological challenges needed to be overcome prior to initiating SVEP testing: 1) removal of a PVEP flash artefact caused by the LCD monitor to be used for SVEP testing. The flash artefact creates a luminance change during acquisition that contaminates any type of patterned VEP with a flash response; 2) removal of aliasing apparent during the stimulus presentation with the LCD monitor

3.7.1 Removal of LCD Monitor Flash Artefact: Preliminary Trials with PVEP

The transient SVEP protocol developed by EDI required the use of LCD monitors. As it is crucial to assure that there is no flash component in a PVEP (see Sections 2.4.1, 2.4.2), prior to using the new LCD monitor we viewed the display through a LP Bangerter foil; we visually detected a flash artefact. Comparative trials using our standard PVEP with both the CRT and LCD monitors would therefore be necessary to obtain a valid PVEP, and consequently a valid SVEP, with the new LCD monitor. A few reports published after the initiation of this project confirmed the presence of a flash effect in the stimulus presentation linked to LCD technology and not present with the traditional CRT monitors (Fox et al., 2014; Matsumoto et al., 2013; Matsumoto et al., 2014) (also see Section 2.4.2)

To study the flash artefact, matched PVEP stimulus parameters were created using the CRT monitor (PVEP-CRT) and the LCD monitor (PVEP-LCD). Eventually, m-sequence modifications were introduced (PVEP-LCDm) that resolved the flash artefact. For exact acquisition details for the PVEP- CRT, PVEP-LCD and PVEP- LCDm see Appendix A.

To investigate the flash artefact, 8 of 11 PVEP participants (age range: 21-59; 4 males; mean VA -.08 logMAR) who completed two PVEP test types (PVEP-CRT, PVEP-LCD, or PVEP-LCDm) were included. Control trials with routine levels of optical defocus and BFs, as

well as extreme visual reduction using a +5.00 lens and LP Bangerter foil, were recorded. In summary, as seen in Figure 7A, with the CRT monitor, the introduction of a LP Bangerter foil (left side) or a +5.00 lens (right side) reduced the large evoked potentials obtained in control conditions to noise level, confirming the efficacy of the types of image degradation to reduce the VA but also to demonstrate the absence of a flash artefact due to the stimulus presentation. With the LCD monitor, both image degradation types resulted in the presence of a large amplitude evoked potential that was likely due to a flash artefact. This flash artefact was significantly reduced when a black frame was interposed in the m-sequence (LCDm monitor; bottom part of the figure). The significance of this flash effect and its efficacious reduction is documented in Figure 7B with the use of an ANOVA procedure corrected for multiple comparisons (Bonferroni post hoc analysis).

3.7.2 Removal of Aliasing with LCD Monitor

By visual observation of the new LCD monitor, it was apparent that there was a reduction in the contrast of the high spatial frequency gratings (not enough pixels to generate a sinewave grating from white to black). The algorithm that created the horizontal gratings on the monitor allowed the generation of multiple spatial frequencies- image aliasing was visible. After discussion with EDI, a change in the image-generation algorithm was implemented to provide antialiasing pixel-based gratings. This afforded high contrast white/black gratings at high spatial frequencies.

Once these quirks were ironed out, the final transient SVEP protocol was finally developed.

3.8 Sweep Visual Evoked Potential (Population-Averaged Estimates)

Visual acuity predictions based on grating stimuli can show valid and reliable results for population-averaged data but may show significant variability for individuals (Lauritzen et al., 2004; Prager et al., 1999). However, population-averaged (“group”) data is needed to validate a new test such as our transient SVEP. This section will describe how we obtained the individual recordings that were compiled to create our group data and the eventual development of 6 analysis models. Section 3.9 will then describe our application of the modelling results based on group data back to the individual SVEP results.

3.8.1 Acquisition

The final SVEP protocol included a step-wise sweep of 16 horizontal sine wave gratings (0.51, 0.73, 1.07, 1.26, 1.54, 1.98, 2.31, 2.77, 3.46, 4.62, 5.54, 6.93, 9.24, 13.86, 18.48, 27.72 c/d). There were two frames per m-step (first frame provided the contrast alternation directed by the m-sequence; second frame provided a uniform black field to decrease the flash effect generated by the LCD monitor). The m-sequence length was 2^5 . With a frame rate of 60 Hz, the recording time for each spatial frequency was 4.67 sec. (a total sweep of 16 spfs. = 72.72 sec.). Four of these complete sweeps were acquired for each of the image degradation conditions and averaged together to produce a consistent waveform to be analyzed. Control trials were done at the beginning and end of each testing session. The first kernel slice was analyzed with an epoch range from 0-350 ms. The amplifier gain was set at 50,000 with a low frequency cut-off of 1 Hz and a high frequency cut-off at 100 Hz. After acquisition, the data was post-processed with a 45 Hz low pass filter. The fixation target was a 3° red cross with a free central zone of 1° with an outline 3% of the image diameter. The average overall luminance value for the SVEP (15 cd/m²) was measured during acquisition using the same technique as for the PVEP tests (see Appendix A.)

3.8.2. *Measurement of Waves and Linear Regression*

The SVEP responses for the 16 tested spfs are displayed after acquisition and waves are marked after each trial (see Figure 8). During the initial phase of the study, it was apparent that choosing the wave to be measured was, at times, arbitrary. At this point we decided that an objective automated approach would be an asset so wavelet analysis (WA) was initiated and compared to the human interpretation of response wave markings (Expert).

For both WA and Expert, SVEP response curves were created based on amplitude of response to the various spatial frequencies in the sweep (see Figure 8). Linear regressions were created along the descending slope of the response curve with an extrapolation to zero to indicate the SVEP predicted acuity marked in c/d along the X axis. This method of SVEP visual acuity prediction was suggested by early studies using steady-state SVEP (Sokol, 1978; Tyler et al., 1979) (see Figure 4) and has been in continual use since then. Although several criteria for data points to include in the linear regression were trialed, the final criteria for both the Expert and WA was to take the data point with the highest amplitude of the SVEP response curve and include all data points in succession until the last point just above noise level. The linear regression was extrapolated to zero and all other data points beyond this were disregarded. At least 3 data points were required for the linear regression. Expert noise level was set at $2\mu\text{V}$ based on trials removing all pattern responses (light perception BF) and the WA noise level was linked to individual recordings (see below).

The resultant SVEP predicted acuity was then compared to the ETDRS visual acuities for control and image degradation conditions by subtracting the SVEP predicted acuity from the ETDRS acuity (ETDRS-SVEP). Positive values indicate SVEP under prediction of ETDRS acuity and negative values indication SVEP over estimation of ETDRS acuity. Conversion from

ETDRS to c/d: spatial frequency in c/d = 180/ metric denominator for recognition acuity (also see conversion chart based on Holladay (1997) (see Appendix B).

The Expert chose the most prominent positive peaks for measurement but inconsistencies did arise particularly when measuring waves at the very high or low spatial frequencies. After extensive experience a specific criterion for Expert wave marking was outlined (see also Appendix C for examples).

The guidelines for the experienced observer method were as follows:

- 1) The base and apex of the first positive wave showing a consistent response throughout the sweep was marked.
- 2) If a prominent wave for marking was equivocal, attention was directed to the response at the middle spatial frequencies of the sweep and the most prominent wave form at that location was chosen as a guide.
- 3) Using the guide as a starting point, for each spatial frequency, the most prominent wave (at or within a time window of 10 ms.) of the previously marked wave was marked.
- 4) If no obvious wave was present using the set time window (step 3), two marks were made yielding a zero amplitude value close to the time window.
- 5) Negatively oriented waves were not included in the analysis and were marked to yield a zero value.

3.8.3. *Automated Wavelet Analysis*

Wavelet analysis provides correlations of an original signal with a finite duration base function (the wavelet) that is translated in time to allow the analysis of the various parts of the signal and dilated or contracted to allow the determination of the spectral content of the

signal (see Section 2.7 and Figure 6). This yields two sets of parameters (the translation and the scale parameters) that are plotted as a scalogram (translation as X axis, scale as Y axis and correlation as Z axis). The base function (the wavelet) can be any oscillatory function and many wavelets are available to study neural functions. The automated WA method for our study was based on the continuous wavelet transform (MATLAB[®] 2015b, Wavelet Toolbox 4.15, Mathworks, Natick, MA, USA).

The continuous wavelet transform yields a large number of coefficients both in the time and frequency domains. For this study, we elected to use the series of coefficients corresponding to a pseudo frequency of 66 Hz which corresponds to the fast oscillation of the evoked potentials recorded (see Figure 6). This means that the low and high frequencies of the signal were purposely omitted as they are often related to recording artefacts such as head movements and muscle contraction. The coefficients were summed within a chosen temporal window of typical SVEP responses (60-180ms) to yield a dimensionless single value that was used to build the response curve. The noise level was evaluated by using a temporal window (280-340 ms.) of the SVEP response. The MATLAB[®] code used to extract the wavelet coefficients is provided in Appendix D. Comprehensive tutorials of the application of wavelet analysis to evoked responses and EEG signals can be found in Herrmann et al. (2014) and Samar et al. (1999).

We considered many wavelets such as Haar, Simlet, Coiffet, Frequency B-Spline and even complex Morlet. It was found that each wavelet provided slightly different profiles of the original signal. The strict analysis of the best wavelet function to represent the SVEP is beyond the scope of the present study; however, we determined that the Haar function (a simple square wave) was providing an adequate decomposition of the SVEP signal and consequently, it was used for all the wavelet computations found in this study. One consistent scaling level was

chosen for analysis using this wavelet and data generated by control trials and image degradation conditions were compared to this baseline scaling.

3.8.4. *Additional Analysis Models*

It became apparent that analysis by linear regression, commonly seen in SVEP literature, had limitations. For instance, the linear regression (Model 1) is highly dependent on a set of endpoint data where the SNR is at its lowest, this causes inconsistencies in the points to be included in the regression and yields dramatic changes in the VA estimate.

To overcome these limitations, we developed a series of curve determinants that were based on the regions of the curve where the SNR was at its maximum. As the most abrupt change in amplitude generally occurs between the low spatial frequency stimuli (0.73- 1.54 c/d) and peak amplitude stimuli (2.77-5.54 c/d), two ratios were derived from the mean response amplitude from sets of three points: 1,2,3/8,9,10 (spatial frequencies: 0.73, 0.93,1.07 / 2.77, 3.46, 4.62 c/d) and 3,4,5/ 9,10,11 (spatial frequencies: 1.07, 1.26, 1.54 / 3.46, 4.62, 5.54 c/d) (Model 2- Ratios). Ratio numerators represent responses from low spatial frequency stimuli (points 1,2,3 or 3,4,5) and denominators represent responses from higher spatial frequency stimuli (points 8,9,10, or 9,10,11).

We also considered the region where the maximum recording amplitude was obtained for both stimulus spatial frequency (Model 3) and amplitude values (Model 4), the number of points in the curve that were significantly above noise level (pre-determined at a level corresponding to 1.6 times the base noise level- Model 5) and finally the area under the curve as determined by integration of the data points (sum of all amplitudes-Model 6) (see Figure 11). For each of the models (excluding linear regression where VA is directly estimated), the determinant values

obtained from each type of visual degradation were associated with the corresponding ETDRS visual acuity (from Figures 9 and 10) and linear regression equations were obtained.

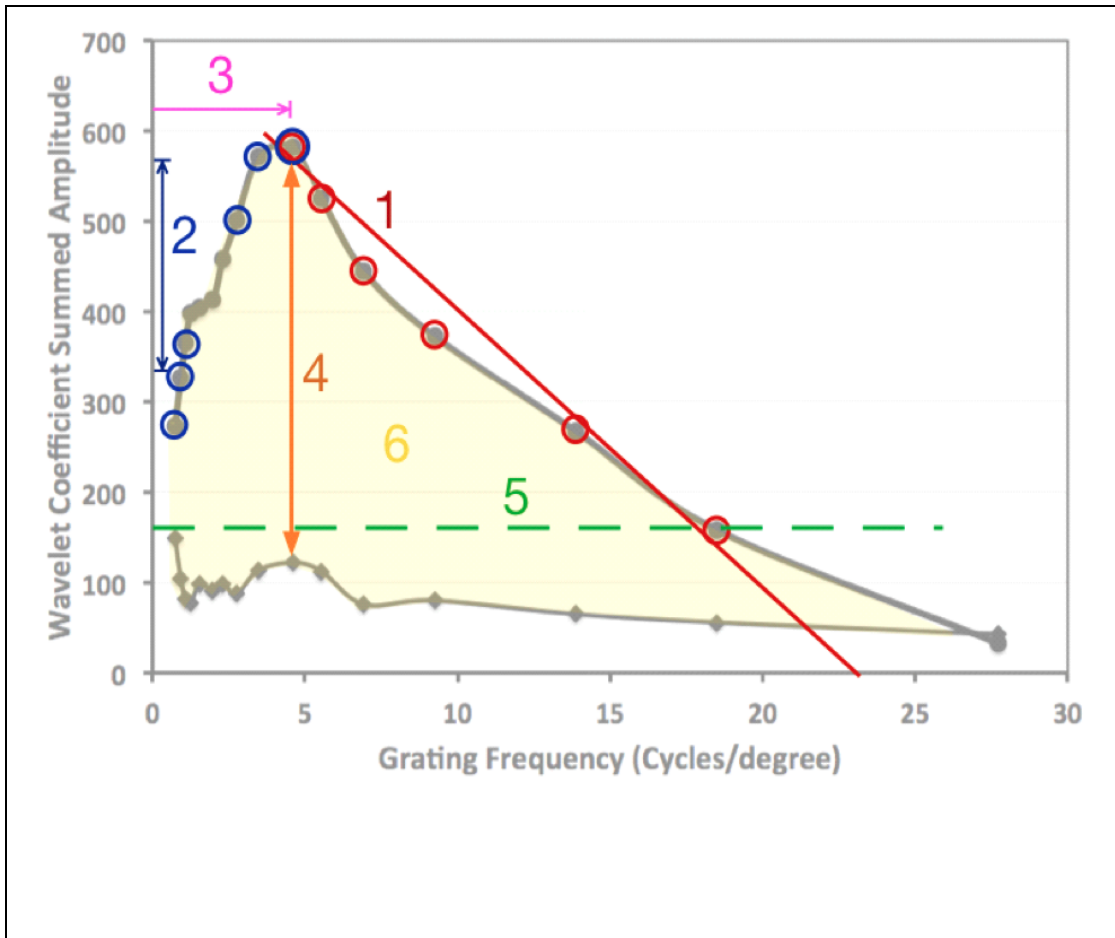


Figure 11: Illustration of a SVEP Response Curve Showing Analysis Models (1-6) Based on Response Curve Parameters. Gray circles on the ascending and descending slope of the curve represent the 16 spatial frequencies tested (#1- low spatial frequency far left to #16 high spatial frequency far right). The gray line connecting the diamonds indicates noise level. Model 1 (red line) shows the linear regression technique for visual acuity prediction from last peak point to noise level. Model 2 (blue line and circles) showing the two ratios derived from the mean response amplitude from sets of three points: 1,2,3/8,9,10 and 3,4,5/ 8,9,10 on the SVEP response curve. Model 3 (pink arrow) shows the location of the peak that is normally at ~5 c/d but shifts to lower spatial frequencies with image degradation. Model 4 (orange arrow) show the peak amplitude measured from noise level. Model 5 (green dash) represents the cut-off point for data points to be included in the calculation of number of points 1.6 X the noise level. Model 6 (yellow 6) symbolize the calculation of the summed amplitude of all point under the curve to the noise level.

3.9 Sweep Visual Evoked Potential (Individual Estimates)

As the linear equations based on Models 1-6 from population-based data were obtained under circumstances of known ETDRS visual acuities and unknown visual acuity is often the clinical presentation of individuals for SVEP testing, we applied the equations from Models 1-6 back on our data from individuals. We also combined the data from both image degradation types as cause for reduced visual behavior is often unknown. The resultant scattergrams were thought to be more representative of individual variability in routine clinical conditions. We then considered all binary combinations of Models 1-6 in an attempt to optimize the accuracy of SVEP predictions for individuals.

It has been proposed that the SVEP would be a valuable tool for pediatric vision screening (Simon, Siegfried, Mills, Calhoun, & Gurland, 2004). Regarding the potential of our SVEP test to be used as a vision screening tool, we applied a receiver operating curve (ROC) to our individual data. The ROC technique can be used to analyze medical tests regarding accuracy for screening or diagnosis; the analysis yields a graphical display of the sensitivity and specificity of the test in question (Hajian-Tilaki, 2013; Zou, O'Malley, & Mauri, 2007) To obtain the ROC curves, our SVEP predicted acuities were rated to ETDRS visual acuities using MATLAB[®] (see Appendix E). The specificity/sensitivity of the SVEP for four visual acuity groups was determined: high VA (> 27 c/d; ETDRS better than ~ 6/7.5); high intermediate VA (27-17c/d; ETDRS ~ 6/7.5 - 6/9.6); low intermediate VA (15-10 c/d; ETDRS ~ 6/12 - 6/19); low VA (< 10 c/d; ETDRS- 6/24 or worse). The derived indices of accuracy showing area under the curve (AUC) were also computed for each acuity group.

3.10 Statistical Consideration

Most of the analyses presented in this work are in the form of simple linear regressions, as determined by the algorithms resident in Excel for Mac 2011 (version 14.5.8; Microsoft Corporation, Redmond, Washington, USA). Bland-Altman plots were performed when pertinent to test repeatability and agreement and to afford assessment of bias of the mean (J. M. Bland & Altman, 1986). A singular comparison of a Bland-Altman graph to a plot of the linear regression residuals was done to qualitatively assess the two methods. To document the effect of repeated measures on individual data, calculation of correlation coefficients with repeated measures for “within subjects” (J.M. Bland & Altman, 1995) was performed using Stata[®] (Statacorp LP, College Station, TX). The ROC and AUC were computed using the probability estimates from the logistic regression models as predefined in MATLAB[®] ‘perfcurve’ function.

CHAPTER 4: RESULTS

4.1 Data Presentation

The SVEP raw data was analyzed using two different methods. The first method (Expert), involved the subjective human measurement of the peak amplitude of the first prominent positive wave of individual SVEP responses. The second method involved Wavelet Analysis (WA) that provided an automated computerized summation of wavelet coefficients between 60 and 180 ms for the evoked potential signal and between 280 and 340 ms for the noise signal. From an analysis perspective, one advantage of the WA method over the Expert is the calculation of a noise threshold obtained during each recording session that provides objective criteria to either accept or reject low amplitude data points. For the Expert, independent of individual variation and based on our data characteristics, a broad noise level of 2 nV was subjectively accepted and applied to the Expert data during post-recording processing. All data points falling below noise values were not included in the subsequent analyses.

Both analysis methods yielded a response-frequency scattergram presenting the amplitude measurement of the evoked potential as a function of the spatial frequency of the stimulus grating presented. The alignment of data points is termed the SVEP response curve. A SVEP response curve was obtained for each viewing condition including control trials (unaided or best corrected vision with glasses or contact lenses) as well as successive conditions of image degradation imposed by BFs or plus lenses. The SVEP response curves were characterized by parameters that were subsequently used in modeling the fit of the SVEP visual acuity predictions with ETDRS visual acuity. The repeatability of measurements and the agreement between the techniques were further characterized by Bland-Altman plots.

In the first sections of the results, Section 4.2 shows an overview of results from all individuals (“individual data”) that underwent image degradation. The following sections (4.3-

4.5) used population-averaged data (“group data”) for analysis, i.e. SVEP response curves were analyzed using data points composed from averaged data of evoked potential responses from several individuals to: (1) minimize noise levels and allow better discrimination of spatial frequency points on the response curve; and (2) to reduce the inter-individual variations and allow fundamental validation of the SVEP method. In the final result sections (4.6-4.7), the most promising forms of analysis were repeated, and focused back on individual data to determine the accuracy of such methods in a more clinically-oriented context.

4.2 Comparisons between Expert and Wavelet Analysis Techniques (Individual Data)

Both analysis techniques for SVEP data (Expert and WA) were used for this study. The Expert method consisted of the experienced “expert” subjectively marking one prominent response wave with the highest amplitude (in nV) for each of the evoked potentials generated by the 16 grating spatial frequencies presented during the SVEP (see Figure 8). Although there is no ISCEV standard for SVEP acquisition and analysis, the Expert technique is modeled after ISCEV standards for transient VEPs that is historic, well documented and considered to be the gold standard (Brigell, 2001; Odom et al., 2006). The innovated alternative analysis technique (WA) offers automation and independence from subjectivity. Wavelet Analysis yields unitless data that corresponds to the overall evoked potential activity within a predetermined time window and a noise estimate (see Figure 6).

An all-encompassing linear regression was performed between the individual data obtained by WA and Expert methods. Control trials as well as image degradation by plus lenses and BFs were included in this analysis, yielding 160 points for the BF condition (2 control trials plus 8 grades of foils for 16 SVEP spatial frequencies) and 128 points for the plus lens condition (2 control trials plus 6 lens powers for 16 SVEP spatial frequencies). The Expert and WA

techniques show excellent R^2 values (0.92 and 0.95) for plus lenses and BFs respectively (see Figure 12). The data points for BFs are well aligned along the regression line, whereas the plus lens data shows more variability in the middle to high amplitude values. This indicates that with optical defocus, the WA measures higher summed amplitude values compared to the Expert technique that would have marked one main prominent peak. With low amplitude values (generally related to worse visual acuity), the two analysis methods show points falling closer to the regression line. The excellent overall R^2 values between WA and the gold standard (Expert) justifies the continued use of WA for this study.

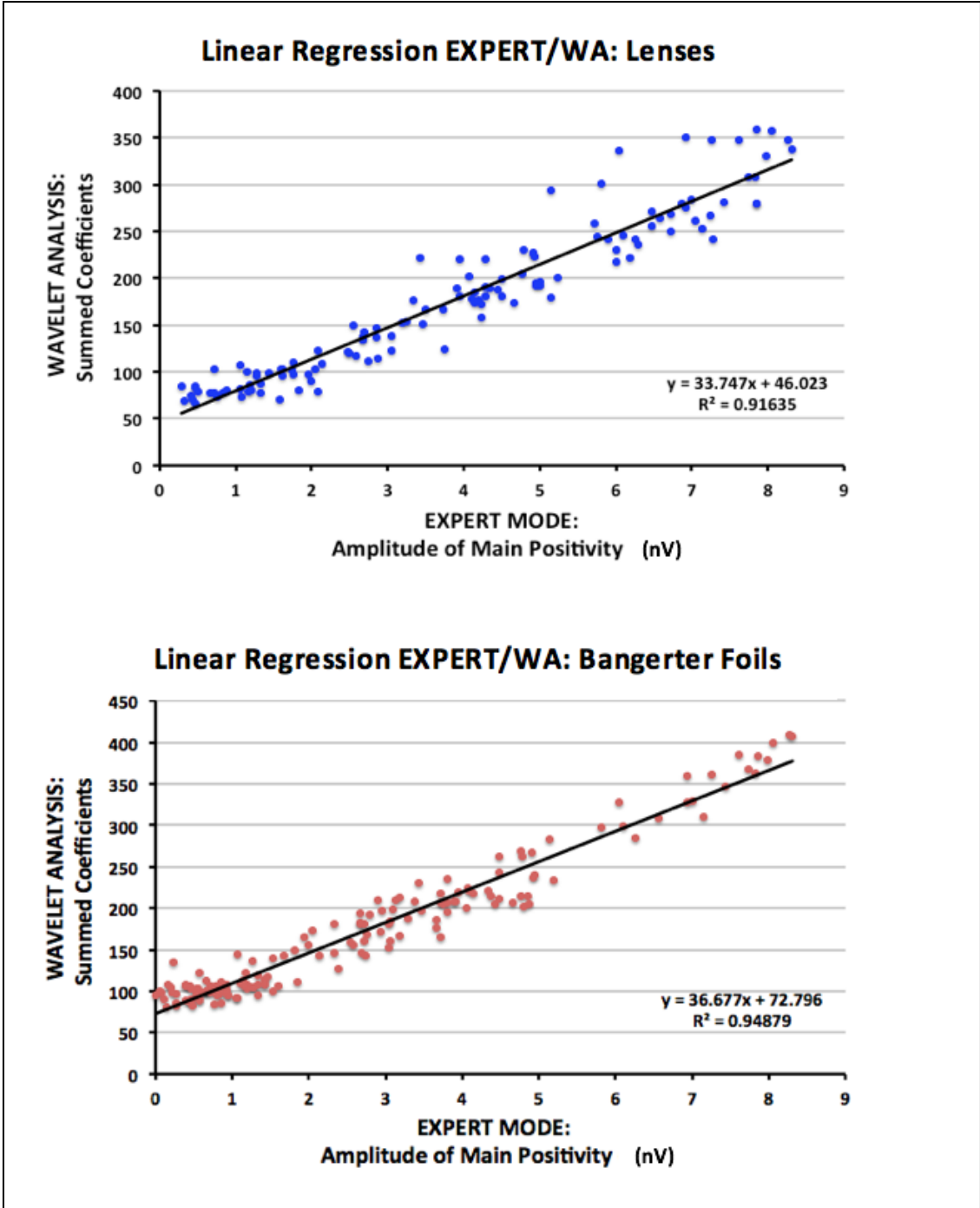


Figure 12: Linear Regression between the Expert and Wavelet Analysis (WA) using Group Data with Plus Lenses and Bangerter Foils.

4.3 Effect of Image Degradation on the SVEP Response Curve (Group Data)

Based on the good overall linear relationship between the Expert and WA techniques and the advantage of the WA to readily provide a noise level, this technique was chosen over the Expert technique to display the effects of image degradation (all plus lenses and BFs) on SVEP visual acuity predictions.

For these analyzes, SVEP response curves were created based on group averages of the summed amplitude responses for each of the grating frequencies presented during the SVEP protocol. The SVEP visual acuity prediction was determined by linear regression from the peak amplitude to the zero intercept point on the x-axis including all points in series to the point lowest in amplitude above the noise level (further responses beyond this final point were disregarded); this technique is comparable to various previous SVEP reports (Bach et al., 2008; Kurtenbach et al., 2013; Norcia & Tyler, 1985b; Ridder, 2004; Tyler et al., 1979). Also SVEP and ETDRS visual acuities were compared by subtracting the SVEP predictions from the ETDRS acuity (ETDRS – SVEP); positive results indicating that the SVEP underestimated the ETDRS acuity; negative results indicating that SVEP overestimated the ETDRS acuity (see Section 3.8.2).

4.3.1 Effect of Optical Defocus (Plus Lenses)

Seven participants (age range: 21-59; 4 males) each completed two control trials and a total of 36 plus lens trials (6 lenses; range: +0.50 to +3.00). The resultant SVEP response curves are presented in Figure 13 including a control curve derived from the average of two control trials (first and last trials of the session) and curves derived from data obtained with various degrees of optical defocus by plus lenses. The blue dots represent the response amplitudes for each spatial frequency in the sweep, with red dots overlying those dots included in the linear

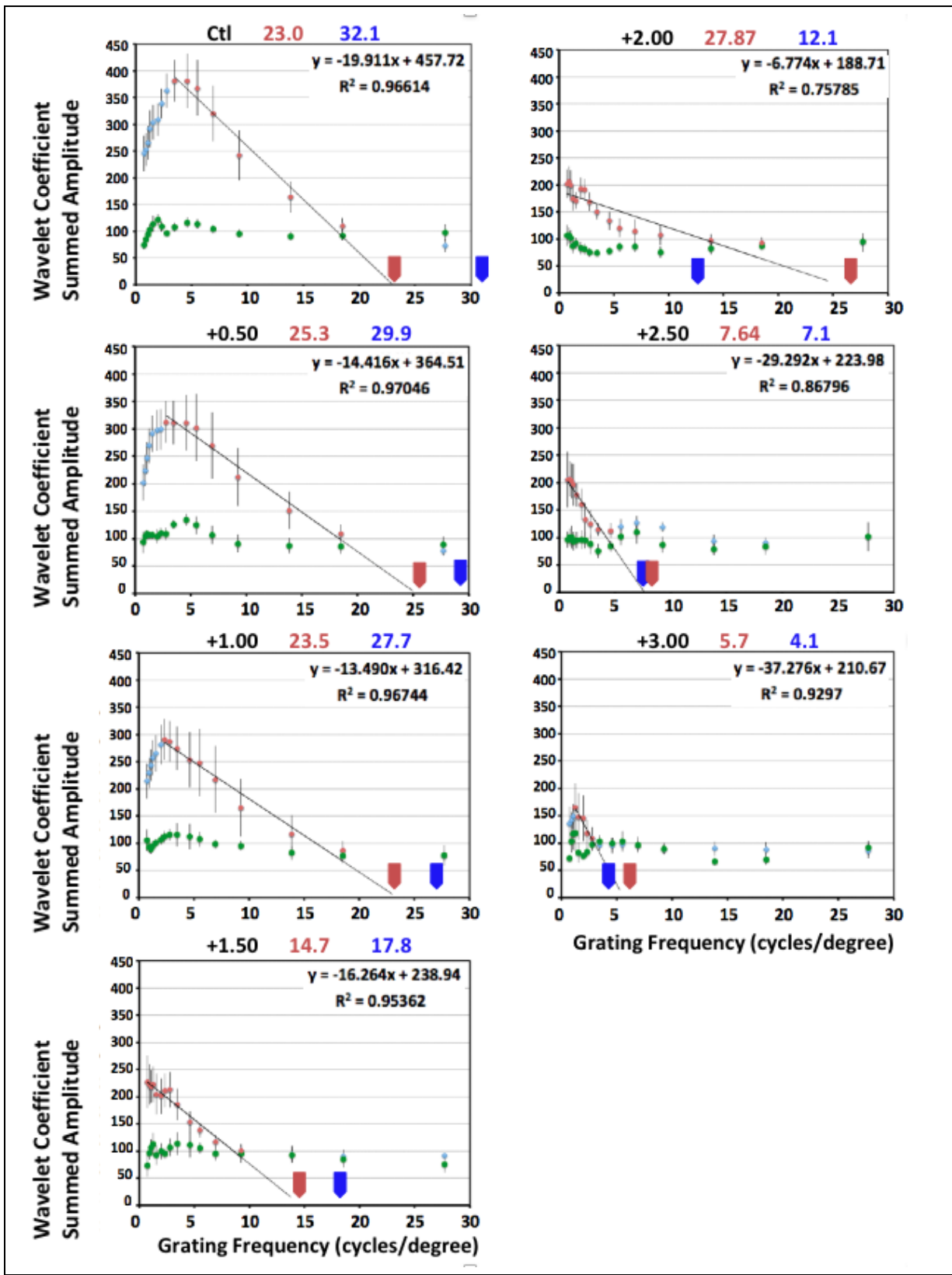
regression applied to determine the SVEP visual acuity prediction. The green dots show the level of noise in each recording. Figure 13 also allows comparison between the value of the SVEP linear extrapolation at the crossing of the x axis (red arrow and numeric value in red) to the ETDRS visual acuity (blue arrow and numeric value in blue) as measured with plus lenses prior to SVEP testing (see Figure 9). The standard error of the mean (SEM) is represented by vertical black bars for each data point of the SVEP response curves. The results of the linear regression for the SVEP predicted acuity are displayed the upper right corner of each graph (R^2 value and the slope-intercept equation).

An overview of the effect of increasing optical defocus seen in Figure 13 shows a well formed SVEP response curve for the control data with low amplitude responses at low spatial frequencies that increase to a peak amplitude at 4-5 c/d followed by a series of declining amplitudes to the last point just above the noise level at 18.5 c/d. The addition of even a +0.50 lens shows a reduction in the peak amplitude and an apparent reduction in the area under the curve that continues to decline as the plus lenses are increased. The resulting collapse of the SVEP response curve is associated with a shift of the peak towards low spatial frequencies and the morphology of the response “curve” eventually becomes a line. This effect can first be observable with the +1.50 lens (ETDRS acuity ~ 6/10). The tendency for responses at the low spatial frequencies to be the peak amplitude continues to the extent of the optical defocus experiment with the +3.00 lens (ETDRS acuity ~6/48). With this maximum defocus, both the number of viable data points above noise level and the peak amplitude decline by approximately 50% compared to the control data.

More specifically, the results of the linear regression of the SVEP predicted acuity compared to the ETDRS acuity for the control data shows SVEP visual acuity predictions to

underestimate the ETDRS visual acuity (ETDRS acuity = 32.1 c/d; SVEP prediction = 23 c/d; ETDRS-SVEP = +9.1 c/d). The trend for SVEP underestimation of ETDRS acuity reduces with +0.50 lens (ETDRS acuity = 29.9 c/d; SVEP prediction = 25.3 c/d) and this level of underestimation (~3-4 c/d) continues with the +1.00 and +1.50 lenses. However, with the +2.00 lens, and abiding by the strict criteria for point inclusion in the linear regression (see Method Section 3.8.2) a substantial SVEP overestimation of ETDRS visual acuity is present (ETDRS acuity = 12.1 c/d (~ 6/12); SVEP prediction = 27.9 c/d (~ 6/6); ETDRS- SVEP acuity = -15.8 c/d). After this point, only a minimal SVEP overestimation of ETDRS visual acuity is seen with the +2.50 and +3.00 lenses (ETDRS-SVEP acuity of -0.50 c/d and -1.6 c/d respectively).

Figure 13: Effect of Increasing Power of Plus Lenses on ETDRS Visual Acuity and SVEP Linear Extrapolated Visual Acuity using Wavelet Analysis and Group Data. Blue markers indicate total SVEP response; red markers indicate the section of the response chosen for linear extrapolation (last peak point to noise level); green markers indicate the noise level; red arrow indicates the SVEP predicted acuity; blue arrows indicate group averaged ETDRS acuity for that lens power. Vertical bars indicate standard error.



4.3.2 *Effect of Image Obscuration (Bangerter Foils)*

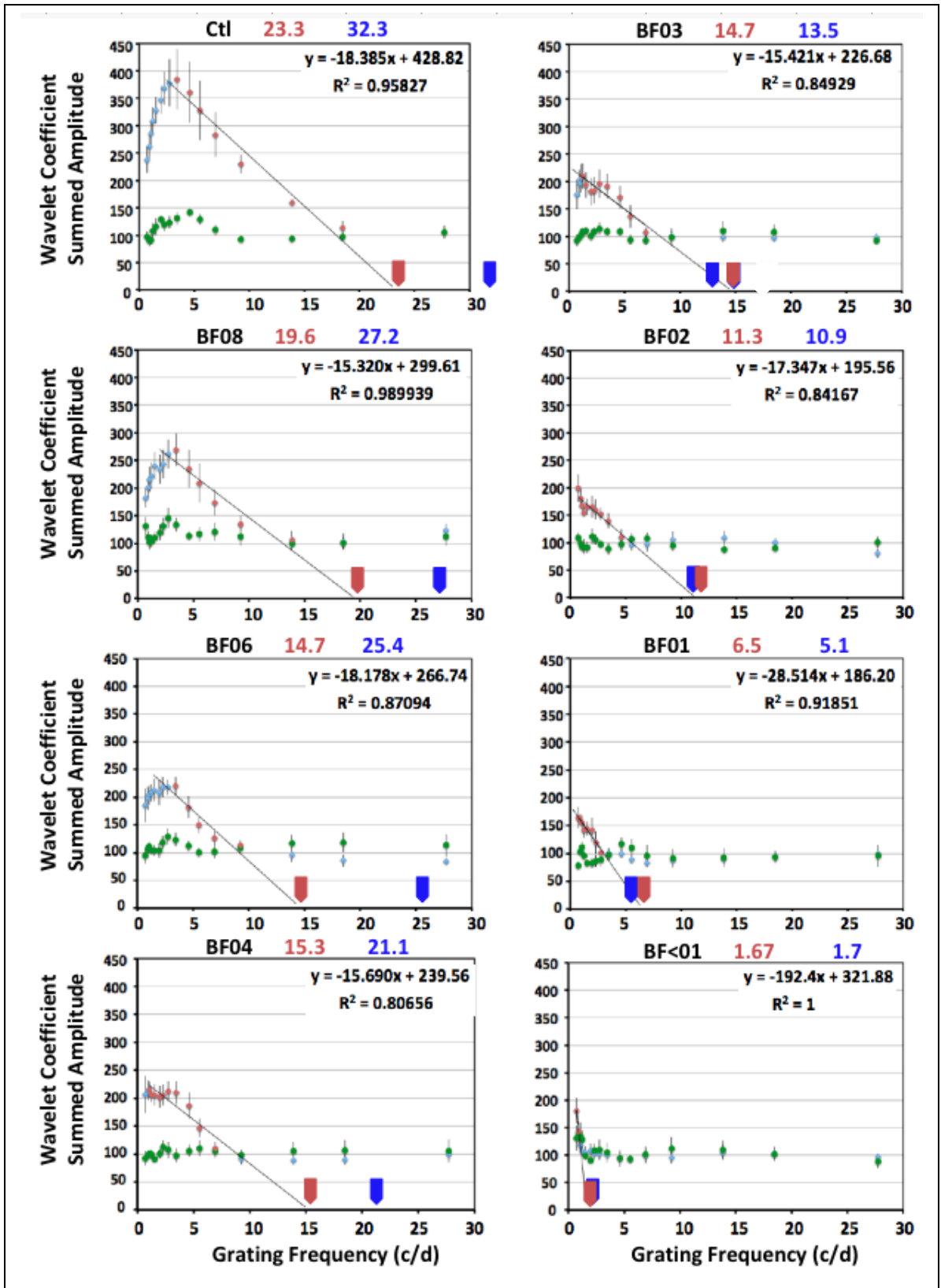
Five participants (age range: 21-58; 3 males) each completed 2 control trials and a total of 49 BF trials (8 foils; range: 0.8 to light perception). The results are displayed in Figure 14 using the same presentation format as in Figure 13 and using the ETDRS visual acuity levels as measured with the BFs prior to SVEP testing (see Figure 11).

An overview of the results of increasing BF strength seen in Figure 14 shows a well formed response curve for the control data with low amplitude responses at low spatial frequencies that increase to a peak amplitude at 4-5 c/d followed by a series of declining amplitudes to the last point just above the noise level at 18.5 c/d. (similar in appearance to the plus lens trial control data). The addition of the 0.8 BF shows a drop in the peak amplitude that continues to decline as the BF strength is increased. The response curve undergoes morphologic changes with increasing BFs and resultant declining visual acuity similar to the plus lens experiment. With the 0.4 BF (ETDRS acuity ~ 6/10), the responses for the lowest spatial frequencies become the peak amplitude and morphology of the response “curve” becomes a line. The tendency for responses at the low spatial frequencies to be the peak amplitude continues to the extent of the BF experiment with the 0.1 and <0.1 BF (ETDRS acuity: ~ 6/48 and < 6/60 respectively). At the point of maximally reduced vision, there are minimal viable data points above the noise level to include in the linear regression and the peak amplitude declines by approximately 50% compared to the control data.

More specifically, the results of the linear regression of the SVEP predicted acuity compared to the ETDRS acuity for the control data, similar to the plus lens experiments, show that the SVEP visual acuity predictions underestimate the ETDRS visual acuity, (ETDRS acuity = 32.3 c/d; SVEP prediction = 23.3 c/d; ETDRS-SVEP = +9.0 c/d). The trend for SVEP

underestimation of ETDRS acuity continues in a fairly stable manner with increasing BF strength, averaging an underestimation of +8.0 c/d from BF 0.8 to BF 0.4.(ETDRS-SVEP values for BFs: 0.8 = +7.6 c/d; 0.6 BF = +10.7 c/d; BF 0.4 = + 5.8 c/d). At BF 0.3 (ETDRS acuity~ 6/12) the SVEP prediction starts to overestimate the ETDRS visual acuity (BF 0.3: ETDRS-SVEP = -1.2 c/d). After this point, only a minimal SVEP overestimation of ETDRS visual acuity is seen with the BFs 0.2 and 0.1 (ETDRS-SVEP acuity of -0.40 c/d and -1.4 c/d respectively). The SVEP prediction appears to equal the ETDRS acuity level at BF <0.1.

Figure 14: Effect of Increasing Power of Bangerter foils (BF) on ETDRS Visual Acuity and SVEP Linear Extrapolated Visual Acuity using Wavelet Analysis (WA) and Group Data. Blue markers indicate total SVEP response; red markers indicate the section of the response chosen for linear extrapolation (last peak point to noise level); green markers indicate the noise level; red arrow indicates the SVEP predicted acuity; blue arrows indicate group averaged ETDRS acuity for that BF power. Vertical bars indicate standard error.



4.3.3 *Comparison of Image Degradation Techniques on SVEP Acuity*

Broad comparisons can be made by viewing the displays of the effect of plus lenses and BFs on the SVEP response curves in Figures 13 and 14. As the image is increasingly degraded, both techniques show a drop in the SVEP peak amplitude, and a loss of spatial tuning as the rise in amplitude from the low to middle spatial frequencies dissolves and, at the extent of degradation, the response “curve” becomes essentially a small cluster of points just above noise level with a linear regression that approaches a vertical line.

The BF data shows less variability as the BF SVEP responses at each spatial frequency display an overall reduced SEM compared to the optical defocus lens data. The BF data shows more consistent SVEP prediction of ETDRS visual acuity devoid of outlying data as occurred with the plus lenses (+2.00 data). The inherent challenge of using linear regression to analyse the SVEP can be seen when comparing the +2.00 lens and the BF 0.3 data; both conditions have similar ETDRS visual acuity (12-13 c/d) and similar appearing data except for the responses with the 14 and 19 c/d stimuli for the +2.00 lens. These responses were above the noise level and thus were included in the linear regression. Inclusion of these two data points in this area of middle to high spatial frequencies yields a dramatic difference in SVEP predicted visual acuity based on linear regression.

A summary of the BF and plus lens data can be seen in Figure 15A. Although the BF data shows more initial drop in the SVEP responses than the plus lens data, the two types of image degradation are quite agreeable at low levels of ETDRS visual acuity. To relate this to clinical practice, a comparison was made between the SVEP predictions and the reported ETDRS acuity at three ETDRS acuity levels: 30 c/d (~6/6), 20 c/d (~6/10), 5 c/d (~6/30) (See Figure 15B). At the level of ~30 c/d, the BFs show a more detrimental effect on the SVEP than

the plus lenses with the SVEP predicted acuity ~ 6 c/d worse than the plus lens predicted acuity and an increased difference between the SVEP and ETDRS acuities (BF 0.8: ETDRS- SVEP = 7.6; +.50 lens: ETDRS-SVEP = 4.6). The difference is slightly reduced with increasing image degradation to the level of ETDRS ~ 20 c/d (BF 0.4: ETDRS-SVEP = 5.8 c/d; +1.50 lens: ETDRS-SVEP= 3 c/d). At the level of ETDRS ~ 5 c/d, the effect of the image degradation techniques equalize with the SVEP showing minimal overestimation of the ETDRS visual acuity with both techniques (BF 0.1: ETDRS-SVEP = -1.4 c/d; +3.00 lens: ETDRS-SVEP = -1.6). Although discrepancies occur in SVEP predictions of ETDRS acuity for control data and mildly reduced visual acuity, the ETDRS visual acuity predictions appear quite reliable for severely reduced visual acuity levels using group average data.

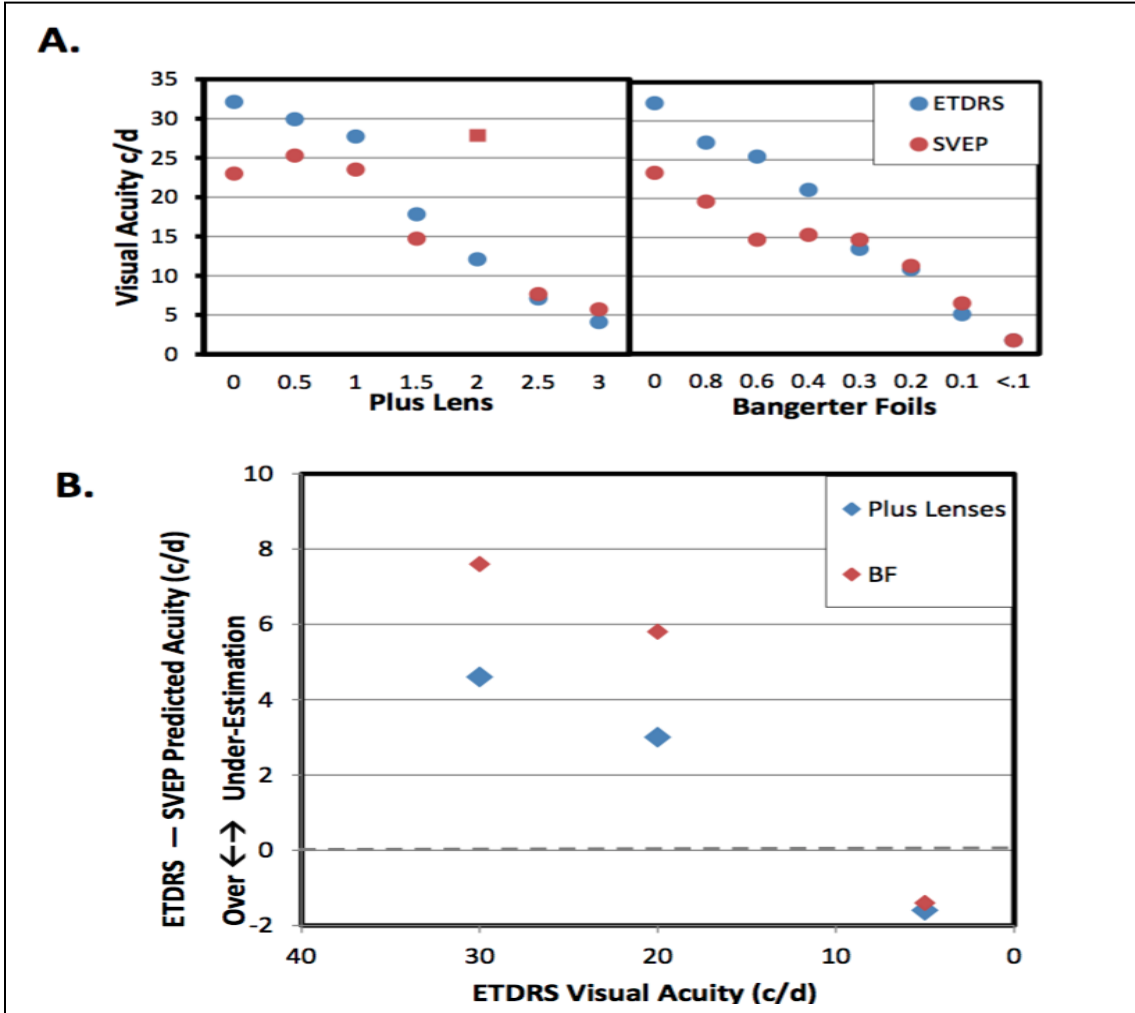


Figure 15: Summary of Comparisons between ETDRS Visual Acuity and SVEP Predicted Acuity. A. ETDRS acuity (blue circles) SVEP acuity (red circles) for plus lenses and Bangerter foils. Outlier present with +2.00 lens (red square). B. Summary of the difference between ETDRS and SVEP acuities at three selected spatial frequencies. Plus lenses (blue diamonds) and Bangerter foils (red diamonds).

4.4 Initial Models Related to SVEP Response Curve Parameters (Group Data)

Although WA has shown some advantages for data analysis and noise assessment for visual electrophysiology research (Barraco et al., 2014; Thie et al., 2012), there are no reports of WA being used to build SVEP response curves. To further illustrate the use of WA in visual electrophysiology in this context, this section includes a comparison between WA and the Expert techniques related to SVEP predictions of visual acuity using SVEP response curve parameters.

Two analysis models will be compared in this section:

Model 1- SVEP predicted acuity based on extrapolation by linear regression

Model 2- SVEP predicted acuity related to response amplitude ratios

Linear regression was applied to this data as a good overall linear relationship between WA and the Expert was seen in section 4.2 (see Figure 12).

4.4.1 Model 1: SVEP Predicted Acuity by Linear Extrapolation

R^2 values were determined for SVEP acuity predictions to compare the Expert and WA techniques for the control trials as well as image degradation conditions. The ETDRS visual acuity for each condition of image degradation was correlated with the SVEP estimated visual acuity derived from linear regression extrapolation as displayed in Figures 13 and 14.

Comparisons between the plus lens and BF conditions can be seen in the twin graphs in Figure 16A. The linear regression results for the Expert versus WA using plus lenses reveals that the Expert shows an excellent R^2 value (0.86) as compared to WA (0.56). However, the WA coefficient is highly influenced by an outlier; with this point omitted, the coefficient of determination improves to 0.93. However, the slope of the Expert results is lower (0.49 vs. 0.66 for the WA); this suggests that the WA results are a closer fit to the line of equality ($y = x$ represented by the black line). The y intercept is at ~ 3.5 c/d for both cases, suggesting that there

is some residual VEP activity above the noise level when the ETDRS visual acuity level approaches zero. Also, agreeable with Section 4.3, the linear regression intercept technique shows an increasing trend for the SVEP predictions to underestimate the ETDRS visual acuity as acuity levels improve; underestimation is most apparent with the control trials at levels better than 30 c/d, while overestimation is evident at low levels of ETDRS visual acuity.

Figure 16B shows the same comparison between the Expert and WA using BFs. In this case, the WA has the better R^2 value (0.92) with an outlier influencing the Expert data (R^2 : 0.67). Recalculation with this outlier removed improved the Expert coefficient to 0.92, again suggesting a fairly good agreement between the Expert and WA. Here again, the slope of the linear regression is lower with the Expert method (Expert 0.44, WA 0.65) suggesting that the WA computation produces results closer to the gold standard ETDRS visual acuity.

Regarding the presence of outliers in the data, it appears that both the Expert and WA data can be contaminated; these discrepancies tend to occur with ETDRS acuities of approximately 15 c/d (6/12 visual acuity) in our data. Discrepancies in the descending portion of the SVEP response curve is not uncommon and frequently affect middle to high spatial frequency locations (may be noted as the presence of a double peak or notch). Such inconsistencies have yielded several approaches by authors such as: 1) using two different methods of data analysis—one for clear linear regressions and one for unclear regressions due to double peaked data (Ridder & Rouse, 2007; Ridder et al., 2012; Ridder et al., 2014); 2) using numerous criteria to optimize the linear regression and SVEP acuity predictions (Yadav et al., 2009); 3) using a heuristic formula to deal with notched data (Bach et al., 2008).

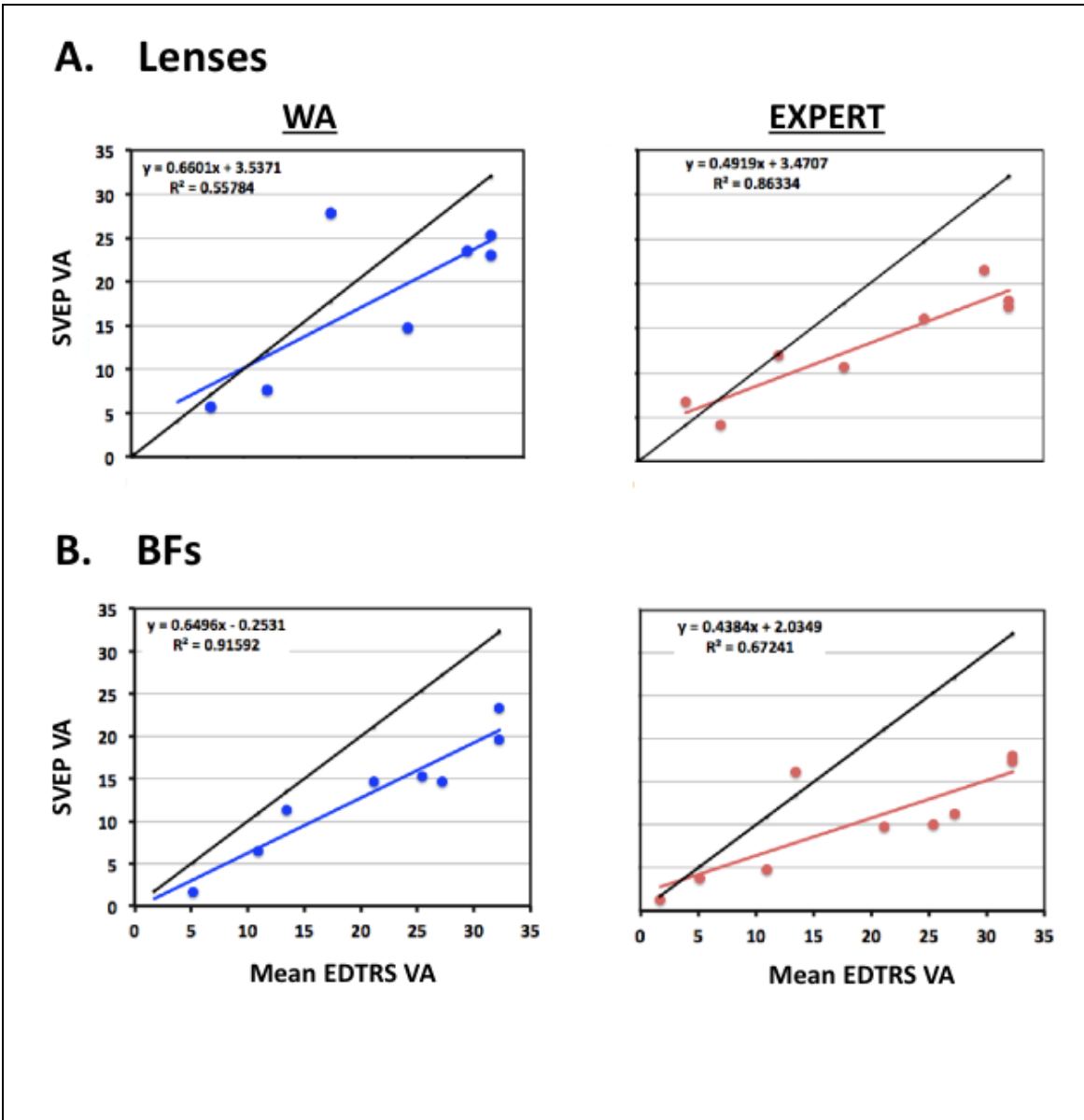


Figure 16: Comparison between ETDRS Visual Acuity (VA) and SVEP Linear Extrapolated VA using Expert and Wavelet Analysis (WA) with Group Data. **A.** Image degradation by plus lenses. Note: removal of outlier in the WA graph at SVEP VA ~27 c/d changes R^2 value to 0.93. **B.** Image degradation by Bangerter foils (BF). Note: removal of outlier in the Expert graph at SVEP VA ~16 c/d changes R^2 value to 0.92.

4.4.2 *Model 2: SVEP Predicted Acuity Related to Response Amplitude Ratios*

A major impediment related to using linear regression with SVEP data is that data points crucial to the final linear regression prediction of acuity are often responses to high spatial frequency stimuli with amplitudes that are close to noise level (minimal SNR). This is to be expected as the rationale for visual acuity testing, in general, is threshold related. It is thus not surprising to find that the linear regression method yields a strong tendency for the SVEP to underestimate the ETDRS visual acuity, particularly in the high spatial frequency ranges where it is difficult to differentiate small amplitude responses from the noise. At the lower levels of visual acuity, as seen with our increased image degradation conditions, very few points above noise level may be available for the determination of the regression line. Linear regression based on few points is prone to substantial variation and is not uncommonly encountered in SVEP literature that includes low visual acuity conditions (Arai et al., 1997; Good & Hou, 2006; Katsumi et al., 1996; Tyler et al., 1979).

Related to our concerns regarding linear regressions, we devised an innovative approach using the data from points with maximal SNR. As the most abrupt change in amplitude of the SVEP response curve generally occurs between the low and middle spatial frequency responses, two ratios were derived from the mean response amplitude from sets of three points: 1,2,3/8,9,10 (corresponding to spatial frequencies of 0.73, 0.93, 1.07/ 2.77, 3.46, 4.62 c/d) and 3,4,5/ 9,10,11 (corresponding to spatial frequencies of 1.07,1.26, 1.54/ 3.46, 5.54 c/d) (see Figure 11). Comparisons were made between the Expert and the WA techniques for all image degradation conditions using these two sets of ratios (see Figure 17).

For the plus lens condition using WA, both ratios show good linear regressions with the ETDRS visual acuity with the 1,2,3/ 8,9,10 ratio and the 3,4,5/9,10,11 ratio yielding coefficients

of determination values of 0.91 and 0.96 respectively. The ratios using Expert derived data and under the same plus lens condition show reduced coefficients of determination with the 1,2,3/8,9,10 ratio and the 3,4,5/9,10,11 ratio yielding R^2 values of 0.53 and 0.68 respectively (see Figure 17A). Despite the lower R^2 values due to the presence of a broad data point spread in conditions of reduced visual acuity for the Expert, the regression lines and the coefficients of determination for each type of ratio are fairly similar for both the WA and Expert data; one ratio type does not appear to change the predictive potential of this type of measurement under plus lens conditions.

For the BF condition, the R^2 values between the ratios and the prediction of the ETDRS acuity are again higher with WA as compared to the Expert: Wavelet Analysis (ratio 1,2,3/8,9,10 = 0.92; ratio 3,4,5/9,10,11 = 0.66); Expert (ratio 1,2,3/8,9,10 = 0.63; ratio 3,4,5/9,10,11 = 0.46) (see Figure 17B). In this case, both ratios for the Expert technique, as with the plus lenses, show a wide spread of points at the lowest levels of ETDRS visual acuity; this also affected the WA ratio of 3,4,5/9,10,11 that shows a linear fit slope not parallel to the 1,2,3/8,9,10 ratio. With image degradation by BFs, the ratio of 1,2,3/8,9,10 yields a better coefficient of determination compared to the alternative ratio, for both the WA and the Expert techniques.

Overall, these results indicate that WA yields higher coefficients of determination for SVEP prediction of ETDRS visual acuity compared to the Expert technique and that the ratio of 1,2,3/8,9,10 showed consistently higher R^2 values than the ratio using points 3,4,5/9,10,11. Therefore, the change in amplitude from the lowest spatial frequency responses in our series (points 1,2,3) to the peak amplitude region shows a stronger relationship to ETDRS visual acuity than ratios involving points closer to the peak (points 3,4,5), making this curve parameter another useful index to characterize the SVEP response curve prediction of visual acuity. It also

is evident the ratio of 1,2,3/8,9,10 affords higher coefficients of determination between the SVEP predicted acuity and the ETDRS acuity than using the linear regression extrapolation technique alone.

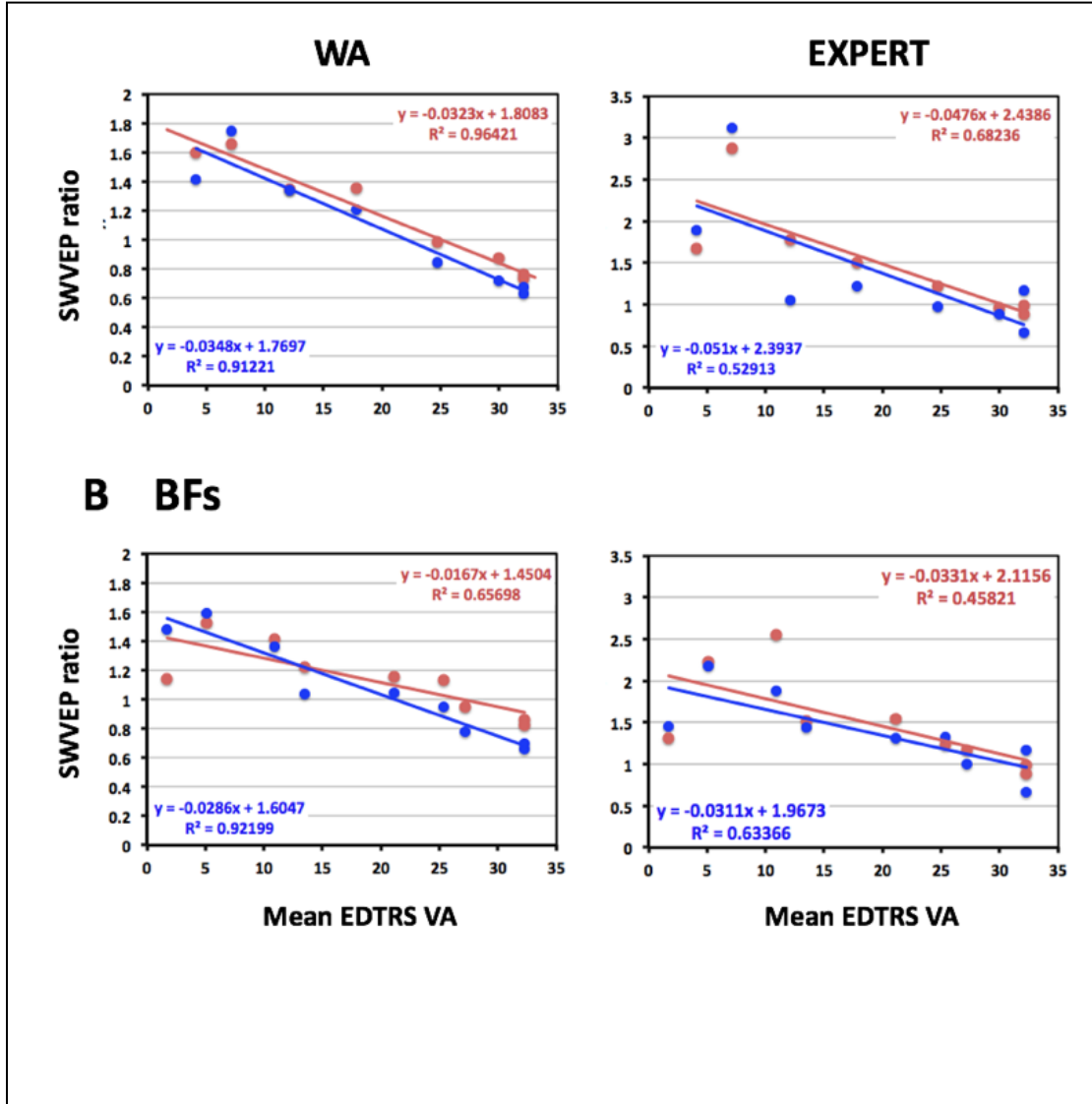


Figure 17: Comparison between ETDRS Visual Acuity (VA) and Two Ratios Based on SVEP Response Amplitudes at Designated Points on the SVEP Response Curve. The two ratios include points 1,2,3/8,9,10 (blue) and points 3,4,5/9,10,11 (red). A. Image degradation using plus lenses. B. Image degradation using Bangerter foils (BF).

4.4.3 *Models 1&2: Measurement Repeatability*

This section provides an assessment of the level of repeatability between the data obtained using our various methods. For this purpose, we used the control trials that were consistently done at the beginning and end of each recording session (total 32) and plotted the results according to the method proposed by Bland & Altman (J. M. Bland & Altman, 1986; M. Bland, 2000). Bland-Altman plots that reveal good repeatability demonstrate a mean that is close to zero and differences from the mean that cluster symmetrically within two standard deviations.

The Bland-Altman graphs for repeatability of control trials (session beginning minus session end) using linear regression extrapolation values obtained by WA and Expert methods can be seen in Figure 18A. Although the main purpose of these graphs is to demonstrate the repeatability of the control trials, note that all participants had good ETDRS acuities ($\sim 6/6$; 30 c/d), that were often underestimated by the SVEP predictions (range: ~ 10 -30 c/d). Both graphs show the difference of the mean to be close to zero with a minimal positive bias. The positive bias of the mean indicates that the intercept values were higher at the beginning than at the end of the testing session; this could indicate a fatigue effect but the values are minimal and likely inconsequential. Whereas the WA graph indicates good repeatability with fairly symmetrical distribution of the data, the Expert graph shows a more positive bias of the mean, increased standard deviations and an asymmetrical distribution of the data with increased variance particularly for higher spatial frequency intercept values (20-30 c/d). A possible explanation for this could be that as the amplitude of the SVEP responses reduces with high frequency stimuli, marking a single prominent peak for the Expert could be more variable compared to the automated WA technique that uses a sum of all the activity in the region of interest.

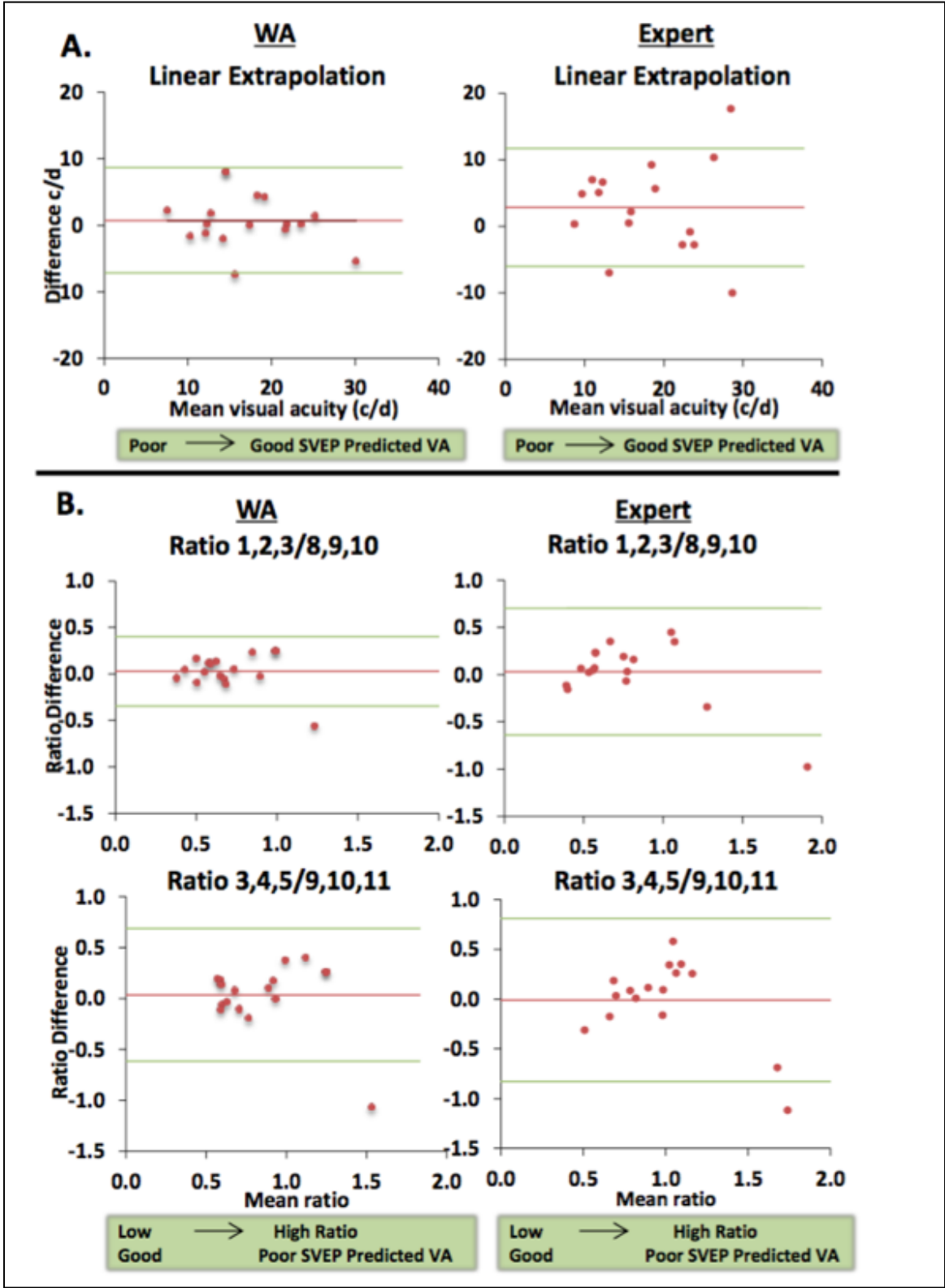
Bland-Altman analyses were also done for the Expert and WA techniques using the two set of ratios (SVEP response curve points 1,2,3/8,9,10 and 3,4,5/9,10,11). Ratio numerators represent responses from low spatial frequency stimuli (points 1,2,3 or 3,4,5) and denominators represent responses from higher spatial frequency stimuli (points 8,9,10, or 9,10,11) (see Section 3.8.4). The Bland- Altman graph using the WA ratio of points 1,2,3/ 8,9,10 shows the smallest standard deviation and optimal repeatability of data amongst the four ratio graphs(see Figure 18B). All graphs show means at approximately zero, small clusters of data at ratios of ~ 0.5 , and increasing data variance with ratios greater than 1.0. This trend can be noted, in particular, with an outlying point found in each graph that has a ratio up to ~ 2.0 (response amplitudes nearing the peak were actually lower than the responses from the low spatial frequency locations) and marked variance (~ -1.0) between control trials.

Our observation of individual control data related to ratios indicates that ratios of ~ 0.5 are associated with typical SVEP response curve morphology (reduced amplitude responses at the lowest spatial frequency stimuli with a peak amplitude for stimuli $\sim 4-8$ c/d) and higher ratios of ~ 1.5 to 2.0, are associated with an atypical SVEP response curve with a peak amplitude occurring with low frequency stimuli. A review of the SVEP waveform morphology for participants and the SVEP trials contributing to the average revealed that some participants were more prone to these atypical waveform morphologies and that repeated trials may show more or less of this atypical SVEP response curve. Such atypical responses may relate to merely individual variation or factors related visual processing (attention, variable fatigue, or retinal rivalry/ binocular inhibition related to monocular occlusion).

The overall Bland-Altman results shows superiority of the WA method compared to the Expert using linear regression intercept and ratios for data analysis; further analysis will use only

WA and the 1,2,3/8,9,10 ratio. However, variability of our control data suggests that analysis methods must be further optimized to afford accurate SVEP visual acuity prediction.

Figure 18: Bland-Altman Analysis Comparing Expert and Wavelet Analysis (WA) using Control Trial Data for SVEP Linear Extrapolated Visual Acuity Levels and Response Amplitude Ratios. A. Repeatability of trials using SVEP linear extrapolated visual acuity. B. Agreement of trials using amplitude ratios at points related to spatial frequencies during the sweep. Ratios using points 1,2,3/8,9,10 (top) and 3,4,5/9,10,11 (bottom).



4.5 Additional and Combined Models for SVEP Predicted Acuity (Group Data)

Using the same group averaged data in above Sections 4.4.2 and 4.4.3 four additional models of the relationship between SVEP predicted visual acuity and ETDRS visual acuity were created based on various parameters of the SVEP response curve (see Figure 11). The additional models and related SVEP parameters are:

Model 3- SVEP Response Curve Peak Position

Model 4- SVEP Response Curve Peak Amplitude

Model 5- Number of Points > 1.6 Times the Mean Noise Level

Model 6- Total Area under the SVEP Response Curve

Using WA data that included group averaged control and image degradation trials, linear regressions between ETDRS visual acuity and the SVEP response curve parameters were generated for the additional Models. Results were compared to the statistics for the Models 1 and 2 from Section 4.4 (see Table 2 and Figure 19).

An overview of the 12 linear regressions seen in Figure 19 reveals that 50% of the models show excellent R^2 values of greater than 0.90 based on this group averaged data. Of the R^2 values > 0.90, Models 2 and 5 (ratio points 1,2,3 and the number of points > 1.6 above the noise level respectively) show the most consistency between image degradation by lenses and BFs. Models 2 and 5 also avoid the outlier that interferes with consistency for Model 1 (lens data).

Dissociation between coefficients of determination based on type of image degradation can be seen in Model 3 and Model 4; the peak position shows a higher R^2 value with BFs (0.82) compared a reduced value with plus lenses (0.66) with a nearly complete reversal of these findings with the peak amplitude (BF: 0.66; plus lenses: 0.81). This dissociation in regards to

peak amplitude could reflect the difference between lenses and BFs on SVEP amplitudes at the initial stages of image degradation seen in Figure 15. The effect of peak position can be seen in Figures 13 and 14 where lenses show a more gradual effect compared to BFs.

In regards to intercept values, the BF data shows overall more consistency and smaller values compared to the lens data.

Figure 19: Various Models for SVEP Visual Acuity Prediction using Linear Regression between ETDRS Visual Acuity and SVEP Response Curve Parameters. Models include: 1) Linear extrapolation; 2) Ratio using points 1,2,3/8,9,10; 3) Position of SVEP response curve peak; 4) Overall peak amplitude; 5) Points $> 1.6 \times$ noise level; 6) Area under the curve. Results include group averaged control trials as well as image degradation trials.

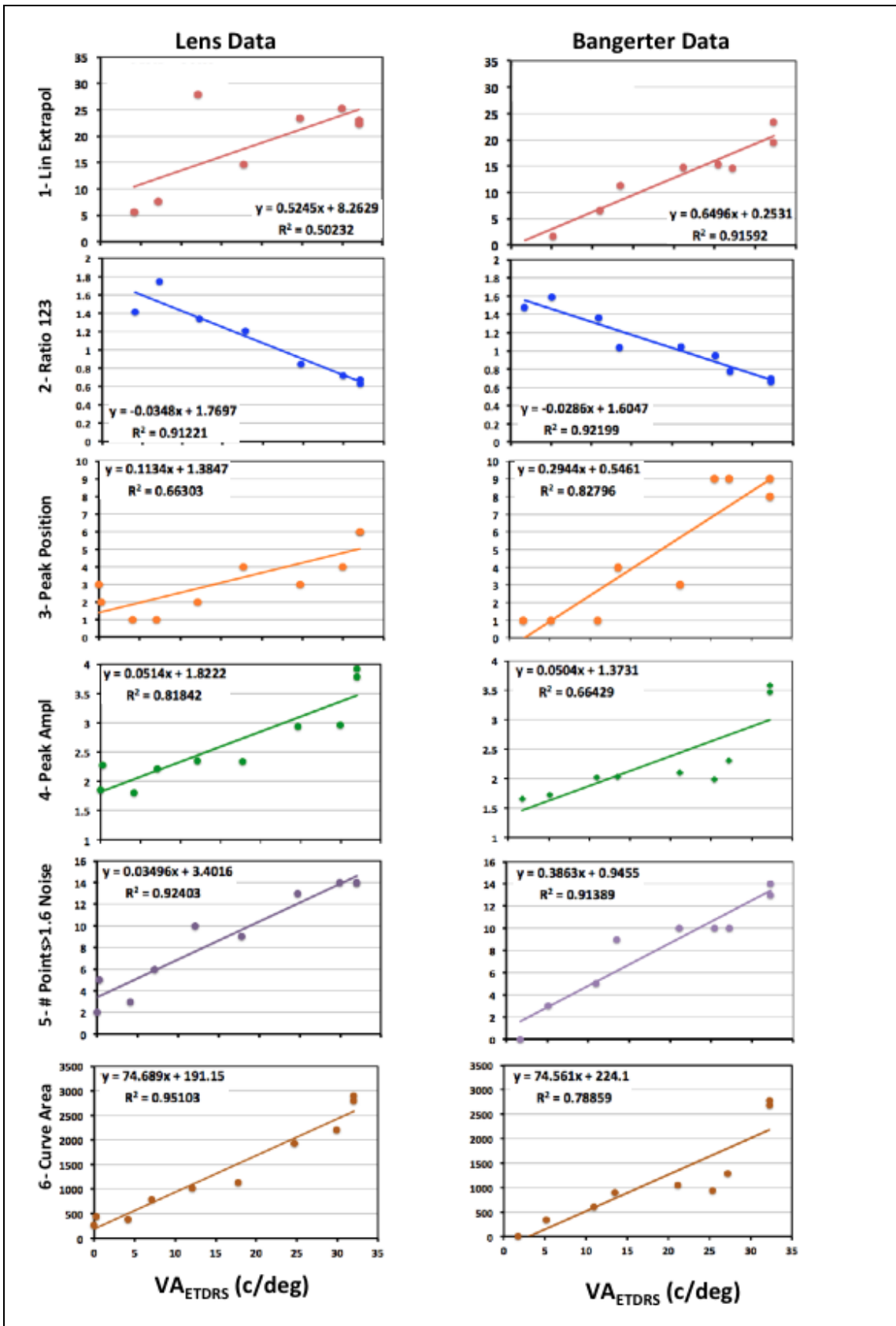


Table 2: Statistics for SVEP Models (Group Data)

Model	Parameter	Condition	Slope	Intercept	r2
1	Linear Regression	Lens	0.525	8.263	0.502
		BF	0.650	0.253	0.916
2	Ratio 123	Lens	-0.035	1.770	0.912
		BF	-0.029	1.605	0.922
3	Peak Position	Lens	0.113	1.385	0.663
		BF	0.294	0.546	0.828
4	Peak Amplitude	Lens	0.051	1.822	0.818
		BF	0.050	1.373	0.066
5	Number of points >1.6X noise level	Lens	0.035	3.402	0.924
		BF	0.386	0.946	0.914
6	Surface under the curve	Lens	74.689	191.15	0.951
		BF	74.561	224.1	0.789

4.6 Additional and Combined Models for SVEP Predicted Acuity (Individual Data)

Although it may be of interest to compare the effects of image degradation related to plus lenses versus BFs using group averaged data, the clinical mandate of the SVEP would likely involve an individual patient that presents with an unknown ETDRS visual acuity and undetermined or combined causes of reduced vision. To address this scenario, data from all individual trials using both types of image degradation (plus lenses and BFs) was analyzed using the six models separately and then combined. In this case, we are treating each data point as independent. However, in the process of combining all image degradation trials in our study, the data set includes repeated measures from individual study participants. Considerations in this regard will be noted and the effect on coefficients of determination will be discussed.

4.6.1 Additional Models for SVEP Predicted Acuity

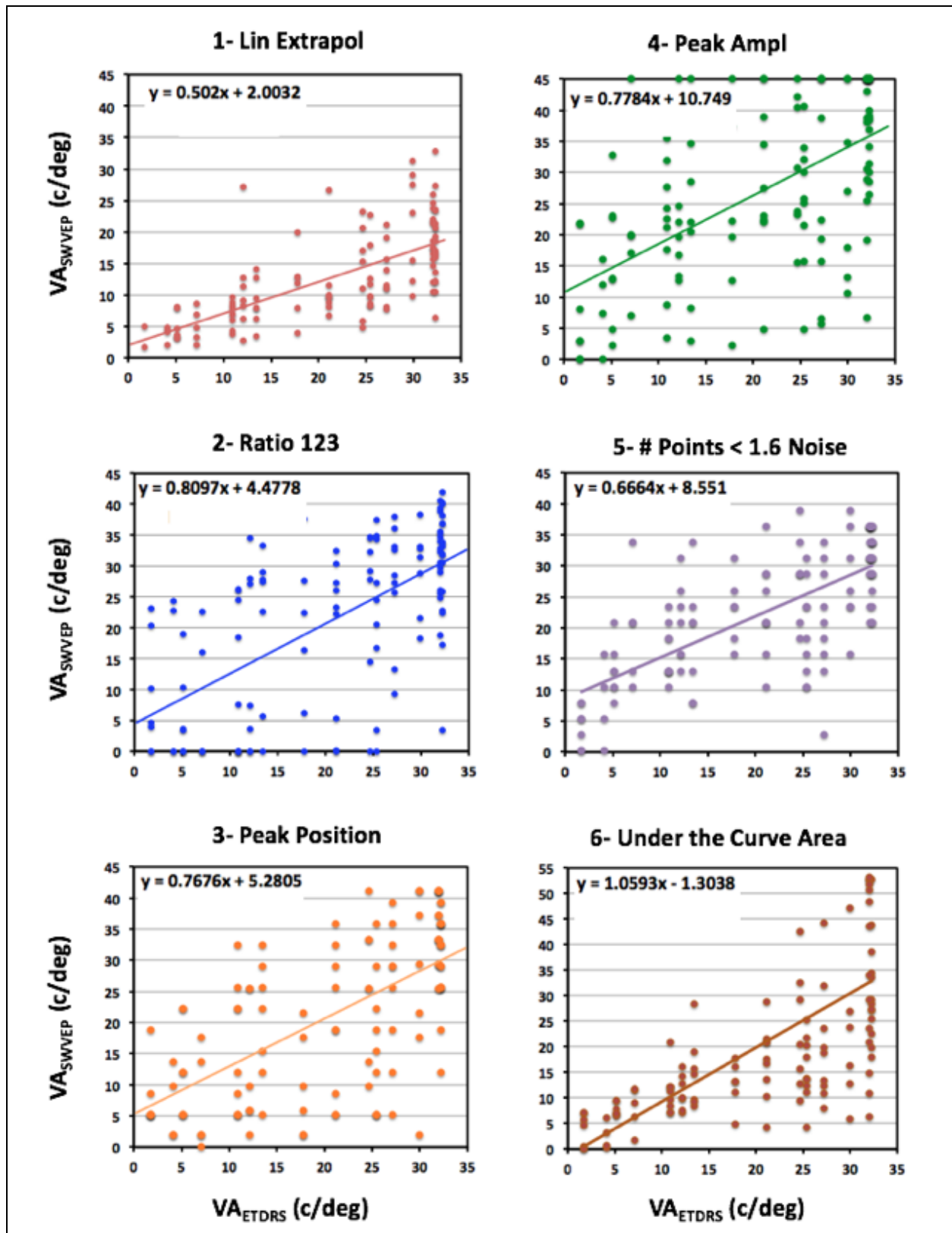
The six models, as applied to the individual data of all image degradation trials, can be seen in Figure 20. Marked variability can be observed in all the models and coefficients of determination are reduced (range: 0.33 to 0.49) compared to the group averaged data shown in Figure 19.

Model 4 shows the lowest R^2 value (0.33) and the highest intercept value (+10.7); this indicates that on an individual basis, the peak SVEP amplitude alone has minimal relationship to ETDRS visual acuity. The highest R^2 values can be seen in Models 1, 5, and 6. Of these, Models 1 and 6 show overall less variability in the data and low intercept values indicating a relationship between SVEP predicted visual acuity and ETDRS acuity. However, the data variability related to the wide range of SVEP predicted visual acuity (even with control trials of ETDRS acuity ~ 32 c/d) would prevent each of these models alone from predicting accurate ETDRS acuity from SVEP data. More accuracy can be seen in Models 1 and 6 at the low range of ETDRS acuity (less than 10 c/d).

The least amount of variability at high levels of ETDRS acuity (~ 32 c/d) can be seen with Model 5 that has the highest R^2 value (0.49) but significant data variability at other ETDRS acuity levels throughout the graph indicates this model alone would be a poor predictor of ETDRS visual acuity. However, it is of interest that Model 5 reduces data variability at high levels of ETDRS acuity. The SVEP amplitudes are small at this location on the response curve and variability could be due to the including data points adjacent to noise level that fall within the inclusion criteria for the linear regression. Such data points are very influential on the final SVEP linear regression and data points in this location can create outlying results (see +2.00 data Figures 13, 15A, 16A).

Although high levels of variability can be seen in the individual data, some models show potential along the spectrum of ETDRS visual acuity and a combination of all models may show an improved overall coefficient of determination between ETDRS acuity and SVEP predicted acuity.

Figure 20: Models for SVEP Visual Acuity Prediction using SVEP Response Curve Parameters Compared to ETDRS Visual Acuity. Models 1-6 include: 1) Linear extrapolation; 2) Ratio using points 1,2,3/8,9,10; 3) Position of SVEP response curve peak; 4) Overall peak amplitude; 5) Points > 1.6 x noise level; 6) Area under the curve. Results show participant individual data (not group average) with control and image degradation trials using wavelet analysis.



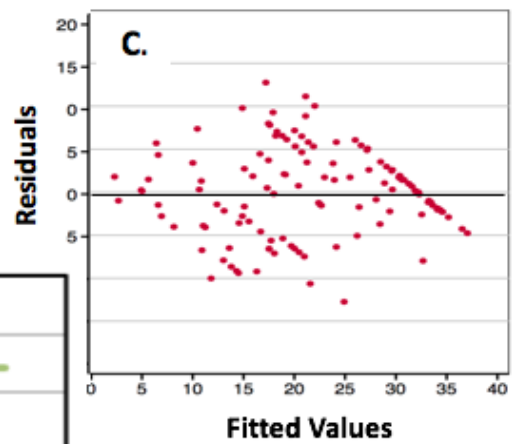
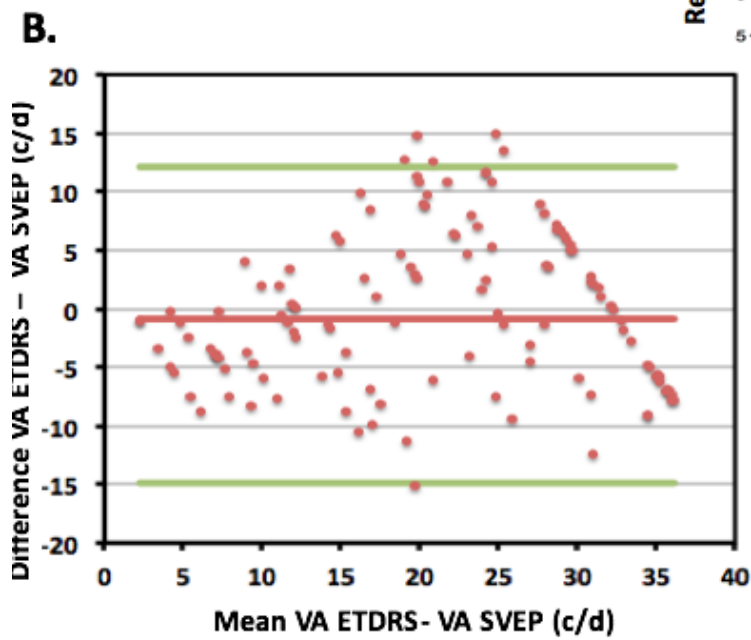
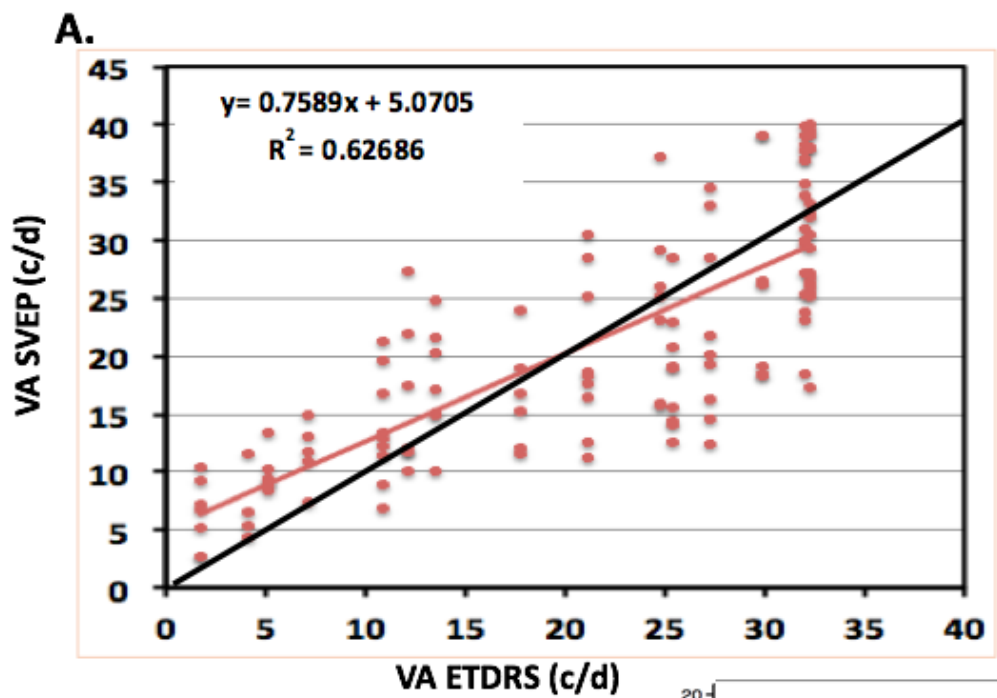
4.6.2 *Combined Models for SVEP Predicted Acuity and Agreement with ETDRS Acuity*

Continuing on with individual data and all image degradation conditions, Models 1-6 were combined and associated with a Bland-Altman analysis to assess overall linear regression and agreement between SVEP predicted visual acuity and ETDRS acuity (see Figure 21). The overall linear regression yields a R^2 value of 0.62 and displays the tendency for the SVEP to underestimate high levels of ETDRS acuity and overestimate low levels of ETDRS acuity as afforded by image degradation (see Figure 21A). The variability generally decreases as ETDRS visual acuity declines, but the highest levels of acuity with the control data shows SVEP predicted acuity variation ranging approximately 20 c/d (~ 4 lines on ETDRS chart). The data variation at the lowest ETDRS visual acuity levels spans less than 10 c/d (~ 2 ETDRS lines). This level of variation approximates the clinical standard related to the adult test/retest variability of ETDRS acuity that requires > 2 ETDRS line difference to indicate a significant change in visual acuity (Arditi & Cagenello, 1993; Rosser et al., 2003). This would suggest that the SVEP shows accuracy in detecting true markedly reduced visual acuity (based on our imposed image degradation) but is otherwise subject to substantial variability.

However, it must be noted that our set of individual data does involve participants who underwent repeated measures. Bland & Altman (1995) has proposed analyzing such repeated measures data using an analysis of covariance technique that shows the best fit lines between the repeated measures in the data and can yield a coefficient of determination. We analyzed our combined Models 1-6 data with this technique; an improved R^2 value of 0.72 was obtained (see Appendix F). Although such repeated measures data and a R^2 value of 0.72 would not be used for clinical assessments, this does suggest that as our R^2 value of 0.62 may be inherently overestimated due to the presence of repeated measures.

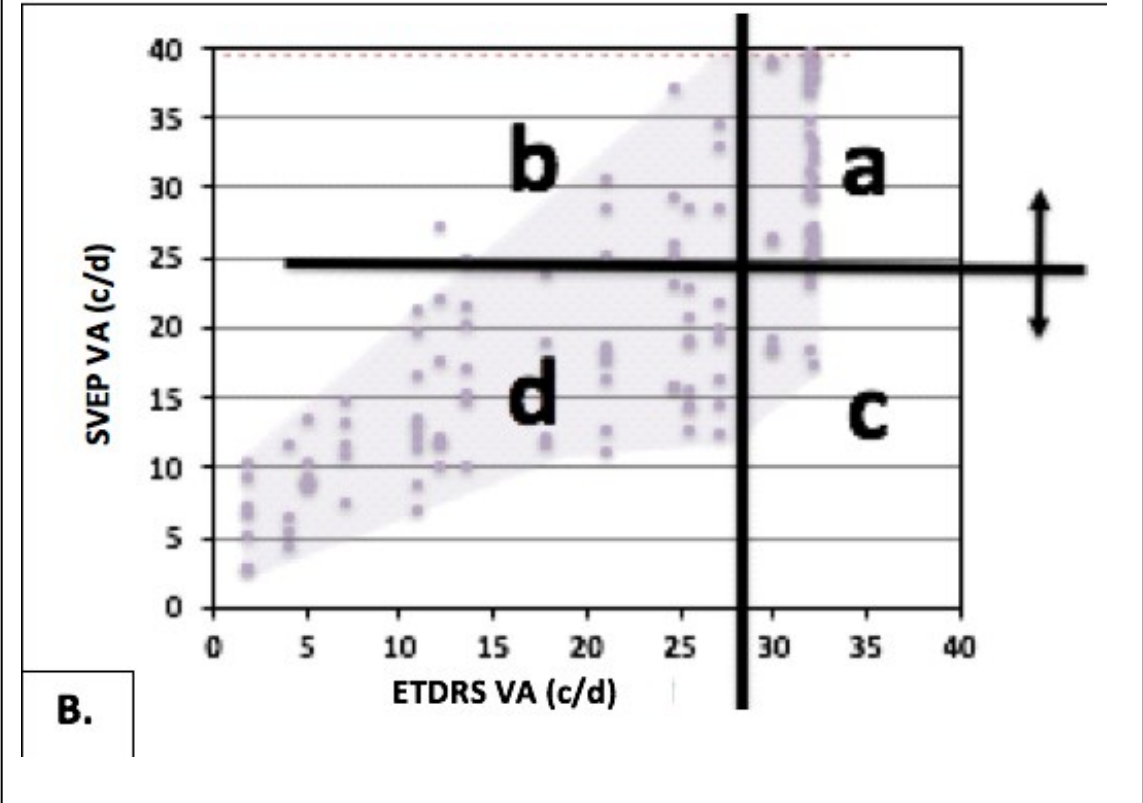
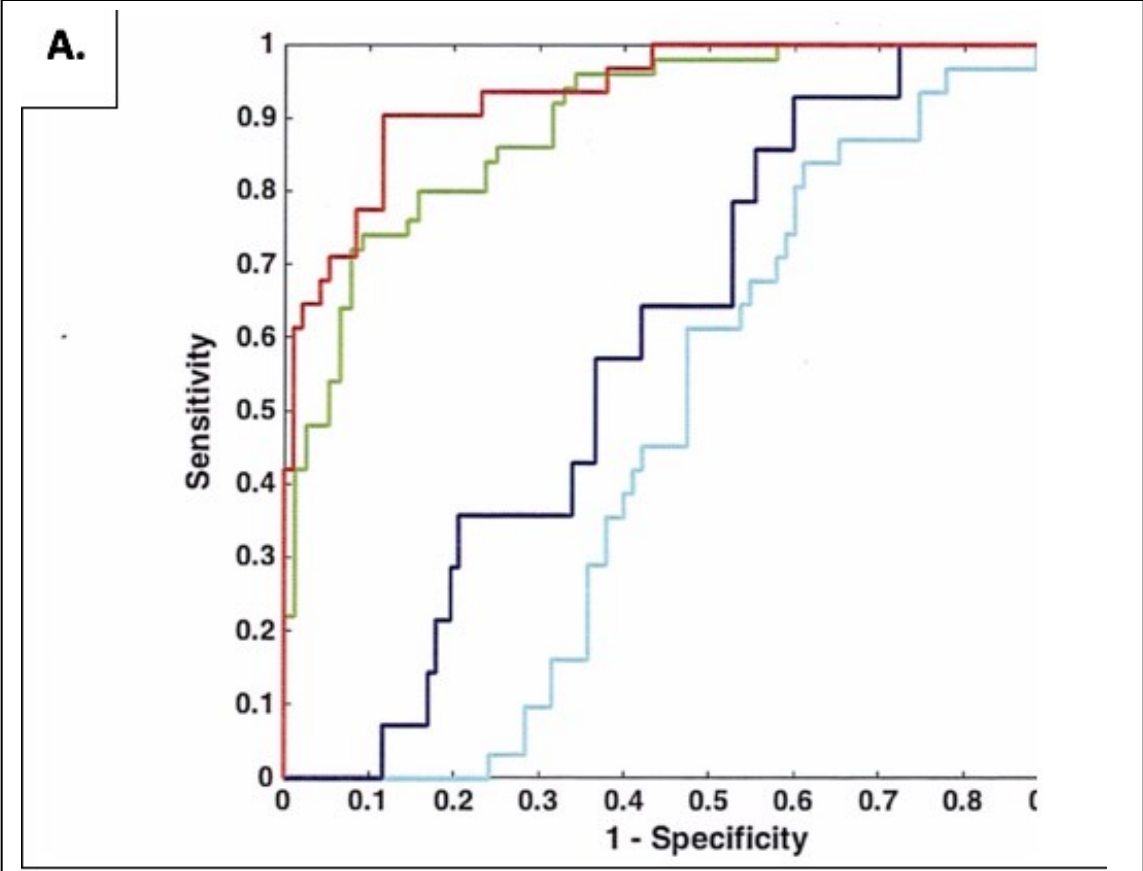
The associated Bland-Altman graph based on the combination of Models 1-6 (Figure 21B) shows an overall poor agreement between SVEP predicted acuity and ETDRS visual acuity. The mean (ETDRS-SVEP = -0.95 c/d) is slightly below zero indicating that overall mean ETDRS acuity is minimally lower than SVEP predicted acuity. The 95% CI is shown based on 1.96 SD from the mean (SD: 7.11 c/d). Also, the data points are not equally distributed around the mean. The inconsistent variation shows poor agreement between the two methodologies at the middle range of mean visual acuity levels from 10-30 c/d with better agreement beyond this range where data points are more tightly clustered (<10 and > 30 c/d). Adjacent to the Bland-Altman graph is a small graph showing the plotting of residuals related to the linear regression—yielding essentially identical conclusions about the data distribution.

Figure 21: Combination of all Models (1-6) for SVEP Visual Acuity Prediction using SVEP Response Curve Parameters and ETDRS Visual Acuity Levels. A. Overall correlation showing data variation and tendency for SVEP to underestimate high levels of ETDRS acuity and overestimate low levels of ETDRS acuity. B. Bland-Altman analysis showing the level of agreement between SVEP and ETDRS visual acuities. C. Small graph shows plotting of the linear regression residuals showing similarity with the Bland-Altman plot. Results show participant individual data (not group average) with control and all image degradation trials using wavelet analysis.



To assist in obtaining a general overview of the sensitivity and specificity of our SVEP to predict ETDRS visual acuity levels, we divided our individual data into four acuity levels and applied ROC curves to each of the acuity subgroups (see Figure 22). The visual acuity subgroups were: high VA (> 27 c/d; ETDRS better than $\sim 6/7.5$; green line); high intermediate VA (27-17c/d; ETDRS $\sim 6/7.5 - 6/9.6$; light blue line); low intermediate VA (15-10 c/d; ETDRS $\sim 6/12 - 6/19$; dark blue line); low VA (< 10 c/d; ETDRS- 6/24 or worse; red line). The AUC levels for each group were as follows: normal VA: 0.90; high intermediate VA: 0.51; low intermediate VA: 0.62; low VA: 0.94. These results, based on our simulated VA levels using image degradation techniques, indicate that the SVEP test is accurate to determine both ends of the VA spectrum (VA better than 6/7.5 or worse than 6/24), but show near chance levels to predict intermediate levels of acuity (6/7.5-6/19).

Figure 22: Receiver Operating Curve for SVEP Individual Data and Chart Illustrating the Method Related to ROC Calculation. A. Red line: Low visual acuity (ETDRS 6/24 or worse; AUC = 0.94). Green line: High visual acuity (ETDRS better than 6/7.5; AUC = 0.90). Dark blue line: Low intermediate visual acuity (ETDRS $\sim 6/12 - 6/19$; AUC =0.62). Light blue line: High intermediate visual acuity (ETDRS 6/7.5- 6/9.6; 0.51). B. The classic categories related to ROCs are shown superimposed on the SVEP/ETDRS (also seen in Figure 25). The ROC categories are as follows: a = true positives, b = false positives, c = false negatives, d = true negatives. The arrows indicate the technique for determining the number of responses that fall into categories a. or c. at the chosen location of ETDRS 27 c/d (green line on the ROC). The process was then repeated at each of the other 3 ETDRS acuity locations that relate to the remaining lines on the ROC.



4.6.3 *Models Combinations for SVEP Predicted Acuity*

Although the overall linear regression yields a coefficient of determination of 0.62 using all Models 1-6 combined for individual data, and each model alone showed poor R^2 values (<0.50), it is possible that various combinations of the models could yield coefficients of determination with higher values than all models combined. Binary combinations were performed using all 6 models to see if the coefficient of determination results could be further optimized (e.g. binary combinations 000000, 000001...111110, 111111). Binary combination results with coefficients of determination higher than 0.61 are shown in Table 3.

Potential optimization using various combinations of models seen in Table 3 indicates that the coefficient of determination can be improved to 0.65 (still not as high as group data but improved over the R^2 value of 0.62 for individual data using Models 1-6 combined). Although this is a minimal improvement, it is interesting to look at the models that contribute to the highest values. The effect of using a ratio (Model 2) has a high frequency (100%) for higher coefficient values above 0.61. For coefficient of determination values of over 0.62, Models 1,2,4 are the most frequent and consistent contributors. Of the remaining models, it appears that using points > 1.6 times the noise level (Model 5) is more useful than the total area under the curve (Model 6) with the position of the SVEP peak (Model 3) as the less useful model for optimization.

Table 3: Combination Analyzes of Various SVEP Parameter Models

1	2	3	4	5	6	r^2
						0.6527
						0.65101
						0.63668
						0.63546
						0.63173
						0.62686
						0.62584
						0.62498
						0.62064
						0.6132
						0.61266
						0.60957
						0.60918
						0.60917
						0.60879
						0.60712
10/16 62.5%	16/16 100%	6/16 37.5%	13/16 81.2%	10/16 62.5%	9/16 56.2%	

4.7 Review of Normative SVEP Response Curves and Subgroups (Individual Data)

Due to the overall high data variability seen between individuals, the raw data of the SVEP response curves were reviewed. Seven participants that had accomplished all testing conditions (all control and image degradation trials) were chosen. The control trials for this group can be seen in Figure 23A. Despite the presence of good ETDRS visual acuity in all of these individuals (≥ 30 c/d) a variety in SVEP response curves can be seen. In particular, the peak amplitude of the SVEP response curves shows an apparent dichotomy that appears to be organized into two groups: 1) normative large peak amplitude; 2) normative small peak amplitude (see Figure 23B). Although such a dichotomy in normative SVEP literature has not been highlighted in other SVEP reports, one study does indicate that recordings from two normal subjects were excluded from their analyses due to reduced SVEP amplitudes (Ridder, McCulloch, & Herbert, 1998).

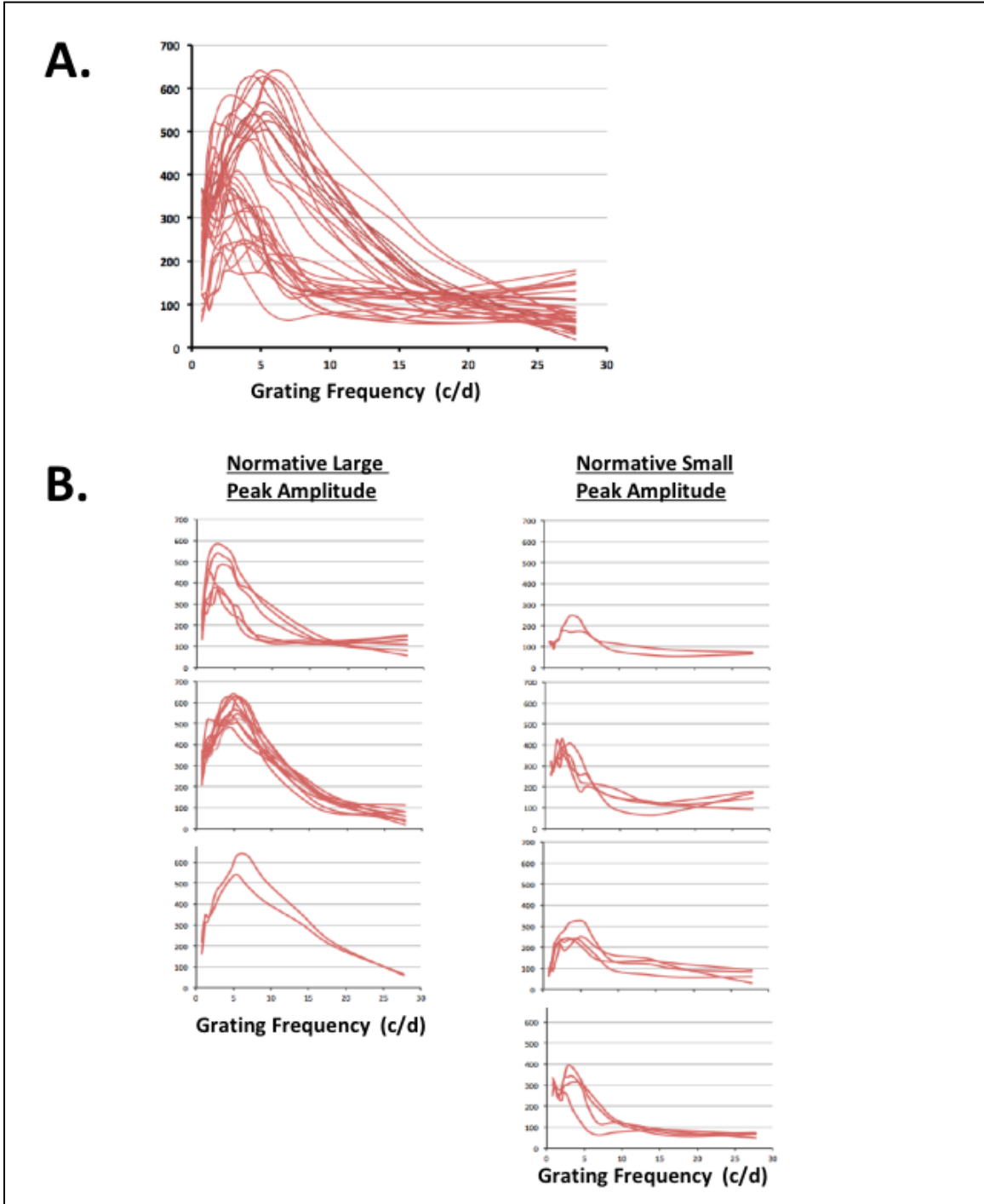
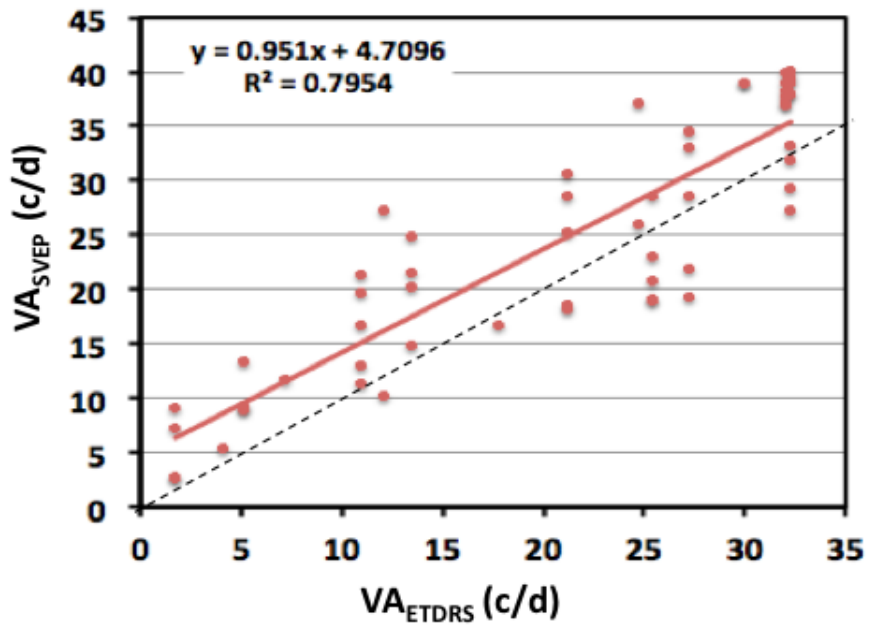


Figure 23: Variation in Normative SVEP Response Curves. A. Composite of seven individuals showing a variety of peak amplitudes. B. Separation into two subgroups (normative large versus small peak amplitude).

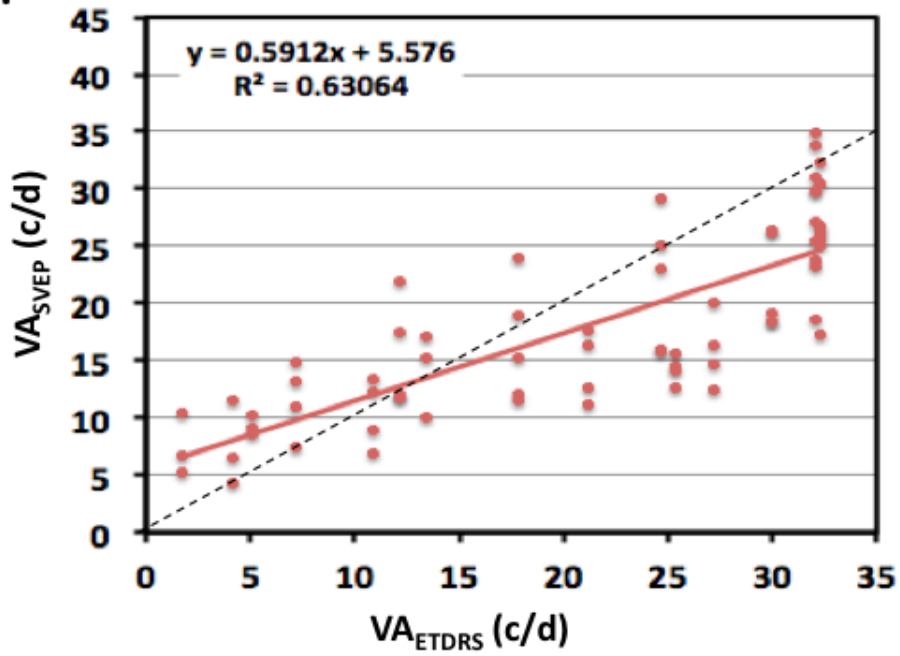
Using the combined analysis Models 1-6 on the two subgroups of normative SVEP response amplitudes shows generally less variability in the data. A high coefficient of determination (0.80) is present for the group with normative large SVEP peak amplitudes and, although the SVEP shows an overall tendency to overestimate ETDRS acuity, the variability is reduced and the slope of 0.95 yields consistency over the span of ETDRS visual acuity levels (see Figure 24A). The variability of SVEP predicted visual acuity is within one octave at most locations, a reasonable variation related to clinical ETDRS visual acuity test/retest values. The combined analysis Models 1-6 for the normative low SVEP amplitude group shows reduced coefficient of determination (0.63) compared to the high normative amplitude group; the relationship is similar to the initial linear regression (see Figures 24 B and 21A). Although noting high vs. low normative amplitude of the SVEP response curve may be a useful clinical tool in some cases (if high amplitude responses, likely more accurate SVEP acuity prediction), low normative amplitudes appear to be quite common in our population thus suggesting increased inaccuracy in SVEP visual acuity predictions in such cases.

Figure 24: Combination of all Models (1-6) for SVEP Visual Acuity Prediction (SVEP Response Curve Parameters Compared to ETDRS Visual Acuity) for Two Subgroups. A. Subgroup with normative large SVEP peak amplitude. B. Subgroup with normative small SVEP peak amplitude. Results show participant individual data (not group average) with control and image degradation trials using wavelet analysis.

A.



B.



CHAPTER 5: DISCUSSION

Clinical application of SVEP technology has been relatively slow to be adopted and is not in widespread use currently. This may be partially due to the fact that SVEP research has utilized steady state acquisition systems (whereas transient state acquisition is more common in clinical settings) as well as substantial variability in SVEP data — particularly in clinical populations with a variety of ocular system disorders (Arai et al., 1997; Gottlob et al., 1990). This project addresses these factors by outlining procedures to utilize new transient SVEP technology (VERIS™) that may be more adaptable to clinical settings. In this section, we will relate our design considerations and technical modifications, compare our findings to previous SVEP studies, and discuss new analysis models to address SVEP data variability.

5.1 Transient Sweep Visual Evoked Potential

5.1.1 Population Design Considerations

After reviewing SVEP literature from the initial studies in the 1970s, there were several design characteristics that appeared to be appropriate going forward. We chose to use a visually mature adult population. This avoids visual developmental issues that eventually became clear and impacted the validity of early SVEP and PVEP studies that predicted adult recognition acuity levels in infants 6-8 months old (Norcia & Tyler, 1985b; Sokol, 1978). Since these early studies, several advances improved our understanding of pediatric visual acuity and predictions of recognition acuity based on grating stimuli: development of ETDRS comparable childhood recognition acuity test; eventual improved understanding as to how resolution and recognition acuity compare; comprehension of developmental processes that impact these acuity types with resolution tests overestimating recognition acuity prior to ~ age 6 yrs. and underestimating recognition acuity beyond this age; detection of developmental improvements for optotype

acuity between age 6 -18 yrs. (Hargadon et al., 2010; Kushner et al., 1995; Leone et al., 2014; Mulla, 2007; Ohlsson & Villarreal, 2005; Prager et al., 1999; Riddell et al., 1997). These factors and the history of SVEP acuity predictions from early studies informed our current expectations.

To get an initial overview of our transient SVEP technology, we preferred to reduce variability as much as possible by having a small number of subjects tested under numerous conditions, when possible. We were able to gather a small population that had many characteristics typical of our clinical practice including refractive errors (corrected myopia and hyperopia, uncorrected latent hyperopia). However, unlike some individuals in our clinical population, our SVEP test population was composed and cooperative and thus provided ideal SVEP testing conditions. Although development of a new test is best done under ideal conditions initially, the results may not be predictive of clinical populations. However, even our preliminary results reveal that a stellar SVEP response curve is very unlikely to be related to low vision and vice versa (see Figure 22) may be applied cautiously at this point for cases of low vision and suspected functional vision loss that comprise a good portion of our referral base.

5.1.2 Technical Considerations and Modifications

Attention to the stimulus is of utmost importance when developing a new SVEP test. The acquisition system and the monitor must provide: high resolution; no aliasing or raster effects that might contribute to the evoked potential separately from the pattern; no luminance change during acquisition (flash artefact) that contaminates the PVEP. Flash artefacts interfere with the PVEP response that should be obtained under luminance neutral conditions (no luminance change due to balanced black and white check alternation). Flash effects during PVEPs evoke a cortical response not related to visual acuity (contrast between high spatial frequency gratings) but rather solely due to a change in luminance.

With our initial VERIS™ Version 6.4 we tried our routine CRT monitor and an available used LCD monitor but both set-ups yielded image aliasing with high spatial frequencies. We obtained a new LED/LCD high definition monitor (further referred to as the LCD monitor) and increased the viewing distance but resolution was still suboptimal. We were then able to obtain a VERIS™ Version 6.4 update that afforded a new synchronization interface and software adjustment that matched the monitor pixel size. At this point resolution was optimized. However, by observation, we suspected a flash effect due to the LCD monitor and detected related increases in implicit time. As the LCD monitor was to be used for the SVEP test, all flash effects and the related implicit time delays had to be resolved prior to proceeding.

We investigated the flash effect by comparing our routine PVEP test conditions with a CRT monitor to the new LCD monitor under conditions of a light perception BF (see Methods section 3.1). Concurrently reports became available relating a problematic flash component with LCD monitors (Fox et al., 2014; Matsumoto et al., 2013; Matsumoto et al., 2014). Matsumoto (2013) found this to be due to an inherent reduction in the monitor luminance related to the timing between the shifting of liquid crystal molecules to align for light passage especially when shifting from black to white stimuli. Although such a flash effect may not be obvious to casual observers, under testing conditions, it was found that the flash was sufficient to trigger an electroretinogram as well a flash VEP (Matsumoto et al. 2013). Matsumoto et al. (2013) promoted reducing stimulus contrast, through polarizing layers. Our flash effect was ameliorated with an adaption to the m-sequence that added one black frame in the sequence. This innovative adaptation reduced contrast and luminance slightly but resolved the flash effect with PVEP (see Figure 7) and was utilized for our SVEP.

The new OLED (organic light emitting diode) monitors show more agreement with the CRT monitors and, although expensive at this time, these may afford a viable alternative to LCD monitors (Matsumoto et al., 2014). These monitor issues are important considerations for visual electrodiagnostic laboratories as CRT monitors are being phased out and it appears that LCD monitors may either require acquisition modifications, a translation factor to assist with patient follow-up, or laboratories will need to create a new LCD- related normative data bank.

5.1.3 SVEP Trials and Response Curve Characteristics

After technical modifications, our initial SVEP response curves trials with visually normal participants were readily accessible using VERIS™ Version 6.4. We did note that individual sweeps showed substantial variation even under optimal testing conditions; therefore, one trial was an average of 3 or 4 sweeps depending on noise levels during acquisition. Based on the variability that we noticed for individual sweeps, we consider averaging at least 3 sweeps should be necessary for a reliable trial; optimally the trial could then be repeated. Based on our SVEP experience, we would be cautious to report SVEP results if a clinical scenario allows an insufficient number of sweeps to be included in a trial or a repeat of that trial.

We did not investigate if the best trial result should be reported or the average of two trials. Although this has been debated in other SVEP reports, there is no definite conclusion at this time (Gottlob et al., 1990; Kurtenbach et al., 2013; Lauritzen et al., 2004; Norcia & Tyler, 1985a; Prager et al., 1999). Based on our experience with routine clinical PVEPs and now the transient SVEP, we see the benefit of averaging several sweeps to obtain a trial (an average of 3-4 sweeps) but amongst trials we would generally consider the best trial to be indicative of the potential of the visual system — barring noise levels or the presence of artifacts that might be

exaggerating the results. With our current transient SVEP test, accuracy of the test in clinical settings would be a concern if patient cooperation prevents sufficient averaging.

Initially, we used only subjective marking of the response waves (Expert) with the resulting data points contributing to the SVEP response curve and peak to base linear regression. It was very apparent that responses to high spatial frequency stimuli (low amplitudes near visual threshold) highly influenced the SVEP predicted acuity (one data point at this low end response curve could swing the linear regression substantially). Although some visually normal participants showed promising prediction of ETDRS acuity by SVEP linear regression, this was not consistent between participants in our early trials. As our objective is to implement SVEP testing for predictions of visual acuity for individual patients, we became very aware that understanding both population-averaged data (group data) and individual data would be necessary for clinical application.

Historically it is not uncommon to see mainly population-averaged data shown in SVEP literature with only samples of individual data displayed, however the importance of showing the overall individual variability will be key to clinically based studies (Lauritzen et al., 2004; Prager et al., 1999). Although SVEP data used to predict visual acuity can show substantial variability, the SVEP appears to work well for interocular comparison such as comparing an amblyopic eye to the fellow eye (Ely et al., 2014). The SVEP has also shown high sensitivity and specificity for pediatric vision screening as reported by Simon (2004). However, despite the apparent good results for vision screening, the SVEP has not become a widespread vision screening tool (Committee on Practice and Ambulatory Medicine, 2016; Sabri et al., 2016; American Association of Pediatric Ophthalmology, 2014).

As related to our previous experience with clinical PVEPs, we were quite accustomed to not only look at VEP measures of amplitude and implicit time, but to also consider wave form morphology (Regan, 1989). With early pilot experiments using image degradation, other than noting changes in the peak to base linear regression, we noted changes in SVEP response curve morphology. As the image was degraded several morphological changes occurred: the peak shifted towards low frequencies; the peak amplitude reduced; the ratio between the low frequency responses and the SVEP peak changed; the area under the curve reduced; and it occurred to us that points substantially above a noise level may be more contributory to the determining SVEP results than small amplitude points at high spatial frequency (see Figures 13 and 14). Observing these fundamental characteristics offered a gestalt of SVEP morphological changes related to image degradation; these factors eventually became contributory to our study as analysis Models (1-6). We have not seen a similar modelling approach to SVEP analysis, but preliminarily, this approach appears to be a useful alternative to linear regression alone.

5.1.4 Challenges to Expert Markings and Use of Wavelet Analysis

Studies based on the Diva and Enfant systems use high frequency stimulus presentations that yield steady state evoked potentials that can be easily quantified automatically by extracting the power of the Fourier transform. The VERIS™ technology is based on generation by m-sequence and, even though the stimulus presentation related to the m-sequence is more rapid than all previous methods, the extraction algorithm produces transient waveforms. The transient waveform depends on visual identification of components and thus is subjective. Although adhering to the strict criterion for wave marking was upheld by the Expert this was not always satisfying as consistency yielded variable SVEP predicted acuity estimates. Wave marking was most problematic at the extreme spatial frequencies when amplitudes could be small and noisy

for control trials and throughout the sweep under conditions of extreme image degradation. For these reasons, we decided to use the WA as a way to automate the quantification of our evoked potentials.

Matching a signal to a wavelet is done by generating correlations between the wavelet and the signal and also by subjective visual quality of the match. Through trial and error we chose to use the Haar wavelet although several wavelets appeared to match very well to the SVEP waveform. Our work with WA started prior to a report by Hassoney et al.(2012) who ran a systematic analysis using the longest common subsequence and basic local alignment search tool to determine the optimal wavelet match for a standard visual evoked potential. Their best results were with the *coiflet5* wavelet that showed optimal results for a high amplitude VEP with noise; it is yet to be determined if this wavelet would also be optimal for the low amplitude SVEP responses as seen with our image degradation conditions or as reported with organic disease (Arai et al., 1997; Good & Hou, 2006; Thompson, Moller, Russell-Eggitt, & Kriss, 1996).

5.2 SVEP Parameters Related to Image Degradation: Initial Analysis Models

As is typical with research and development of new techniques, many SVEP studies have gathered normative data involving well seeing populations. However, clinical populations show a range of visual acuities related to functional, refractive, or organic conditions — singularly or in combination. Our purpose with vision degradation models is to determine an analysis technique that is robust with various levels of visual acuity, albeit simulated at this point. However, this information will likely contribute to comprehension of eventual data acquired on clinical populations.

Another purpose related to our design involving two types of image degradation techniques is to ostensibly differentiate the causative factors of visual complaints in some

patients based on SVEP data characteristics. With further research and by incorporating clinical findings, SVEP results with organic disorders may relate more so to our BF results (reduced contrast typical of optic nerve pathologies). Also, as optical defocus alone is present at times in our referral population, identification based on SVEP results may assist in ruling out purely refractive disorders from organic concerns. Despite previous reports of SVEPs tested with optical defocus (Katsumi et al., 1996; Ridder et al., 1998; Thompson et al., 1996; Tyler et al., 1979) or Bangerter foils (Bach et al., 2008; Kurtenbach et al., 2013), we could not find a study that offers a comparison between the two image degradation conditions in the same setting similar to our design.

5.2.1 Image Degradation Data: Expert versus Wavelet Analysis

As WA appeared to offer many advantages compared to the Expert for our SVEP data analysis, it was important to assess the relationship between WA and Expert over the range of SVEP amplitudes associated with each type of image degradation.

The linear regression results between the WA and Expert for SVEP based on individual data shows amplitude measurements had high coefficient of determination values for both image degradation conditions (see Figure 12). However, the distribution of the data points varied between the two conditions with the BF condition showing data closely aligned to the regression line throughout the amplitude range and the optical defocus data displaying more variability particularly in the middle to high amplitude region. It is apparent from these results that low amplitude responses (generally related to poor visual status/severe image degradation) are quite consistently measured by WA and the Expert for both types of image degradation. However, the WA tends to yield higher and more variable amplitudes than the Expert as the amplitude

increases with the plus lens condition (generally related to better visual status/ reduced power of plus lenses).

One might consider that the higher amplitude measurements by WA compared to the Expert with optical defocus could relate to the fact that the WA amplitude measurements are derived from a region rather than the single point chosen by the Expert. However, as the BF data shows consistency through the amplitude spectrum, the difference between the BF and optical defocus data is more likely due to the nature of the image degradation. The BFs yield a diffuse image obscuration related to microbubbles in the plastic whereas optical defocus affects spatial frequencies in an irregular fashion that can yield lighter and darker bands (spurious resolution or phase shifts) (Perez et al., 2010). It may be possible that optical irregularities with defocus could contribute to an evoked potential particularly as amplitudes decline with moderate powers of plus lenses. Also, the high amplitude, somewhat sporadic, irregularity in plus lens data as compared to the BF data may relate to minimal plus lenses correcting small amounts of latent hyperopia found in some subjects.

Although we incorporated a two meter SVEP viewing distance to reduce accommodative effects and our subjects with small amount of latent hyperopia rejected the plus correction for ETDRS visual acuity, such a minimal correction may have resulted in higher SVEP amplitudes from our participants with latent hyperopia. In this circumstance, plus lens correction could yield an overall higher amplitude for the WA (more activity in the region of interest) compared to the Expert who marks a single wave. Our SVEP sine wave display could also relax accommodation in the presence of latent hyperopia as opposed to the mainly square wave spatial frequencies present on ETDRS charts and correction of the latent hyperopia could be beneficial for SVEPs.

This information supports our clinical impression that the correction of latent hyperopia,

in certain individuals, can improve a PVEP considerably despite the rejection of plus lenses for ETDRS acuity testing. For example with anisometric latent hyperopia, we have seen the resolution of an asymmetric PVEP (reduced amplitude and increased implicit time of the more hyperopic eye) resolve with plus lens correction. Testing with and without lenses in such a case can rule out more ominous causes for an asymmetric PVEP.

Although one might suggest that cycloplegia and lens correction should be implemented to avoid data variations due to latent hyperopia, optimal VEP conditions include a natural pupil (Brigell, 2001; Odom et al., 2006). A perusal of other SVEP and PappVEP studies related to visual acuity prediction and optical defocus revealed typically no mention of cycloplegia (Katsumi et al., 1996; McBain et al., 2007; Ridder et al., 1998; Thompson et al., 1996; Tyler et al., 1979). Displays of individual subject data in some of these studies show some examples of maintenance of good acuity with minimal plus correction suggesting that slight amounts of latent hyperopia are likely present in such studies (Katsumi et al., 1996; McBain et al., 2007).

Overall, despite some minimal differences, our application of WA to SVEP data shows a good linear relationship to the Expert for transient SVEP amplitude measurements.

5.2.2 SVEP Acuity Predictions: Linear Regression Model

Related to the overall good relationship between WA and Expert, the WA data was used to display the specific effects of each level of image degradation on the SVEP response curves. The response curves and a comparison between the ETDRS acuity and the SVEP estimated acuity by linear regression for the group data are displayed in Figures 13 and 14. Our transient SVEP response curves show similarities to other reports using steady state SVEP methodology and image degradation (Bach et al., 2008; Katsumi et al., 1996; Kurtenbach et al., 2013; Ridder

et al., 1998; Tyler et al., 1979); however, methods of creating the linear regression and determining which data points to include in the regression vary.

In regards to points included in our linear regression, we consistently took the peak amplitude of the SVEP response curve and from that point (in the direction of higher spatial frequencies) included any data point above noise level to the final descending amplitude beyond which point the linear regression was extrapolated to zero. Data points beyond this location were disregarded. We did not veer from our criteria even though data outliers were created as can be seen in Figure 13 with +2.00 lens where inclusion of the last data point, that could otherwise be debatable, changed the SVEP predicted acuity substantially to yield a marked over prediction of the ETDRS acuity. For any criterion that is determined for the choice of points to be included in the linear regression, one must consider that in a clinical situation, there would be no prior knowledge of the ETDRS acuity. The difficulty in choosing one consistent method to create the linear regression can be seen in reports by Ridder et al. (2007; 2014) that allow a choice between three options either: 1) a peak to base linear regression; 2) if there is a high amplitude data point beyond the linear regression, directly extrapolate to zero from that one point; 3) if the two methods can both be applied to the data, the one with the higher SVEP predicted acuity is chosen. As the measurement of visual acuity carries significant clinical and social importance, having two methods of predicting acuity and potentially basing the estimate on one data point would likely not suffice for our clinical standard.

In regards to using linear regression to determine the SVEP predicted acuity, we found that the SVEP predicted acuity using our linear regression Model 1 did not necessarily reflect the changes we noted in the SVEP response curve with image degradation such as a decline in peak amplitude. For example, although the group ETDRS acuity declined with +.50 and +1.00 lenses

and the SVEP response curves show the drop in peak amplitude, the SVEP predicted acuity by linear regression does not match these decreases and shows a trend for the SVEP predicted acuity by linear regression to slightly improve (see Figure 12). Although these are small differences between ETDRS visual acuity and SVEP predicted acuity, the drop in the peak amplitude of the SVEP response curve is fairly substantial and would suggest that the peak amplitude of the response curve is fairly sensitive to the reduced ETDRS acuity induced by minimal plus lenses in this group averaged data.

The dissociation between the ETDRS acuity and the SVEP acuity for minimal plus lenses can also be seen in Figure 15A where minimal plus lenses reduce the ETDRS-SVEP difference whereas the BF data reveals an immediate drop in the SVEP predicted acuity with the least amount of BF power and the levels decline steadily with increasing BF power. Figure 15A also shows an outlier in the defocus experiment revealing, again, more variability in SVEP predicted acuity with image degradation by optical defocus as compared to BFs. However, as seen in the summary shown in Figure 15B, the optical defocus and BFs data converge to show similar differences in ETDRS- SVEP acuity in the middle range of image degradation with this group data and equalize with an overestimation of ETDRS acuity at the extreme levels of image degradation. This trend for SVEP predicted acuity to underestimate optotype acuity at near normal levels of vision and to overestimate optotype acuity at poor levels of acuity can be seen in our Figure 16 and in SVEP reports of both simulated and organic causes of reduced vision (Arai et al., 1997; Gottlob et al., 1990; Katsumi et al., 1996; Kurtenbach et al., 2013; Ridder et al., 1998; Ridder & Rouse, 2007; Thompson et al., 1996).

Regarding the substantial difference between optical defocus and BF at minimal levels of image degradation, one might suspect that SVEP predicted acuity may show a particular

discrepancy with VA (underestimation) in disorders with reduced contrast and good optotype acuity as can occur in optic neuritis. Arai et al. (1997) compared SVEP predicted visual acuity to Snellen acuity in 100 patients with a variety of ocular disorders and reported that the 27 patients with optic nerve disorders had the lowest correlation coefficient between SVEP and optotype acuity (0.44). Gottlob et al. (1990) saw a wide range of children with ocular disorders and gives no specific disease-related SVEP results, but does comment that optic nerve disease, amblyopia, and disorders of central processing are unlikely to yield a good SVEP. Ridder (2004) and Bach et al. (2008) who both report SVEP results with ocular disease appear not to include participants with optic nerve disease.

It must also be considered that SVEP data with extremely reduced levels of visual acuity forms a small cluster of points that can be problematic for the creation of a linear regression. At the extent of reduced vision, very few data points above the noise level may be available for the regression. We required at least three data points above the noise level to create the linear regression. If only one or two data points were available, the SVEP predicted acuity was labelled as undetermined (occurred with Expert data but not with WA). Reports have shown regressions using two points (Thompson et al., 1996) or with Ridder et al. (1998; 2007; 2014), the option to use just one data point has been advised.

Figure 16 shows the summary of WA and Expert linear extrapolated visual acuities between ETDRS and SVEP for all image degradation conditions. Again, SVEP acuity predictions by linear regression (with image degradation) show the familiar trend for high spatial frequency ETDRS acuity is underestimated and low acuity conditions to be overestimated using the Expert as well as WA. Data inconsistency that creates outliers in the middle range of ETDRS acuity affected both the WA (for plus lenses) and the Expert (for BF). Removal of the

outliers improves data considerably, but indicates that both WA and Expert can show inconsistencies.

5.2.3 *SVEP Acuity Predictions: Analysis by Ratio Model 2*

Due to data inconsistencies and the reliance of the linear regression method on the high frequency data points that are close to noise levels, we decided to focus on the overall change in the SVEP response curve morphology from control conditions to increasing image degradation. Our initial observations noted a change in the relationship between the low frequency responses and the peak amplitude with increasing image degradation, this area of the SVEP response curve appeared to show consistent decline as vision was degraded. We speculated that change in this portion of the SVEP response curve may show more consistency than SVEP acuity predictions by linear regression. We proposed an innovative SVEP analysis technique involving the creation of ratios between the low spatial frequency responses and the responses at the peak of the SVEP response curve location ~ 5 c/d. For a robust comparison, we created two ratios types, used both Expert and WA data, and compared the repeatability of the linear regression (Model 1) to the new ratio technique (Model 2).

The ratios were devised from the average of the extreme points on the ascending slope of the SVEP response curve (points 1,2,3/8,9,10) versus further points along the ascending slope (points 3,4,5/9,10,11). There was no definitive theoretical basis for the points chosen for each ratio; as this is an innovative technique, no other reports are available for comparisons. One could speculate that early responses may be more variable due to initiation effects or later responses more affected by fatigue, retinal rivalry, interocular effects, or habituation.

The results of the ratio comparison showed superiority for WA rather than the Expert and the ratio of 1,2,3/8,9,10 rather than ratio 3,4,5/9,10,11 for both types of image degradation. The

Expert data showed marked variability for both types of image degradation as ETDRS visual acuity declined, this is a location where SVEP responses approach noise level and can appear as a small cluster of points (see Figures 13 and 14); subjective marking of waves that contribute to the ratio may therefore be more difficult and inconsistent. Analysis by automated WA appears to be superior for this type of data. It is undetermined as to why a difference existed between the two ratios other than taking the furthest points at the lowest spatial frequencies (points 1,2,3) may just afford more amplitude difference from the peak amplitude than points closer to the peak (3,4,5). Also, we could speculate that as the lowest spatial frequencies are more so magnocellular stimuli and moving to higher spatial frequencies at the peak may then include some parvocellular activity, the furthest separation between the two areas may reflect a change in visual acuity related to contribution from the parvocellular system.

5.2.4 Data Repeatability

Related to the relationships described above between two SVEP analysis techniques (Expert and WA) and two models for SVEP acuity predictions (linear regression, response amplitude ratios) repeatability or agreement between correlated entities should be assessed using Bland-Altman graphs.

The Bland-Altman graphs for WA versus Expert analysis techniques compared the group averaged control trials (session beginning minus session end) using the standard method of SVEP acuity prediction – linear regression (see Figure 18A). These trials were optimal circumstances for SVEP acuity prediction as no image degradation was used. Despite these optimal circumstances, the SVEP predicted acuity shows a large range for the visually normal participant (10 to 30 c/d; ~ 0.48 to 0.0 logMAR; 1.5 octave) for both WA and Expert data. Although an approximate 1-2 octave range is not atypical for SVEP data for visually normal

adults (Bach et al., 2008; Kurtenbach et al., 2013; Ridder, 2004; Ridder et al., 1998), these levels represents a fair clinical variability (3-4 ETDRS lines). However, in regards to repeatability, the WA shows less variability with a more consistent spread of data points as compared to the Expert and therefore shows superiority over the Expert technique. The Expert variability in the region of high spatial frequency SVEP predicted acuity likely reflects the difficulty of marking the small amplitude responses at near threshold levels and the sensitivity of the linear regression predicted acuity to the data point chosen at this location. As these data points are sensitive to SNR rejection settings, other studies have attempted to optimize the SVEP acuity predictions by reducing the SNR to ≥ 1 to accept smaller amplitude data in this region of the SVEP response curve (Yadav et al., 2009).

The Bland-Altman repeatability for the two ratio types and the Expert and WA as seen in Figure 18B also confirms the variability present in the Expert data. Expert variability in this case was more so with high ratios (the low spatial frequency amplitudes higher than the peak) that would typically relate to increased image degradation and low vision. However as these are control trials with well seeing individuals, this indicates that the ratio method can also be affected by individual variation but less so with analysis by WA and the ratio 1,2,3/8, 9, 10. The tendency for the negative outlying data point in the ratio graphs would relate to a participant showing a “good ratio” (normal peak appearance, small ratio numerical value) at the beginning of the session and a “poor ratio” (abnormal SVEP response curve, high ratio numerical value) at the end of the session. This could be due to end of session inattention, retinal rivalry or interocular effects related to occlusion, or fatigue that can yield less than optimal VEP recordings (Brigell, 2001; Eysteinnsson, Barris, Denny, & Frumkes, 1993; Fahle & Bach, 2006; Pardhan, Gilchrist, Douthwaite, & Yap, 1990; Regan, 1989).

Based on the findings of Sections 5.2.3 and 5.2.4, WA was considered to be the only analysis technique to be used for any further work in this study and going forward, only the Model 2- Ratio using points (1,2,3/8, 9, 10) was included in analysis.

5.3 Transient SVEP Parameters: Additional and Combined Analysis Models

As Model 2 showed a good relationship to ETDRS acuity, four additional Models were created based on other characteristics of the SVEP response curve that appeared to be affected by image degradation. All six models were separately applied to group averaged data with the results of those analyses applied back to individual data. Then a combination of all models was applied to the individual data. For further optimization, using coefficients of determination, all binary combinations were tallied to find the optimal model or model combinations to afford an accurate ETDRS acuity based on SVEP data.

As linear regression is the standard analysis technique applied to SVEP data, it was interesting to see (Figure 19) that Models 2 (Ratio) and 5 (Number of Points 1.6 X Noise Level) showed high coefficients of determination, reduction of outliers, and consistency for both types of image degradation – such information could be valuable in a clinical scenario where reduced acuity may be related to a combined etiology (see Table 2 and Figure 19). Model 2 shows the most consistent data as the optical defocus and BF graphs are almost identical in slope and R^2 values. Model 2 appears to avoid the inconsistency seen in the middle spatial frequencies (15-25 c/d) where several of the other graphs show data variability especially with the BF data (e.g. Models 3,4,5,6 (see Figure 19). This suggests that Model 2 based on the ascending slope of the SVEP response curve may reflect changes in visual acuity; this data shows a similar consistency obtained with the initial trials of the effect of image degradation on ETDRS acuity (see Figures

10 and 11). Eventually Model 2 may be useful in clinical scenarios where an individual (serving as own control) is being followed over time for changes in visual acuity.

Also, Figure 19 shows that Models 3 (Peak Position) and 4 (Peak Amplitude) may best reflect the difference between image degradation by optical defocus and BFs. The peak position and the peak amplitude show only a gradual decline with optical defocus whereas the BF data shows a dramatic change in these two models between high and lower levels of acuity with increasing levels of BF (reduction of contrast). These differences and the related characteristic of the SVEP response curve may eventually contribute to detecting likely organic causes of vision loss (e.g. with clinical testing, optic neuritis can show good ETDRS acuity with reduced contrast; the SVEP response curve could be sensitive to this) and discerning when subjective visual complaints may be more so refractive (the SVEP response curve maintains good morphology with minimal defocus).

For the individual data, both types of image degradation data were combined using the respective models of visual acuity estimates for optical defocus and BFs. This was done to get a sense of data with unknown combined etiologies of vision loss. The combination of image degradation types may partially be contributing to the marked variation of data seen in Figure 20, but this may more likely represent a clinical population.

When individual data is displayed in SVEP literature, it is common to see substantial variability (Lauritzen et al., 2004; Prager et al., 1999). The coefficients of determination for individual data are much lower than our group data with Models 1,5, and 6 showing the highest coefficient values. This suggests that Models 5 and 6 show a similar relationship to ETDRS acuity as linear regression in our population with a range of VA levels. Whereas populations with normal vision may show optimized SVEP acuity predictions by using linear regression and

increasing acceptable data points by lowering the SNR to ≥ 1 (Yadav et al., 2009), populations with a range of visual acuities may benefit from using various models as we have proposed or a combination of models.

Using a combination of all Models (1-6) improved the coefficient of determination to 0.62 which is substantial compared to the individual models (see Figure 21A). It is also agreeable with Arai et al. (1997) who obtained an overall correlation coefficient of 0.67 in their population of 100 individuals with organic ocular disease. The variability of our data has also been summarized in Figure 25 that shows the comparison between ETDRS visual acuity and SVEP predicted acuity in relationship to octaves of difference (shaded area on the graph shows ± 1 SD from the mean; blue arrows indicate for a given SVEP acuity, the range of the ETDRS acuity; the red arrows indicate for a given ETDRS acuity, the variability of the SVEP acuity). The substantial range from ETDRS 12-24 c/d seen on Figure 25 is also apparent on the Bland-Altman (Figure 21 B) that shows an unequal distribution of data with increased variability at moderately reduced visual acuity levels and more consistency with high and low visual acuity levels.

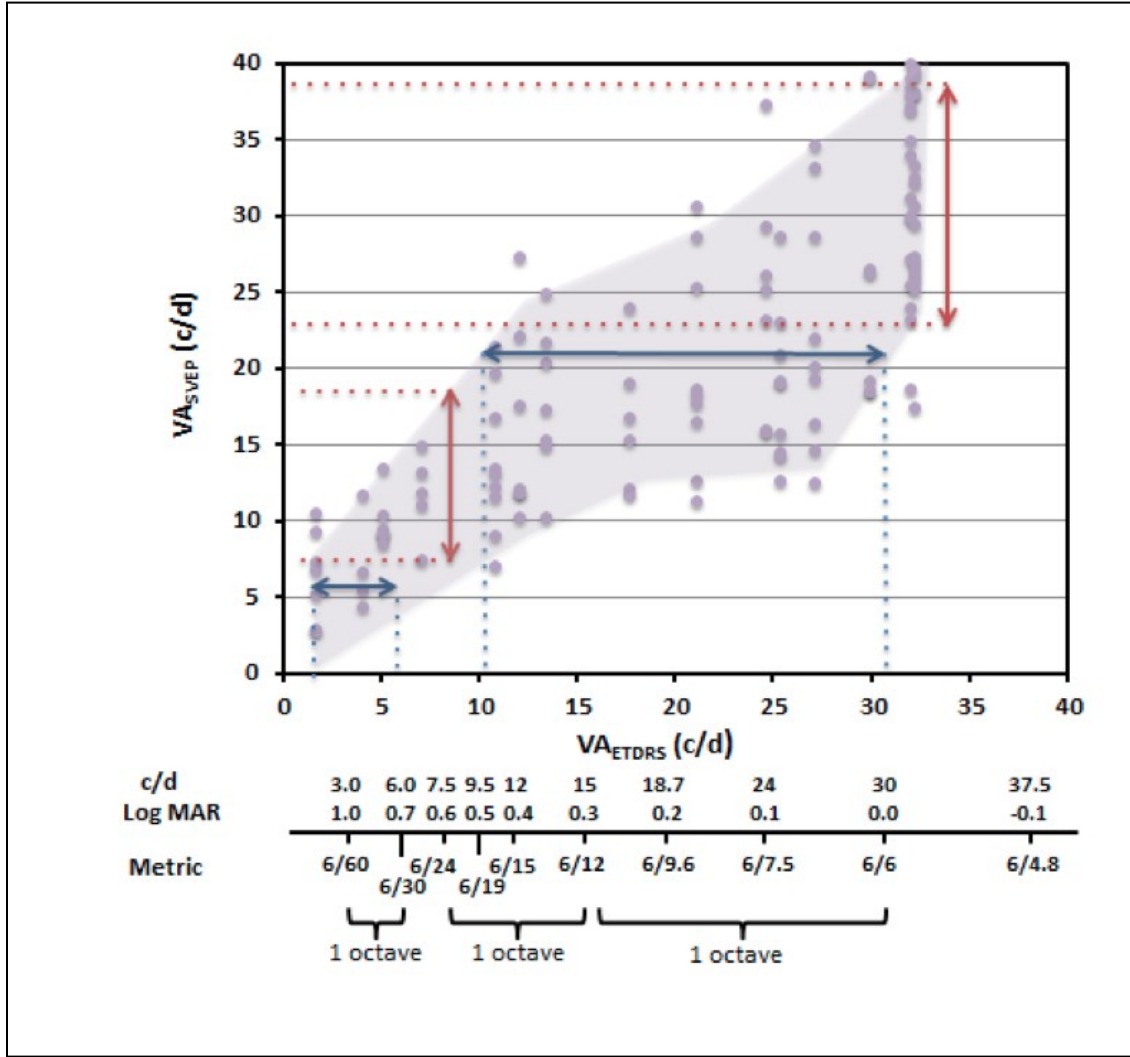


Figure 25: Individual Data Comparing ETDRS Visual Acuity and SVEP Predicted Visual Acuity in Relationship to Octaves of Difference and Various Methods of Recording Visual Acuity. One standard deviation from the mean is indicated by the shaded area on the graph. Horizontal (blue) arrows indicate for a given SVEP acuity, the range of the ETDRS acuity. Vertical (red) arrows indicate for a given ETDRS acuity, the variability of the SVEP acuity.

Figures 25 and 21B are also agreeable with our ROC curve that has shown good sensitivity/specificity for high and low levels of ETDRS acuity (AUC: 0.90 and 0.94 respectively) with much lower AUC values for intermediate acuity levels (See Figure 22). Kurtenbach (2013) who used image degradation by BFs with SVEP testing displays a similar appearing Bland-Altman plot (their Figure 4, “sweepVEP”, LaPlacian trials) showing more variance with moderately reduced vision compared to high and low acuity levels; their ROC curves are similar to our study except for an improved AUC value for intermediate levels of acuity compared to our values (their Figure 6, “sweepVEP”). Our increased variability for intermediate levels of acuity compared to the Kurtenbach study could be related to our inclusion of optical defocus and BFs in this individual data. However, combining the types of image degradation may also model variance that we may see in our clinic population. Also, the Kurtenbach ROC curves involve data points that are either the one best trial or the average of two trials; adopting that approach could also reduce the variability seen in some of our data.

We were able to improve the coefficient of determination for the individual data to 0.65 by using binary combinations of Models 1-6. We searched for a single or combination of models to optimize analysis of the individual SVEP data. The results indicated combined Models 1,2,4 or 1,2,4,5 were needed to optimize the coefficient of determination to 0.65. Under our circumstances with individual data, Model 1 (linear regression) alone did not yield the highest coefficient of determination indicating that model combinations may be the best method for data analysis with individuals showing a wide range of visual acuities. Perusal of the SVEP literature did not detect other reports of using model combinations for comparison with our method.

Our final results for individual data showing the optimized coefficient of determination of 0.65 still shows considerable leeway in ETDRS visual acuity predictions from SVEP data and

would likely be prone to errors if applied to individuals in clinical populations, except for individuals that show either very poor or stellar SVEP response curves.

5.4 Transient SVEP: Normative Subgroups

Although our estimate of ETDRS visual acuity based on SVEP data is fairly agreeable with other studies it appears that the SVEP will provide only broad categorical estimates of ETDRS visual acuity. This might be the extent of recognition acuity predictions possible from grating stimuli as afforded by evoked potentials recorded from the occipital lobe. However, as SVEP predicted acuity was observed to be quite accurate for particular individuals we decided to look again at the raw SVEP recordings.

We observed that the variety of normative SVEP response curves under control conditions (with no image degradation) show significant variability that appears to divide into subgroups: high versus low normative peak amplitudes (See Figure 23). This amount of variability is not surprising, as in regards to VEP amplitude in general, of the two main parameters measured for reports of transient VEPs (amplitude and implicit time), it is well known that amplitude is much more variable than implicit time (Fahle & Bach, 2006). Between and within normally sighted individuals, amplitude can vary up to 25% (Brigell, 2001).

However, when estimating ETDRS acuity from SVEP data, our data with well seeing individuals (control trials) indicates that our subgroup with normative high amplitude SVEP response curves shows a higher coefficients of determination and slope compared to our subgroup with normative low amplitudes (coefficients 0.80 and 0.63; slopes 0.80 and 0.59 respectively) (see Figure 24). This finding may reveal that the concept of predicting visual acuity from a SVEP response curve is inherently just more applicable to people that have high SVEP amplitudes.

The wide range of SVEP visual acuity predictions based on these control trials can be seen Figures 21 and 25 in the location of ETDRS acuity > 30 c/d. In regards to the normative low amplitude subgroup, the question arises as to the ability of the SVEP technique to differentiate normative low amplitude SVEP responses associated with ETDRS acuity of ~30 c/d vs. low amplitude SVEP responses related to ETDRS acuity of ~10 c/d or worse. Figure 22 and Figure 25 indicate that these two SVEP results would likely not overlap; differentiating the normative low amplitude SVEP results from intermediate levels of ETDRS acuity would be more problematic.

Other studies have reported low amplitude responses to the SVEP but have indicated that data from some visually normal participants with low amplitudes were omitted due to visual acuity that could not be determined by SVEP (Ridder et al., 1998). It has yet to be determined if a different electrode placement may improve the amplitude in such individuals or other factors such as fatigue or interocular effects may be reducing their amplitudes. However, it is important to be aware of this normative variation and, particularly with well seeing individuals that show low amplitude SVEP response curves, to be cautious in assuming levels of ETDRS visual acuity.

5.5 Limitations and Future Work

Our study involved numerous testing conditions on a small number of participants for the purpose of assessing a new technique- the transient SVEP. Our interest related to the effect of image degradation on SVEP data rather than normative individual variations within a larger population. With optimization of the transient SVEP technique and analysis methods, future work should involve larger visually normal and visually abnormal populations. Such studies could provide further evidence regarding the suitability of our visual degradation models to mimic ocular disorders and also the validity of our proposal that SVEP normative data segregates

to two main subgroups based on amplitude of response. In this regard, a study testing only individuals with latent hyperopia with and without lens correction and over a large age range would help determine the effect of latent hyperopia on SVEPs.

Provocative testing may be useful to test the resiliency of the SVEP responses by instituting image degradation; SVEP responses from individuals with low amplitudes related to organic vision loss may respond differently to image degradation compared to our subgroup with normative low amplitude SVEPs. Also, for individuals with normative low SVEP amplitudes and latent hyperopia, it would be interesting to correct the latent hyperopia for SVEP testing to determine if amplitudes could be improved.

We detected substantial inter-individual variations in SVEP recordings and also observed that some individuals had sporadic intra-individual test/retest variations. The cause of this variability could be the subject of future study. A modification of our electrode placement or an electrode montage may be helpful to normalize inter-individual differences that may relate to variations in orientation of the occipital lobe and resulting dipoles. Some participants noted a “blinking out” or disappearance of the stimulus during testing. These symptoms may be related to retinal rivalry that may respond to modification in testing luminance or occlusion technique in future studies. Perceptual phenomena may also be related to stimulus display. No standard grating stimulus for SVEP testing has yet been determined. Our horizontal sine wave gratings could contribute to these perceptions. As well, our use of a large monitor (initially considered optimal for a pediatric setting) may be causing inhibitory retinal surround interactions. As VEP responses are derived from the central 10° of the retina, a smaller display could be used. Fatigue can be a cause of intra-individual variation. Test duration could be reduced in future studies by omitting some spatial frequencies in the sweep and including only key data points of the SVEP

response curve. Reduction in test duration will be needed, as well, to institute our SVEP technique clinically.

Wavelet Analysis provided objectivity and automated processing of the large amounts of data generated by this project. By using trial and error with several wavelets, we found the Haar wavelet to be an acceptable match for our data. However, other wavelets or wavelet combinations may eventually prove to be applicable to SVEP data. The automated noise level calculation provided by WA for each SVEP recording was useful to determine viable data points to include in the SVEP response curves. Modification of our method of noise calculation could be instituted in future studies or a readily accessible method may be developed to utilize the VERIS™ second kernel data for simultaneous signal to noise levels data during SVEP acquisition.

A limitation to initiatives using grating type stimuli (resolution acuity) to predict optotype stimuli (recognition acuity) is that these two types of acuity represent different cortical processes and differ in stages of visual system development. Although visual evoked potentials using grating stimuli recorded from the occipital lobe may be valuable as baseline information or for interocular comparison within an individual, our SVEP technique at this point shows the potential to yield misleading approximations of recognition visual acuity for some conditions. However, future studies may refine and further elucidate how visual evoked potentials contribute to the global cortical process of recognition acuity.

5.6 Conclusion

We conclude that our transient SVEP methodology provides SVEP response curves that change in morphology related to image degradation techniques. The response is much more predictable with group- averaged data compared to individual data. As well, automation of data

analysis by Wavelet Analysis correlates well with Expert analysis but Wavelet Analysis takes precedence over the Expert technique due to enhanced objectivity, improved data repeatability, and provision of readily accessible noise data.







Results based on group (population averaged) data revealed that: 1) Image obscuration by the least power of BF reduces the SVEP predicted acuity substantially more than minimal powers of optical defocus, whereas both techniques show similar effects on SVEP predicted acuity at maximal image degradation levels; 2) An innovative model of SVEP acuity prediction based on SVEP response curve ratios shows high coefficient of determination values with ETDRS visual acuity and more consistent data compared to the standard analysis model of linear regression; 3) Four additional models based on SVEP curve parameters (peak position, peak amplitude, number of points $>1.6 \times$ noise level, area under the curve) show variable coefficients of determination and intercept values related to image degradation conditions and do not reach the consistency of the ratio method.

Results based on data from individuals revealed that: 1) All six models show reduced coefficients of determination due to inter-individual variability 2) Despite the inter-individual variability, sensitivity and specificity levels for SVEP predicted acuity are high to detect either excellent or reduced levels of ETDRS visual acuity – this may afford some clinical utility in appropriate cases; 3) Binary combinations between all six analysis models indicate that a combination of three analysis models (linear regression, ratio, peak amplitude) yields the highest coefficients of determination and shows improvement over linear regression alone; 4) Review of the raw data suggests that the presence of two normative subgroups may be generating data variability. Combining all analysis models shows an unchanged coefficient of determination for the low amplitude subgroup but excellent results for the normative subgroup with high peak

amplitude. Visually normal individuals with high peak amplitude SVEP response curves appear to be more likely to show accuracy in SVEP predicted acuity.

APPENDIX A: Removal of Flash Artefact- PVEP Acquisition Details

CRT and LCD PVEP stimuli were checkerboard patterns of black/white squares of 100% contrast, counter phased at 1.3 Hz, and the first kernel slice was analyzed with an epoch range from 0-500ms. Amplifier: gain at 50,000 (low frequency cut-off: 1 Hz; high frequency cut-off: 300 Hz). Settings for the modified LCD version (PVEP- LCDm) were identical except for the insertions of two black frames in the m-sequence to reduce the flash artefact (see Table below). Monitor types: PVEP-CRT: Professional Series P815 20" CRT (ViewSonic® Walnut, CA.); PVEP-LCD and PVEP-LCDm: VX2753mh-LED 1080P HDMI™ monitor (ViewSonic®). Mean luminance: during acquisition PVEPs were measured at monitor center (distance of 1 m.), room lights off and checkerboard (8'). Minolta LS-100 luminance meter (Minolta Camera Company, LTD, Japan) was focused at infinity and aimed centrally.

Parameter	PVEP-CRT	PVEP-LCD	PVEP-LCD(m)
Stimulus Visual Angle (arc')	All same: 8/ 16/ 32/ 64/ 128		
Stimulus Visual Angle (degrees)	All same: .13/ .27/.53/ 1.07/ 2.13		
Monitor Height (cm)	30	34	34
Pixel (width x height)	1024 x 768	1920 x 1080	1920 x 1080
Monitor Width (cm)	40	60	60
Luminance (mean cd/m ²)	20	51	15
Recording Time	51.20 sec.	51.20 sec.	34.13 sec.
Each Segment	12.80 sec.	12.80 sec.	8.53 sec.
M Sequence Exponent	6	6	10
Samples per Frame	16	16	16
Frames per M step	48	48	2
M step Frames	  1-24 25-48	  1-24 25-48	  1 2
Real Time Process	-	-	Kernel Slices 1&0

APPENDIX B: Holladay Visual Acuity Conversion Chart

The *Journal* publishes articles from around the world, where standards for measuring visual acuity vary. This table will help readers interpret visual acuity findings in familiar units.

Visual Acuity Conversion Chart*												
Distance			LogMAR Acuity Chart				Near					
Snellen Feet 20/	Equivalent Meter 6/	Decimal	Line Number	LogMAR†	Spatial Frequency (cyc/deg)	% Central Visual Efficiency	Jaeger Standard	Inches (14/)	Centimeters (35/)	Revised American Point-Type	"M" Notation	
10	3.0	2.00	-3	-0.30	60.00	100	—	7.0	17.5	—	0.20	
12.5	3.8	1.60	-2	-0.20	48.00	100	—	8.8	21.9	—	0.25	
16	4.8	1.25	-1	-0.10	37.50	100	—	11.2	28.0	—	0.32	
20	6.0	1.00	0	0.00	30.00	100	1	14.0	35.0	3	0.40	
25	7.5	0.80	1	0.10	24.00	95	2	17.5	43.8	4	0.50	
30	9.0	0.67	—	0.18	20.00	91	3	21.0	52.5	5	0.60	
32	9.6	0.63	2	0.20	18.75	90	4	22.4	56.0	6	0.64	
40	12.0	0.50	3	0.30	15.00	85	5	28.0	70.0	7	0.80	
50	15.0	0.40	4	0.40	12.00	75	6	35.0	87.5	8	1.0	
60	18.0	0.33	—	0.48	10.00	67	7	42.0	105.0	9	1.2	
63	18.9	0.32	5	0.50	9.52	65	8	44.1	110.3	10	1.3	
70	21.0	0.29	—	0.54	8.57	63	—	49.0	122.5	—	1.4	
80	24.0	0.25	6	0.60	7.50	60	9	56.0	140.0	11	1.6	
100	30.0	0.20	7	0.70	6.00	50	10	70.0	175.0	12	2.0	
114	34.2	0.18	—	0.76	5.26	44	11	79.8	199.5	13	2.3	
125	37.5	0.16	8	0.80	4.80	40	12	87.5	218.8	14	2.5	
150	45.0	0.13	—	0.88	4.00	32	—	105.0	262.5	—	3.0	
160	48.0	0.13	9	0.90	3.75	30	13	112.0	280.0	21	3.2	
200	60.0	0.10	10	1.00	3.00	20	14	140.0	350.0	23	4.0	

*Courtesy Jack Holladay, MD, modified from full Holladay table. For full table, visit www.journalofrefractive.com
†Log minimum angle of resolution; bold values are standard logMAR progression.
Note: 20/2000 is equivalent to count fingers @ 2 feet; 20/20000 is equivalent to hand motion @ 2 feet

Revised Visual Acuity Abbreviations*

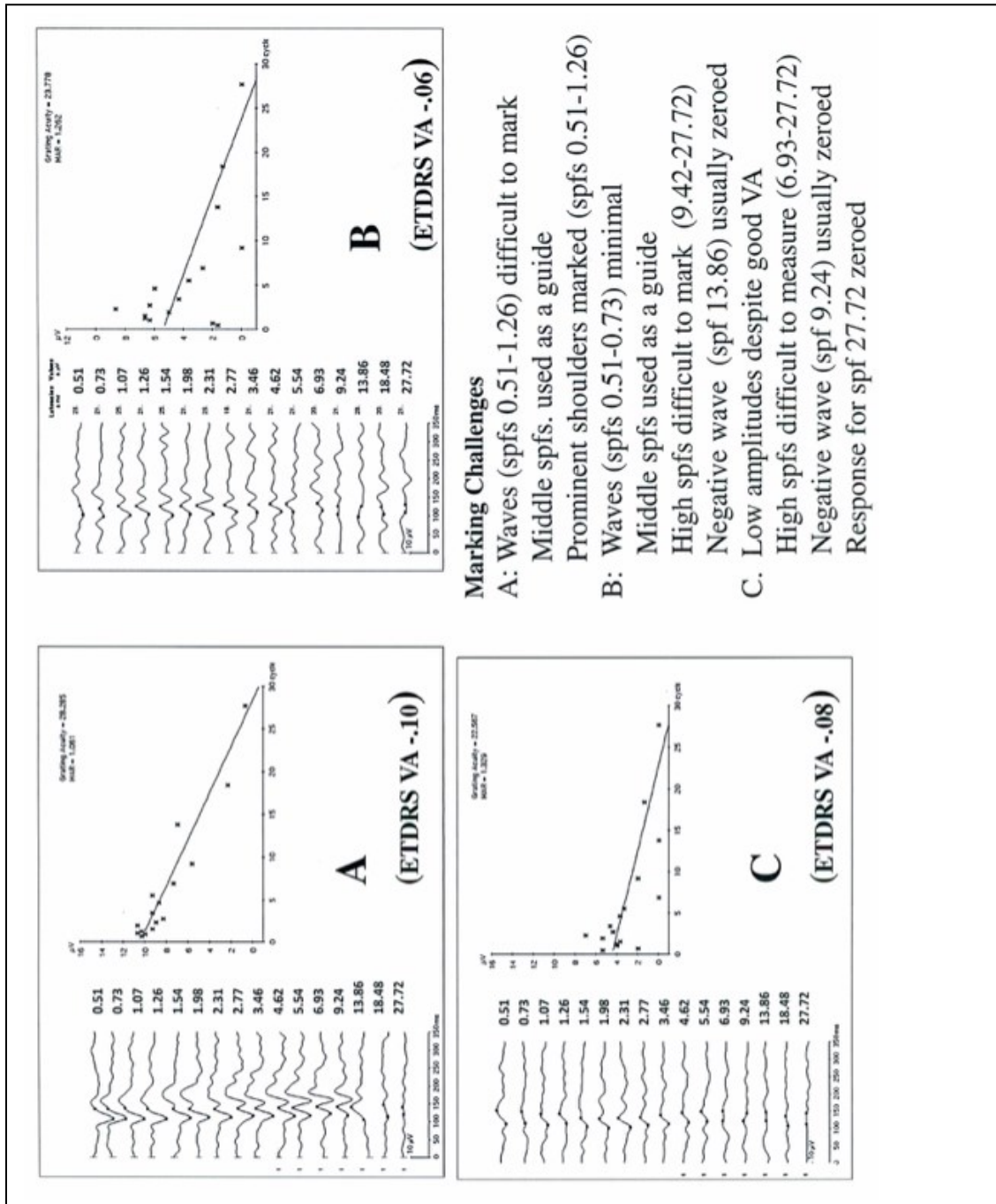
UDVA	uncorrected distance visual acuity
UIVA	uncorrected intermediate visual acuity
UNVA	uncorrected near visual acuity
CDVA	corrected distance visual acuity
CIVA	corrected intermediate visual acuity
CNVA	corrected near visual acuity
DCNVA	distance-corrected near visual acuity

1. Sloan LL. New test charts for the measurement of visual acuity. *Am J Ophthalmol.* 1959;48:808-813.
2. Report of Working Group 39, Committee of Vision, National Academy of Sciences. Recommended standard procedures for the clinical measurement and specification of visual acuity. *Adv Ophthalmol.* 1980;41:103-143.
3. Keeney AH, Durerson HL Jr. Collated near-vision test card. *Am J Ophthalmol.* 1958;46:592-594.
4. Keeney AH. *Ocular Examination: Basis and Techniques.* 2nd ed. St Louis, MO: CV Mosby Co; 1976.
5. Newell FW. *Ophthalmology: Principles and Concepts.* 7th ed. St Louis, MO: CV Mosby Co; 1992.
6. Frisen L. *Clinical Tests of Vision.* New York, NY: Raven Press; 1990.

Holladay Visual Acuity Conversion Chart available from:
www.journalofrefractive.com.
Also specifically:
<http://m3.wyanokecdn.com/8b132ac9d5e5903ccef0235e11f4c850.pdf>.

APPENDIX C: SVEP Response and Marking Challenges as Noted by the Expert

Excerpts are direct prints from VERIS™ Transient SVEP showing a standard linear regression that is generated by the software when all spatial frequencies are marked. For our study, data was all exported and peak to base linear regressions were created offline.



APPENDIX D: Matlab® Codes

Obtaining Mean and Standard Error of the Mean from Matrix of all Individual Data Using One Wavelet Methodology

% Valid for a 4D matrix where x=waveforms, y=results of spatial frequencies, z=conditions and w=individuals

%% Initialization of final variables

```
SwVEPCoeffAVEm=[]; SwVEPCoeffSEMm=[]; SwVEPNoiAVEm=[]; SwVEPNoiSEMm=[];
SwVEPCoeff=[]; SwVEPNoi=[];
% Vector with all grating frequencies in c/deg present in the sweep
x=[ 0.7300  0.9300  1.0700  1.2600  1.5400  1.9800  2.3100  2.7700  3.4600  4.6200
5.5400  6.9300  9.2400  13.8600  18.4800 27.7200];
```

%% Building the matrix of Wavelet Coefficients (reducing dimensionality by one)

```
for j=1:size(SingleTrialDataBase,4) % Number of participants
for i=1: size(SingleTrialDataBase,3) % Condition of the test (degree of blur)
IWC=[]; sIWC=[]; IWN=[]; sIWN=[]; WtA=[]; WCsum=[]; WNSum=[];
WtA= SingleTrialDataBase (:,:,i,j); % initialisation of variables within the loop
for k=1:16
WC= cwt(WtA(:,k),75:1:75, 'haar');
WC=abs(WC);
WCsum=cumsum(WC(300:1:900));
WNSum= cumsum(WC(1400:1:1700));
IWC(end+1)= WCsum(end); IWN(end+1)= WNSum(end);
end %for the 16 frequencies
sIWC=smooth(IWC,'sgolay'); sIWN=smooth(IWN,'sgolay'); % smooting the response curve
SwVEPCoeff(j,:,i)=sIWC; % x=individuals; y=curve; z=conditions
SwVEPNoi(j,:,i)=sIWN*2;
end % i for the conditions
end % j for the participants
```

%% Computing curves with Averages and SEMs

```
SwVEPCoeff=double(SwVEPCoeff); %make sure 0=0
SwVEPNoi=double(SwVEPNoi);
SwVEPCoeff(SwVEPCoeff==0)=NaN; % replace zeros by empty
SwVEPNoi(SwVEPNoi==0)=NaN;
SwVEPCoeffAVE=nanmean(SwVEPCoeff); % averaging on columns (over individuals)
(1:16:10)
SwVEPNoiAVE=nanmean(SwVEPNoi);
%SwVEPCoeffSEM=nanstd(SwVEPCoeff,1,3) ./sqrt(size(SwVEPCoeff,3)-
isnan(SwVEPCoeff));
SwVEPCoeffSEM=nansem(SwVEPCoeff); % Calculate SEM on columns (1:16:10)
SwVEPNoiSEM=nansem(SwVEPNoi);
```

%% Converting long linear vectors into matrix with degradation in rows and grating size in columns before sending to clipboard

```
for i=1:10;
    SwVEPCoeffAVEm(i,:)=SwVEPCoeffAVE(1, :, i);
    SwVEPCoeffSEMm(i,:)=SwVEPCoeffSEM(1, :, i);
    SwVEPNoiAVEm(i,:)=SwVEPNoiAVE(1, :, i);
    SwVEPNoiSEMm(i,:)=SwVEPNoiSEM(1, :, i);
end;
```

%% Copy to clipboard

```
MyTransferToExcel=[SwVEPCoeffAVEm, SwVEPCoeffSEMm, SwVEPNoiAVEm,
SwVEPNoiSEMm]; num2clip(MyTransferToExcel);
```

To determine r^2 for any determinant combination

% Uses

%% Declaration of variable

```
C=[];FinalR2=0;FinalC=[];M=[];Mr=[];MF=[];
VA= SwVEPPopVACoeff; %list of vectors containing values from all individuals
```

%% Determination of the matrix

```
M=permn([0 1],6); %change last number for any size if needed
```

%% Adding the r^2 for each combination

```
for i = 2:size(M,1)
    C=M(i,:); % First permutation (avoiding first row of zeros)
    NewVAEst=C(1).*VA(:,2) + C(2).*VA(:,3) + C(3).*VA(:,4)+ C(4).*VA(:,5)+ C(5).*VA(:,6)+
C(6).*VA(:,7);
    mdl = fitlm(VA(:,1),NewVAEst); % Linear regression model
    beta= mdl.Rsquared.Adjusted; % Get  $r^2$  from model
    Mr=M(i,:);Mr(end+1)=beta; % Building a new matrix with  $r^2$  added
    MF=[Mr;MF];
end
```

%% Order the Matrix by value of r^2

```
Final= sortrows(MF,7)
```

APPENDIX E: MATLAB® Code for Receiver Operating Curve

% Use ROCSwVEP workspace with all variables from Excel "VA inter-individual Variations" Have to load labels individually by pasting using Excel data directly into the variable window.

% Identification of the prediction to be quantified

```
pred=input('Prediction to be assessed: ');
```

% Determination of the 4 ROC corresponding to detection of ctls, lowVA and intermediate VAintH and VAintL

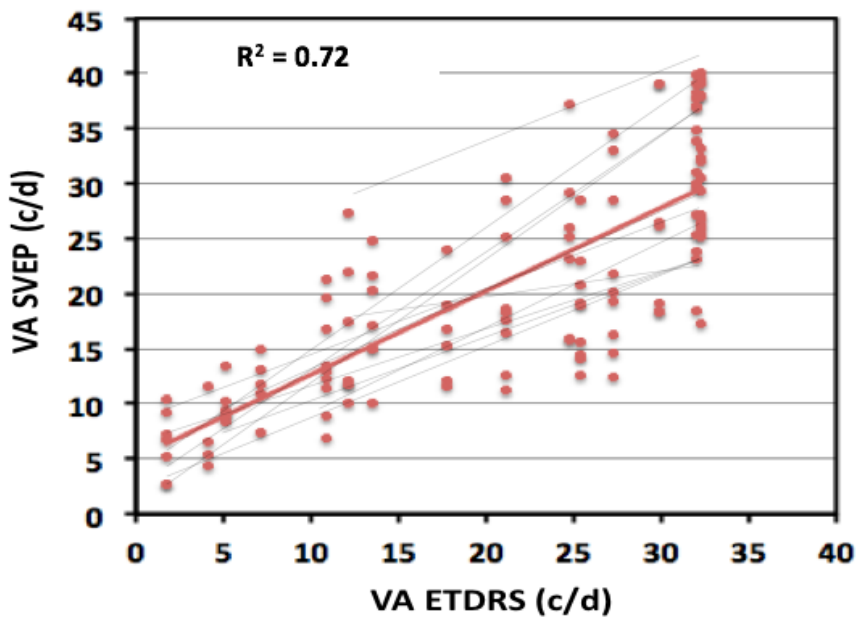
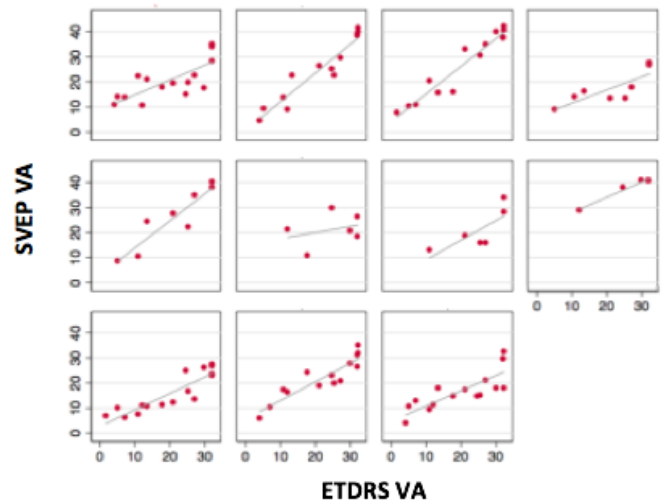
```
mdl = fitglm(pred,binH,'Distribution','binomial','Link','logit');
scores = mdl.Fitted.Probability;
[XH,YH,TH,AUCH] = perfcurve(labelH,scores,'ctl');
mdl = fitglm(pred,binintH,'Distribution','binomial','Link','logit');
scores = mdl.Fitted.Probability;
[XintH,YintH,TintH,AUCintH] = perfcurve(labelintH,scores,'VAintH');
mdl = fitglm(pred,binintL,'Distribution','binomial','Link','logit');
scores = mdl.Fitted.Probability;
[XintL,YintL,TintL,AUCintL] = perfcurve(labelintL,scores,'VAintL');
mdl = fitglm(pred,binL,'Distribution','binomial','Link','logit');
scores = mdl.Fitted.Probability;
[XL,YL,TL,AUCL] = perfcurve(labelL,scores,'LowVA');
% plot data
plot (XH,YH,'g',XintH,YintH,'c',XintL,YintL,'b',XL,YL,'r','LineWidth',3)
```

APPENDIX F: Analysis of Individual Data Related to the Presence of Repeated Measures

It is important to acknowledge the presence of repeated measures in a combined display of individual data as seen in Figure 20. The data was reanalyzed according to the method reported by Bland & Altman (1995); this yielded an overall R^2 (0.72).

Right: Plots of repeated measures for each participant contributing to the combined display of individual data (Figure 20). Some participants underwent both plus lenses and BF testing to various extents.

Below: Combined data showing all individual data with lines of best fit for the repeated measures



REFERENCES

- Aboufadel, E., & Schlicker, S. (1999). *Discovering Wavelets*. New York: John Wiley & Sons, Inc.
- Abrams, M. S., Duncan, C. L., & McMurtrey, R. (2011). Development of motor fusion in patients with a history of strabismic amblyopia who are treated part-time with Bangerter foils. *Journal of the American Association of Pediatric Ophthalmology and Strabismus*, *15*(2), 127-130.
- Adrian, E. D., & Matthews, B. H. C. (1934). The Berger rhythm: potential changes from the occipital lobe in man. *Brain*, *57*, Pt 4, 355-385.
- Agervi, P. (2011). Treatment with Bangerter filters. *Journal of the American Association of Pediatric Ophthalmology and Strabismus*, *15*(2), 121-122.
- Agervi, P., Kugelberg, U., Kugelberg, M., Simonsson, G., Fornander, M., & Zetterstrom, C. (2009). Treatment of anisometric amblyopia with spectacles or in combination with translucent Bangerter filters. *Ophthalmology*, *116*(8), 1475-1480
- Allen, M., & Birse, E. (1991). Stigma and blindness. *Journal of Ophthalmic Nursing and Technology*, *10*(4), 147-152.
- Almoqbel, F., Leat, S. J., & Irving, E. (2008). The technique, validity and clinical use of the sweep VEP. *Ophthalmic and Physiologic Optics*, *28*(5), 393-403.
- Almoqbel, F. M., Yadav, N. K., Leat, S. J., Head, L. M., & Irving, E. L. (2011). Effects of sweep VEP parameters on visual acuity and contrast thresholds in children and adults. *Graefes Archives for Clinical and Experimental Ophthalmology*, *249*(4), 613-623.
- American Association for Pediatric Ophthalmology and Strabismus. (2014). AAPOS Techniques for Pediatric Vision Screening. Retrieved from <http://www.aapos.org/terms/condtions/131>.
- American Electroencephalographic Society. (1994). Guideline Thirteen: Guidelines for Standard Electrode Position Nomenclature. *Journal of Clinical Neurophysiology*, *11*(1), 111-113.
- Anand, A., De Moraes, C. G., Teng, C. C., Liebmann, J. M., Ritch, R., & Tello, C. (2011). Short-duration transient visual evoked potential for objective measurement of refractive errors. *Documenta Ophthalmologica*, *123*(3), 141-147.
- Appel, S. D., & Brilliant, R. L. (1999). The Low Vision Examination. In R. L. Brilliant (Ed.), *Essentials of Low Vision Practice* (pp. 19-46). Boston : Butterworth Heinemann.

- Arai, M., Katsumi, O., Paranhos, F. R., Lopes De Faria, J. M., & Hirose, T. (1997). Comparison of Snellen acuity and objective assessment using the spatial frequency sweep PVER. *Graefes Archives for Clinical and Experimental Ophthalmology*, 235(7), 442-447.
- Arditi, A., & Cagenello, R. (1993). On the statistical reliability of letter-chart visual acuity measurements. *Investigative Ophthalmology and Visual Science*, 34(1), 120-129.
- Bach, M., Maurer, J. P., & Wolf, M. E. (2008). Visual evoked potential-based acuity assessment in normal vision, artificially degraded vision, and in patients. *British Journal of Ophthalmology*, 92(3), 396-403.
- Barraco, R., Persano Adorno, D., Brai, M., & Tranchina, L. (2014). A comparison among different techniques for human ERG signals processing and classification. *Medical Physics*, 30(1), 86-95.
- Baseler, H. A., Sutter, E. E., Klein, S. A., & Carney, T. (1994). The topography of visual evoked response properties across the visual field. *Electroencephalography and Clinical Neurophysiology*, 90(1), 65-81.
- Berman, M. S., & Seki, S. (1982). Blur-induced changes in the visual evoked potential. *American Journal of Optometry and Physiologic Optics*, 59(7), 556-560.
- Bishop, P. O. (1981). Binocular Vision. In R. A. Moses (Ed.), *Adler's Physiology of the Eye: Clinical Applications* (7th ed.). Toronto: C.V. Mosby Company.
- Bland, M. (2000). *An Introduction to Medical Statistics*. New York: Oxford University Press.
- Bland, J. M., & Altman, D. G. (1986). Statistical methods for assessing agreement between two methods of clinical measurement. *Lancet*, 1(8476), 307-310.
- Bland, J. M., & Altman, D. G. (1995). Calculating correlation coefficients with repeated observations: Part 1- correlation within subjects. *British Medical Journal*, (6977), 446.
- Bobak, P., Bodis-Wollner, I., & Guillory, S. (1987). The effect of blur and contrast on VEP latency: comparison between check and sinusoidal and grating patterns. *Electroencephalography and Clinical Neurophysiology*, 68(4), 247-255.
- Boyd, J. D., & Matsubara, J. A. (2011). Extrastriate Visual Cortex. In L. A. Levin, S. F. E. Nilsson, J. Ver Hoeve & S. M. Wu (Eds.), *Adler's Physiology of the Eye* (11 ed., pp. 599-612). Toronto: Saunders Elsevier.
- Brazier, A. B. (1986). The Emergence of Electrophysiology as an Aid to Neurology. In M. J. Aminoff (Ed.), *Electrodiagnosis in Clinical Neurology* (2nd ed., pp. 1-19). New York: Churchill Livingstone.

- Brigell, M. G. (2001). The Visual Evoked Potential. In G.A. Fishman, D.G. Birch, G.E. Holder, M.G. Brigell (Eds.), *Electrophysiologic Testing in Disorders of the Retina, Optic Nerve and Visual Pathway* (2nd ed., pp. 237-278). San Francisco, CA: American Academy of Ophthalmology.
- Campanini, M., Cassinari, P., Ferrigno, L., & Macaluso, C. (2001). ETDRS-fast: implementing psychophysical adaptive methods to standardized visual acuity measurement with ETDRS charts. *Investigative Ophthalmology and Visual Science*, 42(6), 1226-1231.
- Campbell, F. W., & Maffei, L. (1970). Electrophysiological evidence for the existence of orientation and size detectors in the human visual system. *Journal of Physiology*, 207(3), 635-652.
- Casagrande, V., & Ichida, J. (2011). Processing in the Lateral Geniculate Nucleus (LGN). In L. A. Levin, S. F. E. Nilsson, J. Ver Hoeve & S. M. Wu (Eds.), *Adler's Physiology of the Eye* (11 ed., pp.574-585). Toronto: Saunders Elsevier.
- Casagrande, V., & Marion, R. (2011). Processing in the Primary Visual Cortex. In L. A. Levin, S. F. E. Nilsson, J. Ver Hoeve & S. M. Wu (Eds.), *Adler's Physiology of the Eye* (11 ed., pp. 586-598). Toronto: Saunders Elsevier.
- Cavallerano, A. A. (1991). Potential Acuity Assessment. In *Clinical Procedures in Optometry* (pp. 470-481). New York: J.B.Lippincott.
- Chalam, K. V., Ambati, B. K., Beaver, H. A., Grover, S., Levine, L., Wells, T., et al. (2011). *Basic and Clinical Science Course*. San Francisco: American Academy of Ophthalmology.
- Chen, S., Chandna, A., Norcia, A. M., Pettet, M. W., & Stone, D. (2006). The Repeatability of Best Corrected Acuity in Normal and Amblyopic Children 4 to 12 Years of Age. *Investigative Ophthalmology and Visual Science*, 47(2), 614-619.
- Chen, Z., Li, J., Thompson, B., Deng, D., Yuan, J., Chan, L. Y., et al. (2014). The effect of Bangerter filters on binocular function in observers with amblyopia. *Investigative Ophthalmology and Visual Science*, 56(1), 139-49.
- Chiappa, K. H. (1989). Pattern-Shift Visual Evoked Potentials: Methodology. In K. H. Chiappa (Ed.), *Evoked Potentials in Clinical Medicine* (2nd ed .pp. 37-109). New York: Raven Press.
- Cobb, W. A., Morton, H. B., & Ettliger, G. (1967). Cerebral potentials evoked by pattern reversal and their suppression in visual rivalry. *Nature*, 216(5120), 1123-1125.
- Committee on Practice and Ambulatory Medicine. (2016). Visual system assessment in infants, children, and young adults by pediatricians *Pediatrics*, 137(1), 28-30.

- Corboy, J. M. (2003). *The Retinoscopy Book* (5th ed.). Thorofare: Slack Inc.
- da Costa, M. F., Salomao, S. R., Berezovsky, A., de Haro, F. M., & Ventura, D. F. (2004). Relationship between vision and motor impairment in children with spastic cerebral palsy: new evidence from electrophysiology. *Behavioural Brain Research*, *149*(2), 145-150.
- Dagnelie, G. (2013). Age-related psychophysical changes and low vision. *Investigative Ophthalmology and Visual Science*, *54*(14), ORSF88-93.
- Daw, N. (2006). *Visual Development* (2nd ed.). New Haven: Springer.
- Deutman, A. F., Hoyng, C. B., & van Lith-Verhoeven, J. J. C. (2006). Macular Dystrophies. In A. P. Schachat & K. Hagen (Eds.), *Retina* (4 ed., Vol. 2). Philadelphia: Elsevier Mosby.
- Donzis, P. B., Rappazzo, J. A., Burde, R. M., & Gordon, M. (1983). Effect of binocular variations of Snellen's visual acuity on Titmus stereoacuity. *Archives of Ophthalmology*, *101*(6), 930-932.
- Duckman, R. H. (2006). *Visual Development, Diagnosis, and Treatment of the Pediatric Patient*. Philadelphia: Lippincott, Williams & Wilkins.
- Early Treatment Diabetic Retinopathy Study Group (1985). Photocoagulation for diabetic macular edema. Early Treatment Diabetic Retinopathy Study report number 1. Early Treatment Diabetic Retinopathy Study research group. *Archives of Ophthalmology*, *103*(12), 1796-1806.
- Ely, A. L., Weinstein, J. M., Price, J. M., Gillon, J. T., Boltz, M. E., Mowery, S. F., et al. (2014). Degradation of swept-parameter VEP responses by neutral density filters in amblyopic and normal subjects. *Investigative Ophthalmology and Visual Science*, *55*(11), 7248-7255.
- Emmerson-Hanover, R., Shearer, D. E., Creel, D. J., & Dustman, R. E. (1994). Pattern reversal evoked potentials: gender differences and age-related changes in amplitude and latency. *Electroencephalography and Clinical Neurophysiology*, *92*(2), 93-101.
- Evans, D. E., Biglan, A. W., & Troost, B. T. (1981). Measurement of visual acuity in latent nystagmus. *Ophthalmology*, *88*(2), 134-138.
- Eysteinson, T., Barris, M. C., Denny, N., & Frumkes, T. E. (1993). Tonic interocular suppression, binocular summation, and the visual evoked potential. *Investigative Ophthalmology and Visual Science*, *34*(8), 2443-2448.
- Fahle, M., & Bach, M. (2006). Origin of the Evoked Potential. In J. R. Heckenlively & G. B. Arden (Eds.), *Principles and Practice of Clinical Electrophysiology of Vision* (2nd ed. pp. 207-234). Cambridge: Massachusetts Institute of Technology.

- Fannin, T. E., & Grosvenor, T. (1996). *Clinical Optics* (2nd ed.). Boston: Butterworth-Heinemann.
- Faulkner, W. (1983). Predicting acuities in capsulotomy patients: interferometers and potential acuity meter. *Journal of American Intraocular Implant Society*, 9(4), 434-437.
- Ferris, F. L., 3rd, Kassoff, A., Bresnick, G. H., & Bailey, I. (1982). New visual acuity charts for clinical research. *American Journal of Ophthalmology*, 94(1), 91-96.
- Forrester, J. V., Dick, A. D., McMenemy, P. G., & Roberts, F. (2008). *The Eye: Basic Sciences in Practice* (3rd ed.). Toronto: Saunders Elsevier.
- Fourier, J. (1822). *La theorie analytique de la chaleur* (A. Freeman, Trans.). London: Cambridge: At The University Press.
- Fox, M., Barber, C., Keating, D., & Perkins, A. (2014). Comparison of cathode ray tube and liquid crystal display stimulators for use in multifocal VEP. *Documenta Ophthalmologica*, 129(2), 115-122.
- France, T. D., & Ver Hoeve, J. N. (1994). VECP evidence for binocular function in infantile esotropia. *Journal of Pediatric Ophthalmology and Strabismus*, 31(4), 225-231.
- Franklin, A. (2007). Retinoscopy. In A. Keirl & C. Christie (Eds.), *Clinical Optics and Refraction* (pp. 71-87). Toronto: Bailliere Tindall Elsevier.
- Friedman, D. S., Munoz, B., Massof, R. W., Bandeen-Roche, K., & West, S. K. (2002). Grating visual acuity using the preferential-looking method in elderly nursing home residents. *Investigative Ophthalmology and Visual Science*, 43(8), 2572-2578.
- Galli, M. (2012). Diplopia following cosmetic surgery. *American Orthoptic Journal*, 62, 19-21.
- Ginis, H., Perez, G. M., Bueno, J. M., & Artal, P. (2012). The wide-angle point spread function of the human eye reconstructed by a new optical method. *Journal of Vision*, 12(3).
- Glasser, A. (2011). Accommodation. In L. A. Levin, S. F. E. Nilsson, J. Ver Hoeve & J. Wu (Eds.), *Adler's Physiology of the Eye* (11th ed. pp 40-70). Toronto: Saunders Elsevier.
- Good, W. V., & Hou, C. (2006). Sweep visual evoked potential grating acuity thresholds paradoxically improve in low-luminance conditions in children with cortical visual impairment. *Investigative Ophthalmology and Visual Science*, 47(7), 3220-3224.
- Goodwin, R. T., & Romano, P. E. (1985). Stereoacuity degradation by experimental and real monocular and binocular amblyopia. *Investigative Ophthalmology and Visual Science*, 26(7), 917-923.

- Gottlob, I., Fendick, M. G., Guo, S., Zubcov, A. A., Odom, J. V., & Reinecke, R. D. (1990). Visual acuity measurements by swept spatial frequency visual-evoked-cortical potentials (VECPs): clinical application in children with various visual disorders. *Journal of Pediatric Ophthalmology and Strabismus*, 27(1), 40-47.
- Grossmann, A., & Morlet, J. (1984). Decomposition of Hardy functions into square integral wavelets of constant shape. *Society for Industrial and Applied Mathematics Journal on Computing*, 15, 723-736.
- Hajian-Tilaki, K. (2013). Receiver Operating Characteristic (ROC) Curve Analysis for Medical Diagnostic Test Evaluation. *Caspian Journal of Internal Medicine*, 4(2), 627-635.
- Harding, G. (2006). History of Visual Evoked Cortical Testing. In J. R. Heckenlively & G. B. Arden (Eds.), *Principles and Practice of Clinical Electrophysiology of Vision* (2nd ed. pp. 15-19). Cambridge: MIT Press.
- Hargadon, D. D., Wood, J., Twelker, J. D., Harvey, E. M., & Dobson, V. (2010). Recognition acuity, grating acuity, contrast sensitivity, and visual fields in 6-year-old children. *Archives of Ophthalmology*, 128(1), 70-74.
- Harter, M. R., & White, C. T. (1968). Effects of contour sharpness and check-size on visually evoked cortical potentials. *Vision Research*, 8(6), 701-711.
- Hassoney, A. H., Ismail, A. K., & Hamza, H. (2012). Orthogonal and biorthogonal wavelet analysis of visual evoked potentials. *International Journal of Computer Applications*, 60(4), 50-52.
- Herbik, A., Geringswald, F., Thieme, H., Pollmann, S., & Hoffmann, M. B. (2014). Prediction of higher visual function in macular degeneration with multifocal electroretinogram and multifocal visual evoked potential. *Ophthalmic Physiologic Optics*, 34(5), 540-551.
- Herrmann, C. S., Rach, S., Vosskuhl, J., & Struber, D. (2014). Time-frequency analysis of event-related potentials: a brief tutorial. *Brain Topography*, 27(4), 438-450.
- Hersh, L. A., Spinell, M., & Astorino, J. (1999). Low vision distance Systems I: Spectacles and Contact Lenses. In R. L. Brilliant (Ed.), *Essentials of Low Vision Practice* (pp. 131-146). Boston: Butterworth-Heinemann.
- Hildebrand, G. D., & Fielder, A. R. (2011). Anatomy and Physiology of the Retina. In J. Reynolds & S. Olitsky (Eds.), *Pediatric Retina*. Berlin: Springer-Verlag.
- Hiraoka, T., Miyata, K., Nakamura, Y., Miyai, T., Ogata, M., Okamoto, F., et al. (2013). Influences of cycloplegia with topical atropine on ocular higher-order aberrations. *Ophthalmology*, 120(1), 8-13.

- Holder, G. E. (2006). Localizing Lesions in the Visual System. In J. R. Heckenlively & G. B. Arden (Eds.), *Principles and Practice of Clinical Electrophysiology of Vision* (2nd ed. pp. 505-517). Cambridge: The MIT Press.
- Holladay, J. T. (1997). Proper method for calculating average visual acuity. *Journal of Refractive Surgery*, 13(4), 388-391.
- Hood, D. C. (2006). The Multifocal Electroretinographic and Visual Evoked Potential Techniques. In J. R. Heckenlively & G. B. Arden (Eds.), *Principles and Practice of Clinical Electrophysiology of Vision* (2nd ed. pp. 197-205). Cambridge: The Massachusetts Institute of Technology.
- Horton, J. C., & Hoyt, W. F. (1991). Quadrantic visual field defects. *Brain*, 114, 1703-1718.
- Hou, C., Norcia, A. M., Madan, A., Tith, S., Agarwal, R., & Good, W. V. (2011). Visual cortical function in very low birth weight infants without retinal or cerebral pathology. *Investigative Ophthalmology and Visual Science*, 52(12), 9091-9098.
- Howard, I. P., & Rogers, B. J. (1995). *Binocular vision and Stereopsis*. New York: Oxford University Press, Inc.
- Hubbard, B. B. (1996). *The world according to wavelets: The story of a mathematical technique in the making*. Wellesley: A.K. Peters.
- Hyvarinen, L. (1988). *Vision in Children: Normal and Abnormal*. Meaford: The Canadian Deaf-Blind and Rubella Association.
- Hyvarinen, L. (1991). Visual Acuity Testing Principles. In J. R. Heckenlively & G. B. Arden (Eds.), *Principles and Practice of Clinical Electrophysiology of Vision* (1st ed. pp.459-464). Toronto: Mosby Year Book Inc.
- Iacobucci, I. L., Archer, S. M., Furr, B. A., Martonyi, E. J., & Del Monte, M. A. (2001). Bangerter foils in the treatment of moderate amblyopia. *American Orthoptic Journal*, 51, 84-91.
- James, J. F. (2002). *A student's guide to Fourier transforms with applications in physics and engineering* (2nd ed.). New York: Cambridge University Press.
- Jampel, H. D., Singh, K., Lin, S. C., Chen, T. C., Francis, B. A., Hodapp, E., et al. (2011). Assessment of visual function in glaucoma: a report by the American Academy of Ophthalmology. *Ophthalmology*, 118(5), 986-1002.
- John, F. M., Bromham, N. R., Woodhouse, J. M., & Candy, T. R. (2004). Spatial vision deficits in infants and children with Down syndrome. *Investigative Ophthalmology and Visual Science*, 45(5), 1566-1572.

- Kanski, J. J., & Milewski, S. A. (2002). *Diseases of the Macula: A Practical Approach*. Toronto: Mosby.
- Karanjia, R., Brunet, D. G., & ten Hove, M. W. (2009). Optimization of visual evoked potential (VEP) recording systems. *Canadian Journal of Neurological Science*, 36(1), 89-92.
- Katsumi, O., Arai, M., Wajima, R., Denno, S., & Hirose, T. (1996). Spatial frequency sweep pattern reversal VER acuity vs Snellen visual acuity: effect of optical defocus. *Vision Research*, 36(6), 903-909.
- Keirl, A. (2007). Schematic Eyes, Emmetropia and Ametropia. In *Clinical Optics and Refraction* (pp.20-24). Toronto: Elsevier Ltd.
- Kim, J. E., Weber, P., & Szabo, A. (2012). Medical malpractice claims related to cataract surgery complicated by retained lens fragments (an American Ophthalmological Society thesis). *Transactions of American Ophthalmological Society*, 110, 94-116.
- Knob, H. (2014). Simple Anatomy of the Retina. *Webvision; The Organization of the Retina and Visual System* Retrieved from [www.http://webvision.med.utah.edu](http://webvision.med.utah.edu)
- Kurtenbach, A., Langrova, H., Messias, A., Zrenner, E., & Jagle, H. (2013). A comparison of the performance of three visual evoked potential-based methods to estimate visual acuity. *Documenta Ophthalmologica*, 126(1), 45-56.
- Kushner, B. J., Lucchese, N. J., & Morton, G. V. (1995). Grating visual acuity with Teller cards compared with Snellen visual acuity in literate patients. *Archives of Ophthalmology*, 113(4), 485-493.
- Lang, M. A. (2000). The role of psychosocial factors in adaptation to vision impairment and habilitation outcomes for children and youth. In A. Horowitz (Ed.), *The Lighthouse Handbook on Vision Impairment and Vision Rehabilitation* (Vol. 2, pp. 1011-1028). New York: Oxford University Press.
- Lauritzen, L., Jorgensen, M. H., & Michaelsen, K. F. (2004). Test-retest reliability of swept visual evoked potential measurements of infant visual acuity and contrast sensitivity. *Pediatric Research*, 55(4), 701-708.
- Lee, P. P., Cunningham, W. E., Nakazono, T. T., & Hays, R. D. (2009). Associations of eye diseases and symptoms with self-reported physical and mental health. *American Journal of Ophthalmology*, 148(5), 804-808 e801.
- Leone, J. F., Mitchell, P., Kifley, A., & Rose, K. A. (2014). Normative visual acuity in infants and preschool-aged children in Sydney. *Acta Ophthalmologica*, 92(7), e521-529.
- Levi, D. M. (2011). Visual Acuity. In L. A. Levin, S. F. E. Nilsson, J. Ver Hoeve & S. M. Wu (Eds.), *Adler's Physiology of the Eye* (11th ed. pp. 627-647). Toronto: Saunders Elsevier.

- Lim, S. A., Siatkowski, R. M., & Farris, B. K. (2005). Functional visual loss in adults and children patient characteristics, management, and outcomes. *Ophthalmology*, *112*(10), 1821-1828.
- Loudon, S. E. (2007). *Improvement of therapy for amblyopia*. Rotterdam.
- MacCuspie, P. A. (1996). *Promoting Acceptance of Children with Disabilities: From Tolerance to Inclusion*. Halifax: Atlantic Provinces Special Education Authority.
- Mackay, A. M., Bradnam, M. S., Hamilton, R., Elliot, A. T., & Dutton, G. N. (2008). Real-time rapid acuity assessment using VEPs: development and validation of the step VEP technique. *Investigative Ophthalmology and Visual Science*, *49*(1), 438-441.
- Malhotra, R., Then, S. Y., Richards, A., & Cheek, E. (2010). The effect of Bangerter occlusion foils on blepharospasm and hemifacial spasm in occlusion-positive and occlusion-negative patients. *Open Ophthalmology Journal*, *4*, 1-6.
- Mallat, S. (1987). *A theory of multiresolution signal decomposition: The wavelet representation*. Philadelphia: University of Pennsylvania.
- Mallat, S. (1989). The multiresolution approximation and wavelets. *Transactions of the American mathematical society* *315*, 69-88.
- Mallot, H. A. (2000). *Computational vision information processing in perception and visual behavior*. Cambridge: MIT Press.
- Marc, R. E. (2011). The Synaptic Organization of the Retina. In L. A. Levin, S. F. E. Nilsson, J. Ver Hoeve & S. M. Wu (Eds.), *Adler's Physiology of the Eye* (11 ed. pp. 443-458). Toronto: Saunders Elsevier.
- Marr, D. (1982). *Vision: A computational investigation into the human representation and processing of visual information*. New York: W.H. Freeman and Company.
- Masland, R. H. (2012). The neuronal organization of the retina. *Neuron*, *76*(2), 266-280.
- Massey, S. C. (2006). Functional Anatomy of the Mammalian Retina. In D. R. Hinton (Ed.), *Retina* (4 ed., Vol. 1 pp. 43-82). Philadelphia: Elsevier Mosby.
- Matsumoto, C. S., Shinoda, K., Matsumoto, H., Funada, H., Minoda, H., & Mizota, A. (2013). Liquid crystal display screens as stimulators for visually evoked potentials: flash effect due to delay in luminance changes. *Documenta Ophthalmologica*, *127*(2), 103-112.
- Matsumoto, C. S., Shinoda, K., Matsumoto, H., Funada, H., Sasaki, K., Minoda, H., et al. (2014). Comparisons of pattern visually evoked potentials elicited by different response time liquid crystal display screens. *Ophthalmic Research*, *51*(3), 117-123.

- McBain, V. A., Robson, A. G., Hogg, C. R., & Holder, G. E. (2007). Assessment of patients with suspected non-organic visual loss using pattern appearance visual evoked potentials. *Graefes Archives for Clinical and Experimental Ophthalmology*, 245(4), 502-510.
- McCreath, G. (2010). *The Politics of Blindness: From Charity to Parity*. Vancouver: Granville Island Publishing.
- McDonald, M. A., Dobson, V., Sebris, S. L., Baitch, L., Varner, D., & Teller, D. Y. (1985). The acuity card procedure: a rapid test of infant acuity. *Investigative Ophthalmology and Visual Science*, 26(8), 1158-1162.
- McLeod, M. L., Wisnicki, H. J., & Medow, N. B. (2000). Vision Impairment in the Pediatric Population. In J. F. Martone & R. Wilson (Eds.), *The Lighthouse Handbook on Vision Impairment and Vision Rehabilitation* (Vol. 1, pp. 19-31). New York: Oxford University Press.
- Mendoza-Santiesteban, C. E., Fernandez-Cherkasova, L., Echavarria, O. H., Rodriguez, R. C., Columbie-Garbey, Y., & Riesgo, T. J. (2010). Multifocal electroretinography. *Seminars in Ophthalmology*, 25(4), 155-164.
- Milder, B., & Rubin, M. L. (1991). *The Fine Art of Prescribing Glasses* (2nd ed.). Gainesville: Triad Publishing Company.
- Minkowski, J. S., Palese, M., & Guyton, D. L. (1983). Potential acuity meter using a minute aerial pinhole aperture. *Ophthalmology*, 90(11), 1360-1368.
- Misiti, M., Misiti, Y., Oppenheim, G., & Poggi, J. (2010). Wavelet Toolbox™ 4 user's guide.
- Moore, Q., Al-Zubidi, N., Yalamanchili, S., & Lee, A. G. (2012). Nonorganic visual loss in children. *International Ophthalmology Clinics*, 52(3), 107-123, xii.
- Mulla, S. H. (2007). *A correlation between measurements obtained with LEA symbols visual acuity chart and the gold standard ETDRS VA chart for 3 to 7 year old normal children*. (Master's thesis). Retrieved from Dalhousie University Dissertation and Theses database (MR26877).
- Nagy, B. V., Gemesi, S., Heller, D., Magyar, A., Farkas, A., Abraham, G., et al. (2011). Comparison of pattern VEP results acquired using CRT and TFT stimulators in the clinical practice. *Documenta Ophthalmologica*, 122(3), 157-162.
- Nelson, L. B. (1998). *Harley's Pediatric Ophthalmology* (4th ed.). Toronto: W.B.Saunders.
- Neveu, M. M., Jeffery, G., Burton, L. C., Sloper, J. J., & Holder, G. E. (2003). Age-related changes in the dynamics of human albino visual pathways. *European Journal of Neuroscience*, 18(7), 1939-1949.

- Norcia, A. M., & Tyler, C. W. (1985a). Infant VEP acuity measurements: analysis of individual differences and measurement error. *Electroencephalography and Clinical Neurophysiology*, 61(5), 359-369.
- Norcia, A. M., & Tyler, C. W. (1985b). Spatial frequency sweep VEP: visual acuity during the first year of life. *Vision Research*, 25(10), 1399-1408.
- Norcia, A. M., Tyler, C. W., Piecuch, R., Clyman, R., & Grobstein, J. (1987). Visual acuity development in normal and abnormal preterm human infants. *Journal of Pediatric Ophthalmology and Strabismus*, 24(2), 70-74.
- Odell, N. V., Hatt, S. R., Leske, D. A., Adams, W. E., & Holmes, J. M. (2009). The effect of induced monocular blur on measures of stereoacuity. *Journal of the American Association of Pediatric Ophthalmology and Strabismus*, 13(2), 136-141.
- Odell, N. V., Leske, D. A., Hatt, S. R., Adams, W. E., & Holmes, J. M. (2008). The effect of Bangerter filters on optotype acuity, Vernier acuity, and contrast sensitivity. *Journal of the American Association of Pediatric Ophthalmology and Strabismus*, 12(6), 555-559.
- Odom, J. V., Bach, M., Barber, C., Brigell, M., Marmor, M., Tormene, A. P., et al. (2006). Visual Evoked Potential Standard. In J. R. Heckenlively & G. B. Arden (Eds.), *Principles and Practice of Clinical Electrophysiology of Vision* (2nd ed. pp 301-308). Cambridge: The MIT Press.
- Ohlsson, J., & Villarreal, G. (2005). Normal visual acuity in 17--18 year olds. *Acta Ophthalmologica Scandinavica*, 83(4), 487-491.
- Pardhan, S., Gilchrist, J., Douthwaite, W., & Yap, M. (1990). Binocular inhibition: psychophysical and electrophysiological evidence. *Optometry and Vision Science*, 67(9), 688-691.
- Parkinson, J., & Tremblay, F. (2009). Misleading clinical stereoacuity levels in pediatric maculopathy. *Journal of the American Association of Pediatric Ophthalmology and Strabismus*, 13(5), 496-498.
- Parkinson, J., Waterhouse, J., & Tremblay, F. (April, 2009). *The effect of variation in pattern electroretinogram/visual evoked potential stimulus paradigm and clinical considerations*. Presentation at Dalhousie University Department of Ophthalmology and Visual Sciences Resident Research Day, Halifax, Nova Scotia.
- Pei, F., Baldassi, S., & Norcia, A. M. (2014). Electrophysiological measures of low-level vision reveal spatial processing deficits and hemispheric asymmetry in autism spectrum disorder. *Journal of Vision*, 14(11).

- Perez-Rico, C., Ayuso-Peralta, L., Rubio-Perez, L., Roldan-Diaz, I., Arevalo-Serrano, J., Jimenez-Jurado, D., et al. (2014). Evaluation of visual structural and functional factors that predict the development of multiple sclerosis in clinically isolated syndrome patients. *Investigative Ophthalmology and Visual Science*, 55(10), 6127-6131.
- Perez, G. M., Archer, S. M., & Artal, P. (2010). Optical characterization of Bangerter foils. *Investigative Ophthalmology and Visual Science*, 51(1), 609-613.
- Pinter, R. B., & Nabet, B. E. (1992). *Nonlinear vision: Determination of neural receptive fields, function and network*. Ann Arbor: CRC Press.
- Polikar, R. (2006). *Wavelet tutorial*. Retrieved from <http://users.rowan.edu/~poliker/WAVELETS/WTutorial.html>.
- Polit, D. F. B. C. T. (2008). *Nursing research: Generating and assessing evidence for nursing practice* (8th ed.). New York: Lippincott William & Wilkins.
- Prager, T. C., Zou, Y. L., Jensen, C. L., Fraley, J. K., Anderson, R. E., & Heird, W. C. (1999). Evaluation of methods for assessing visual function of infants. *Journal of the American Association of Pediatric Ophthalmology and Strabismus*, 3(5), 275-282.
- Rabbetts, R. B., & Mallen, E. E. A. (2007). Accommodation and near vision. The inadequate-stimulus myopias. In R. B. Rabbetts (Ed.), *Bennett & Rabbetts' Clinical Visual Optics* (4th ed., pp. 125-153). Toronto: Butterworth Heinemann Elsevier.
- Ray, J. S., & Maahs, M. A. (1999). Low Vision Special Populations II: The Stroke Patient. In R. L. Brilliant (Ed.), *Essentials of Low Vision Practice* (pp. 335-349). Boston: Butterworth Heinemann.
- Read, S. A., Collins, M. J., & Sander, B. P. (2010). Human optical axial length and defocus. *Investigative Ophthalmology and Visual Science*, 51(12), 6262-6269.
- Reeves, B. C., Wood, J. M., & Hill, A. R. (1991). Vistech VCTS 6500 charts--within- and between-session reliability. *Optometry and Vision Science*, 68(9), 728-737.
- Regan, D., Richards, W. (1971). Independence of evoked potentials and apparent size. *Vision Research*, 11 (7), 679-684.
- Regan, D. (1973). Rapid objective refraction using evoked brain potentials. *Investigative Ophthalmology and Visual Science*, 12(9), 669-679.
- Regan, D. (1977). Rapid methods for refracting the eye and for assessing visual acuity in amblyopia, using steady-state visual evoked potentials. In J. E. Desmedt (Ed.), *Visual Evoked Potentials in Man: New Developments* (pp. 418-426). Oxford: Oxford University Press.

- Regan, D. (1989). *Human Brain Electrophysiology: Evoked Potentials and Evoked Magnetic Fields in Science and Medicine*. New York: Elsevier.
- Reinhardt, J. P., & D'Allura, T. (2000). Social support and adjustment to vision impairment across the life span. In A. Horowitz (Ed.), *The Lighthouse Handbook on Vision Impairment and Vision Rehabilitation* (Vol. 2, pp. 1049-1068). New York: Oxford University Press.
- Repka, M., & Gramatikov, B. J. (2006). The reproducibility of blur with a Bangerter filter. *Journal of the American Association of Pediatric Ophthalmology and Strabismus*, 10(1).
- Riddell, P. M., Ladenheim, B., Mast, J., Catalano, T., Nobile, R., & Hainline, L. (1997). Comparison of measures of visual acuity in infants: Teller acuity cards and sweep visual evoked potentials. *Optometry and Vision Science*, 74(9), 702-707.
- Ridder, W. H., 3rd. (2004). Methods of visual acuity determination with the spatial frequency sweep visual evoked potential. *Documenta Ophthalmologica*, 109(3), 239-247.
- Ridder, W. H., 3rd, McCulloch, D., & Herbert, A. M. (1998). Stimulus duration, neural adaptation, and sweep visual evoked potential acuity estimates. *Investigative Ophthalmology and Visual Science*, 39(13), 2759-2768.
- Ridder, W. H., 3rd, & Rouse, M. W. (2007). Predicting potential acuities in amblyopes: predicting post-therapy acuity in amblyopes. *Documenta Ophthalmologica*, 114(3), 135-145.
- Ridder, W. H., 3rd, Tong, A., & Floresca, T. (2012). Reliability of acuities determined with the sweep visual evoked potential (sVEP). *Documenta Ophthalmologica* 124(2), 99-107.
- Ridder, W. H., 3rd, Waite, B. S., & Melton, T. F. (2014). Comparing enfant and PowerDiva sweep visual evoked potential (sVEP) acuity estimates. *Documenta Ophthalmologica*, 129(2), 105-114.
- Rodieck, R. W. (1998). *The First Steps in Seeing*. Sunderland, Massachusetts: Sinauer Associates, Inc.
- Rosser, D. A., Cousens, S. N., Murdoch, I. E., Fitzke, F. W., & Laidlaw, D. A. (2003). How sensitive to clinical change are ETDRS logMAR visual acuity measurements? *Investigative Ophthalmology and Visual Science*, 44(8), 3278-3281.
- Rotenstreich, Y., Fishman, G. A., & Anderson, R. J. (2003). Visual acuity loss and clinical observations in a large series of patients with Stargardt disease. *Ophthalmology*, 110(6), 1151-1158.
- Rubin, G. S. (2006). Visual Acuity and Contrast Sensitivity. In D. R. Hinton (Ed.), *Retina* (4th ed., Vol. 1, pp. 227-233). Philadelphia: Elsevier Mosby.

- Rutstein, R. P. (2012). Retinally induced aniseikonia: a case series. *Optometry and Vision Science*, 89(11), e50-55.
- Rutstein, R. P., Foster, N. C., Cotter, S. A., Kraker, R. T., Lee, D. H., Melia, M., et al. (2011). Visual acuity through Bangerter filters in nonamblyopic eyes. *Journal of the American Association of Pediatric Ophthalmology and Strabismus*, 15(2), 131-134.
- Sabri, K., Thornley, P., Waltho, D., Warren, T., Lavery, L., Husain, S., et al. (2016). Assessing accuracy of non-eye care professionals as trainee vision screeners for children. *Canadian Journal of Ophthalmology*, 51(1), 25-29.
- Sadowsky, J. (1996). Investigation of signal characteristics using the continuous wavelet transform. *John Hopkins APL Technical Digest*, 17(3).
- Sagili, S., Malhotra, R., & Elston, J. (2005). Facial palsy-induced blepharospasm relieved by a Bangerter foil. *Movement Disorders*, 20(9), 1231-1232.
- Sakaue, H., Katsumi, O., Mehta, M., & Hirose, T. (1990). Simultaneous pattern reversal ERG and VER recordings. Effect of stimulus field and central scotoma. *Investigative Ophthalmology and Visual Science*, 31(3), 506-511.
- Samar, V. J. (1999). Wavelet analysis of neuroelectric waveforms. *Brain and Language*, 66(1), 1-6.
- Schanel-Klitsch, E., Siegfried, J. B., & Kavanagh, V. (1987). Developmental differences in visual evoked potential slow waves and high frequency wavelets across the lifespan: effects of luminance variation of flash and background. In C. Barber & T. Blum (Eds.), *Evoked Potentials III: The Third International Evoked Potentials Symposium*. (pp.198-204). Toronto: Butterworths.
- Schiffman, H. R. (1976). *Sensation and Perception*. New York: John Wiley & Sons, Inc.
- Schor, P., & Miller, D. (2011). Optics. In L. A. Levin, N. S.F.E., J. Ver Hoeve & S. M. Wu (Eds.), *Adler's Physiology of the Eye* (11 ed. pp.1-27). Toronto: Saunders Elsevier.
- Siddiqi, M. H., Ali, R., Rana, M. S., Hong, E. K., Kim, E. S., & Lee, S. (2014). Video-based human activity recognition using multilevel wavelet decomposition and stepwise linear discriminant analysis. *Sensors (Basel)*, 14(4), 6370-6392.
- Simon, J. W., Siegfried, J. B., Mills, M. D., Calhoun, J. H., & Gurland, J. E. (2004). A new visual evoked potential system for vision screening in infants and young children. *Journal of the American Association of Pediatric Ophthalmology and Strabismus*, 8(6), 549-554.

- Sokol, S. (1978). Measurement of infant visual acuity from pattern reversal evoked potentials. *Vision Research*, 18(1), 33-39.
- Sokol, S. (1986). Visual Evoked Potentials. In M. J. Aminoff (Ed.), *Electrodiagnosis in Clinical Neurology* (2nd ed. pp. 441-456). New York: Churchill Livingstone.
- Stiers, P., Vanderkelen, R., & Vandenbussche, E. (2003). Optotype and grating visual acuity in preschool children. *Investigative Ophthalmology and Visual Science*, 44(9), 4123-4130.
- Struck, M. C., Ver Hoeve, J. N., & France, T. D. (1996). Binocular cortical interactions in the monofixation syndrome. *Journal of Pediatric Ophthalmology and Strabismus*, 33, 291-297.
- Sutter, E. E. (1991). The fast m-transform: A fast computation of cross-correlations with binary m-sequences. *Society for Industrial and Applied Mathematics Journal on Computing*, 20(4), 686-694.
- Sutter, E. E. (1992). A Deterministic Approach to Nonlinear Systems Analysis. In R. B. Pinter & B. Nabet (Eds.), *Nonlinear Vision: Determination of Neural Receptive Fields, Function, and Networks*. Ann Arbor: CRC Press.
- Sutter, E. E., & Tran, D. (1992). The field topography of ERG components in man--I. The photopic luminance response. *Vision Research*, 32(3), 433-446.
- Sutter, E. E., & Vaegan. (1990). Lateral interaction component and local luminance nonlinearities in the human pattern reversal ERG. *Vision Research*, 30(5), 659-671.
- Szlyk, J. P., Fishman, G. A., Grover, S., Revelins, B. I., & Derlacki, D. J. (1998). Difficulty in performing everyday activities in patients with juvenile macular dystrophies: comparison with patients with retinitis pigmentosa. *British Journal of Ophthalmology*, 82(12), 1372-1376.
- Thie, J., Sriram, P., Klistorner, A., & Graham, S. L. (2012). Gaussian wavelet transform and classifier to reliably estimate latency of multifocal visual evoked potentials (mfVEP). *Vision Research*, 52(1), 79-87.
- Thompson, D. A., Moller, H., Russell-Eggitt, I., & Kriss, A. (1996). Visual acuity in unilateral cataract. *British Journal of Ophthalmology*, 80(9), 794-798.
- Tielsch, J. M. (2000). The Epidemiology of Vision Impairment. In J. F. Martone & M. R. Wilson (Eds.), *The Lighthouse handbook on Vision Impairment and Vision Rehabilitation* (Vol. 1, pp. 5-17). New York: Oxford University Press.
- Tinelli, F., Pei, F., Guzzetta, A., Bancalè, A., Mazzotti, S., Baldassi, S., et al. (2008). The assessment of visual acuity in children with periventricular damage: a comparison of behavioural and electrophysiological techniques. *Vision Research*, 48(10), 1233-1241.

- Trobe, J. D. (2001). *The Neurology of Vision*. Toronto: Oxford University Press.
- Tyler, C. W., Apkarian, P., Levi, D. M., & Nakayama, K. (1979). Rapid assessment of visual function: an electronic sweep technique for the pattern visual evoked potential. *Investigative Ophthalmology and Visual Science*, *18*(7), 703-713.
- Underwood, B. J. (1966). *Experimental Psychology* (2nd ed.). Englewood Cliffs: Prentice Hall, Inc.
- Ver Hoeve, J., France, T. D., & Bousch, A. (1996). A sweep VEP test for color vision deficits in infants and young children. *Journal of Pediatric Ophthalmology and Strabismus*, *33*, 298-302.
- Vianya-Estopa, M., Douthwaite, W. A., Funnell, C. L., & Elliott, D. B. (2009). Clinician versus potential acuity test predictions of visual outcome after cataract surgery. *Optometry*, *80*(8), 447-453.
- Victor, J. D. (1992). Nonlinear systems analysis in vision: overview of kernel methods. In R. B. Pinter & B. Nabet (Eds.), *Nonlinear Vision: Determination of Neural Receptive Fields, Function, and Networks* (pp. 1-37). Ann Arbor: CRC Press.
- Vistech Consultants, I. (1986). Preliminary acuity norms in snellen equivalents. In A. 2 (Ed.), *Teller Acuity Cards Manual*. Dayton: Vistech Consultants Inc.
- von Noorden, G. K., & Campos, E. C. (2002). *Binocular Vision and Ocular Motility: Theory and Management of Strabismus* (6th ed.). St. Louis, Missouri: Mosby.
- Vottonen, P., Kaarniranta, K., Paakkonen, A., & Tarkka, I. M. (2013). Changes in neurophysiologic markers of visual processing following beneficial anti-VEGF treatment in macular degeneration. *Clinical Ophthalmology*, *7*, 437-442.
- Walker, J. S. (2008). *A primer on wavelets and their scientific applications* (2nd ed.). New York: Chapman & Hall/CRC.
- Watson, L. M., Strang, N. C., Scobie, F., Love, G. D., Seidel, D., & Manahilov, V. (2012). Image jitter enhances visual performance when spatial resolution is impaired. *Investigative Ophthalmology and Visual Science*, *53*(10), 6004-6010.
- Wendel, K., Vaisanen, J., Seemann, G., Hyttinen, J., & Malmivuo, J. (2010). The influence of age and skull conductivity on surface and subdermal bipolar EEG leads. *Computational Intelligence and Neuroscience*, *2010*, 397272.
- Wolfe, J. M., Kluender, K. R., & Levi, D. M. (2009). *Sensation and Perception* (2nd ed.). Sunderland: Sinauer Associates, Inc.

- Woodhouse, J. M., Morjaria, S. A., & Adler, P. M. (2007). Acuity measurements in adult subjects using a preferential looking test. *Ophthalmic Physiologic Optics*, 27(1), 54-59.
- Wu, Z., Ayton, L. N., Guymer, R. H., & Luu, C. D. (2014). Comparison between multifocal electroretinography and microperimetry in age-related macular degeneration. *Investigative Ophthalmology and Visual Science*, 55(10), 6431-6439.
- Xu, S., Meyer, D., Yoser, S., Mathews, D., & Elfervig, J. L. (2001). Pattern visual evoked potential in the diagnosis of functional visual loss. *Ophthalmology*, 108(1), 76-80; discussion 80-71.
- Yadav, N. K., Almoqbel, F., Head, L., Irving, E. L., & Leat, S. J. (2009). Threshold determination in sweep VEP and the effects of criterion. *Documenta Ophthalmologica*, 119(2), 109-121.
- Young, B., Eggenberger, E., & Kaufman, D. (2012). Current electrophysiology in ophthalmology: a review. *Current Opinion in Ophthalmology*, 23(6), 497-505.
- Young, R. K. (1993). *Wavelet theory and its applications*. Norwell: Kluwer Academic Publishers.
- Zambone, A. M., Ciner, E., Appel, S., & Graboyes, M. (2000). Children with Multiple Impairments. In S. F. Wainapel (Ed.), *Vision Impairment and Vision Rehabilitation* (Vol. 1, pp. 451-468). New York: Oxford Univeristy Press.
- Zou, K. H., O'Malley, A. J., & Mauri, L. (2007). Receiver-operating characteristic analysis for evaluating diagnostic tests and predictive models. *Circulation*, 115(5), 654-657.